

2008

Gas-Phase Formation of Environmentally Persistent Free Radicals from Thermal Degradation of Catechol, Hydroquinone, Phenols and Tobacco

Julien Gnonlonfoun Adoukpe

Louisiana State University and Agricultural and Mechanical College, jadoun1@lsu.edu

Follow this and additional works at: https://digitalcommons.lsu.edu/gradschool_dissertations

 Part of the [Chemistry Commons](#)

Recommended Citation

Adoukpe, Julien Gnonlonfoun, "Gas-Phase Formation of Environmentally Persistent Free Radicals from Thermal Degradation of Catechol, Hydroquinone, Phenols and Tobacco" (2008). *LSU Doctoral Dissertations*. 885.
https://digitalcommons.lsu.edu/gradschool_dissertations/885

This Dissertation is brought to you for free and open access by the Graduate School at LSU Digital Commons. It has been accepted for inclusion in LSU Doctoral Dissertations by an authorized graduate school editor of LSU Digital Commons. For more information, please contact gradetd@lsu.edu.

**GAS-PHASE FORMATION OF ENVIRONMENTALLY
PERSISTENT FREE RADICALS FROM THERMAL DEGRADATION OF
CATECHOL, HYDROQUINONE, PHENOLS AND TOBACCO**

A Dissertation

Submitted to the Graduate Faculty of the
Louisiana State University and
Agricultural and Mechanical College
in Partial Fulfilment of the
requirements for the degree of
Doctor of Philosophy

in

The Department of Chemistry

by

Julien Adoukpe

MS, Université Nationale du Benin, 1990,

MS, Louisiana State University, 2004

May 2008

To my wife, Victoire Adoukpe,

To my sons

Noble Obafemi. Trésor,

Julien Yise Péniel,

Abed Exauce Donatin

With love

ACKNOWLEDGEMENT

Firstly, I want to thank God Almighty, the provider of all my needs, for the assistance I have received from Him during my stay and study here in US. He has put on my path wonderful people from the Chapel on the Campus, and the Baptist Collegiate Ministry on LSU campus that deserve my gratitude.

Secondly, I acknowledge the support and councils provided to me by my academic advisor Dr Dellinger during the course of this research.

I am very grateful to Dr Lavrent Khatchatryan, my mentor, for his patience and guidance throughout this research. His valuable help is appreciated and acknowledged.

I was also fortunate to study in a viable environment made possible by all the post doctorates and graduate students in Dr Barry Dellinger's group. May each of them receive my full appreciation.

Most importantly, I want to thank the Fulbright Scholarship whose financial support enabled me to come to US at the first place and that opened up my six year academic adventure here at Louisiana State University.

I thank my wife and three children for the sacrifice that my student life had imposed upon them. Having them with me, along with its joy and pains was the strength that helped me to succeed in my endeavors.

I thank my brother Jonas Adoukpe for the role of father he humbly and unrelentingly played in my life before and after we lost our dad in March 1983, and for his moral support during my studies in America.

Here is the place to say my thank you to my uncle Dr Clement S. Adoukpe for the model he has represented for me as far as undergoing doctoral studies.

I also want to thank the members of my PhD committee for the time they take to read and help make useful corrections to the present work.

FOREWORD

This Dissertation, divided in 5 chapters, is concerned with the gas-phase formation of environmentally persistent free radicals from thermal degradation of catechol, hydroquinone, phenols and Tobacco. The first chapter, the introductory part of the present work, gives a broad view on the combustion generated persistent free radicals, their health impacts, and the importance of their gas-phase study. The second chapter describes the experimental part of this work which basically relies on radicals' characterization employing the Electron Paramagnetic Resonance (EPR) coupled with the Low Temperature Matrix Isolation technique (LTMI). The formation of Environmentally Persistent Free Radicals was studied at low and atmospheric pressure. Mass analyses of the thermal degradation products of the precursors were performed employing the Gas-Chromatography Mass Spectroscopy (GC-MS). The results are reported in the third chapter. The discussion part of this dissertation presented in chapter 4 shed light on the understanding of gas-phase radical formation depending on their environment. In chapter five, a summary of the main findings is presented.

| TABLE OF CONTENTS | PAGE |
|--|-------------|
| ACKNOWLEDGEMENTS..... | iii |
| FORWORD..... | v |
| LIST OF TABLES..... | ix |
| LIST OF FIGURES..... | x |
| LIST OF SCHEMES..... | xiii |
| ABSTRACT..... | xiv |
| CHAPTER 1: INTRODUCTION..... | 1 |
| 1.1 General Introduction..... | 1 |
| 1.2 Combustion Sources of Total Particulate Matter..... | 1 |
| 1.3 Health Effects of Fine Particles..... | 7 |
| 1.4 Occurrence, Use and Health Impacts of Phenols, Hydroquinone, and Catechol..... | 9 |
| 1.5 Formation of Cyclopentadienyl, Phenoxy, and Semiquinone Radicals..... | 12 |
| 1.6 Hazardous Pollutants Formation from Radicals..... | 17 |
| 1.6.1 Formation of PCDD/Fs..... | 17 |
| 1.6.2 Formation of Naphthalene, Hydroxynaphthalene, di-hydroxynaphthalene, 1H-Indenol, and 1H-Indene..... | 18 |
| 1.7 Rationale for the Current Study..... | 19 |
| 1.8 References..... | 24 |
| CHAPTER 2: EXPERIMENTAL..... | 40 |
| 2.1 Introduction..... | 40 |
| 2.2 The Electron Paramagnetic Resonance Spectroscopy..... | 40 |
| 2.2.1 EPR Theory..... | 42 |
| 2.2.2 Importance and Physical Significance of the EPR g-values..... | 47 |
| 2.2.3 Low Temperature Matrix Isolation..... | 48 |
| 2.2.4 Pyrolysis Experiments..... | 50 |
| 2.2.4.1 Experimental Set-Up..... | 50 |
| 2.2.4.2 Experimental Procedure..... | 53 |
| 2.2.4.2.1 Pyrolysis of Catechol, Hydroquinone and Phenol..... | 53 |
| 2.2.4.2.2 Pyrolysis of Tobacco..... | 56 |
| 2.2.4.2.3 The Time of Residence of the Vaporized Samples in the Reactor..... | 56 |
| 2.2.5 Photolysis Experiments..... | 58 |
| 2.2.6 Annealing Experiments..... | 59 |
| 2.3. Gas Chromatography-Mass Spectroscopy..... | 59 |
| 2.4 References..... | 60 |
| CHAPTER 3: RESULTS..... | 64 |
| 3.1 Low Pressure Pyrolysis of Phenol..... | 65 |
| 3.1.1 Total Radical Yield..... | 65 |
| 3.1.2 Temperature Dependence of Radical Yield..... | 66 |

| | |
|---|-----|
| 3.1.3 Persistent Free Radical Formation from Phenol..... | 67 |
| 3.2 Low Pressure Pyrolysis of Hydroquinone..... | 69 |
| 3.2.1 Total Radical Yield..... | 69 |
| 3.2.2 Temperature Dependence of Radical Yield..... | 69 |
| 3.2.3 Persistent Free Radical Formation from Hydroquinone..... | 71 |
| 3.3 Low Pressure Catechol Pyrolysis..... | 73 |
| 3.3.1 Total Radical Yield..... | 74 |
| 3.3.2 Temperature Dependence of Radical Yield..... | 74 |
| 3.3.3 Persistent Free Radical from Catechol..... | 75 |
| 3.4 Pyrolysis of Tobacco..... | 75 |
| 3.4.1 Free Radical Yield..... | 76 |
| 3.4.2 Persistent Free Radical from Tobacco..... | 77 |
| 3.5 Additional Experiments..... | 78 |
| 3.5.1 Annealing Experiments..... | 79 |
| 3.5.2 Microwave Power Dependence Experiments..... | 80 |
| 3.5.3 Photolysis of Phenol, Hydroquinone, and Catechol..... | 82 |
| 3.5.4 Pyrolysis of Tricarbonylcyclopentadienylmanganese($\eta^5\text{C}_5\text{H}_5\text{Mn}(\text{CO})_3$) at 250°C..... | 85 |
| 3.5.5 Pyrolysis of Di-ter-butylperoxide..... | 87 |
| 3.5.6 Atmospheric Pressure Pyrolysis of Phenol, Hydroquinone, and Catechol..... | 87 |
| 3.5.7 Effects of Trace of Oxygen on Radicals: Case Study of Hydroquinone..... | 91 |
| 3.5.8 GC-MS Analysis of the Products of Atmospheric Pressure Pyrolysis of Phenol, Hydroquinone and Catechol..... | 93 |
| 3.6 References..... | 94 |
| CHAPTER 4: DISCUSSION..... | 98 |
| 4.1 Radicals from Phenol..... | 98 |
| 4.2 Radicals from Hydroquinone..... | 106 |
| 4.3 Radicals from Catechol..... | 114 |
| 4.4 Radicals from Tobacco..... | 118 |
| 4.5 Effects of Oxygen on the Nature of Radicals..... | 121 |
| 4.6 References..... | 123 |
| CHAPTER 5: SUMMARY..... | 129 |
| 5.1 Cyclopentadienyl Radical..... | 129 |
| 5.2 Phenoxy Radical..... | 131 |
| 5.3 Ortho-Semiquinone and Para-Semiquinone Radicals..... | 131 |
| 5.4 Hydroxycyclopentadienyl Radical..... | 133 |
| 5.5 Methylperoxide Radical..... | 134 |
| 5.6 Radical from Tobacco..... | 134 |
| 5.7 Radical from Tobacco Compared to Those from Precursors..... | 135 |
| 5.8 Concluding Remarks..... | 138 |
| 5.9 References..... | 140 |
| APPENDIX 1: ATMOSPHERIC PRESSURE PYROLYSIS OF 2-CHLOROPHENOL, 4-CHLOROPHENOL, ANISOLE, AND CHLOROBENZENE..... | 145 |

| | |
|--|-----|
| APPENDIX 2: COPYRIGHT AND PERMISSIONS..... | 152 |
| VITA..... | 155 |

LIST OF TABLES

| | |
|---|-----|
| 1.1 Sources of Environmentally Persistent Free Radicals..... | 5 |
| 1.2 EPR Spectral Characteristics of PFRs..... | 21 |
| 2.1 Temperature Dependence Variation of Gas Flow for a Constant Residence Time..... | 57 |
| 3.1. Concentration of Free Radical from Four Blends of Tobacco..... | 77 |
| 4.1 Reaction Kinetic Model for the Pyrolysis of Phenol..... | 102 |
| 4.2 CPD and Phenoxy Concentration from the Phenol Reaction Kinetic Model..... | 103 |
| 4.3 Calculated Ratios of K2 to K1..... | 109 |
| 4.4 Bader Valence Electron Charge Densities..... | 113 |
| 5.1 Summary of Key Findings..... | 136 |

LIST OF FIGURES

| | |
|--|----|
| 1.1 Formula Structure of Hydroquinone, Catechol, Phenol, Para-Semiquinone, Ortho-Semiquinone, p-Benzoquinone, o-Benzoquinone, Phenoxy and Cyclopentadienyl Radicals..... | 13 |
| 2.1 Effect of Inclusion of Successive Terms in the Hamiltonian for 1s2p Helium Configuration..... | 46 |
| 2.2 Resonance Condition..... | 46 |
| 2.3 Cold Dewar Assembly..... | 51 |
| 2.4 Assembly for Atmospheric Pyrolysis Experiments..... | 52 |
| 2.5 Photograph of the Experimental Layout..... | 53 |
| 2.6 Cold Dewar in EPR Cavity-Front View, Cold Dewar Connected to the Vaporizer-Rear View..... | 54 |
| 2.7 Tobacco Atmospheric Pyrolysis Assembly..... | 55 |
| 3.1 Time Dependence of Radical EPR Intensity from the Pyrolysis of Phenol..... | 66 |
| 3.2 Temperature Dependence of Radical Yield from the Pyrolysis of Phenol..... | 67 |
| 3.3 A Representative EPR Spectrum from the Pyrolysis of Phenol above 850°C..... | 68 |
| 3.4 Temperature Dependence of Total Yields from Low Pyrolysis of Hydroquinone..... | 70 |
| 3.5 EPR Spectra of Frozen Radical from HQ Pyrolysis at 950°C..... | 71 |
| 3.6 EPR Featureless Singlet Line from the Pyrolysis of HQ at Temperature below 600°C..... | 71 |
| 3.7 Representative EPR Spectrum from the Pyrolysis of HQ at 700-800°C..... | 72 |
| 3.8 A Representative EPR Spectrum from the Pyrolysis of HQ at 800-1000°C..... | 72 |
| 3.9 Time Dependence Accumulation of Radicals from the Pyrolysis of Catechol..... | 73 |
| 3.10 A Representative EPR Spectrum from the Pyrolysis of CT at 400-600°C..... | 74 |
| 3.11 Temperature Dependence of Total Radicals Yield from the Gas-Phase Pyrolysis of Catechol..... | 75 |
| 3.12 Overall Width of Raw Tobacco EPR Spectrum..... | 76 |

| | |
|--|----|
| 3.13 EPR Spectrum of Organic Radical in Raw Tobacco..... | 77 |
| 3.14 Radical Yields Observed in TPM Condensed Directly on the Cold Finger from the Gas-Phase Pyrolysis of Four Tobacco Blends..... | 78 |
| 3.15 The EPR Spectrum of Frozen Radicals Collected on the Cold Finger from the Pyrolysis of Virginia Blend at 380°C..... | 78 |
| 3.16 The Step by Step Annealing of Radicals from Pyrolysis of Phenol at 700°C..... | 79 |
| 3.17 EPR Spectra of Frozen Radical from HQ Pyrolysis at 950°C..... | 79 |
| 3.18 EPR Spectra of Carbon Dioxide Matrix Isolated Radicals from the Pyrolysis of Catechol at 850°C Atmospheric Pyrolysis of HQ..... | 80 |
| 3.19 Microwave Power Dependence of CPD radicals at 77K from the Pyrolysis of $\eta^5\text{-C}_5\text{H}_5\text{Mn}(\text{CO})_3$ at 250°C..... | 81 |
| 3.20 Effect of Microwave Power on the 77K EPR spectra of Radicals from the Pyrolysis of Phenol at 750°C..... | 82 |
| 3.21 Photolysis of Phenol at Room Temperature..... | 83 |
| 3.22 EPR Spectrum of Products of the Photolysis of HQ..... | 84 |
| 3.23 CT Photolysis at Room Temperature Yielded a Very Weak EPR Signal..... | 84 |
| 3.24 CPD EPR Spectrum from the Pyrolysis of Tricarbonylcyclopentadienylmanganese at 250°C..... | 85 |
| 3.25 Comparison and Subtraction of EPR Spectra of Carbon Dioxide Matrix Isolated CPD Radicals from Pyrolysis of $\eta^5\text{-C}_5\text{H}_5\text{Mn}(\text{CO})_3$ at 250°C | 86 |
| 3.26 Step by Step Annihilation of Initial Spectrum A to Final Phenoxy Radical Spectrum C... | 86 |
| 3.27 Atmospheric Pressure Pyrolysis of Phenol at 750°C..... | 88 |
| 3.28 Apparent Superposition of Several Radicals..... | 89 |
| 3.29 Atmospheric Pyrolysis of HQ..... | 91 |
| 3.30 EPR Spectrum of Radicals from the Atmospheric Pressure Pyrolysis of CT..... | 91 |

| | |
|---|-----|
| 3.31 Frozen p-SQ Radicals EPR Spectra from Pyrolysis of HQ at 550° | 92 |
| 3.32 Effect of Oxygen Traces on the Shape of EPR spectra of frozen Radicals from HQ pyrolysis at 750°C | 93 |
| 4.1 EPR Spectra of Frozen Radicals (at 77K) from Phenol Pyrolysis at 950°C | 100 |
| 4.2 77K EPR Spectra of Radicals from Pyrolysis of Phenol in CO ₂ flow at 400°C, (spectrum A) and at 600°C (spectrum B) | 101 |
| 4.3 Comparison of Experimental EPR spectrum from HQ pyrolysis with the Calculated EPR Spectrum of CPD | 106 |
| 4.4 EPR Spectra of Radicals Trapped on the Cold Finger from the Pyrolysis of HQ at 825°C | 108 |
| 4.5 Comparison of EPR Spectra of Frozen Radical from the Pyrolysis of HQ at 550°C, Photolysis of HQ, And photolysis of Phenol at room Temperature | 111 |
| 4.6 Total Radical Yield from the Gas-Phase Pyrolysis of Catechol CT | 114 |
| 4.7 Temperature Dependence of g-values and ΔH_{p-p} of Radicals from the Pyrolysis of HQ in CO ₂ in Presence of Traces of O ₂ | 122 |
| 5.1 A Comparative Total Radical Yields from 0 to 12 minutes Accumulation Time of CT, HQ, and Phenol | 130 |
| 5.2 Temperature Dependence of Total Radical Yield | 133 |

LIST OF SCHEMES

| | |
|---|-----|
| 1.1 General formation of Semiquinone and Phenoxy Radicals in Gas-Phase..... | 14 |
| 1.2 Gas-Phase Formation of CPD from Phenoxy Radical..... | 14 |
| 1.3 Semiquinone and Phenoxy Radical Formation Respectively from HQ or CT and Phenol.... | 15 |
| 1.4 Formation of Phenoxy Radical and Chlorinated Phenoxy Radical on a Metal Surface from Chlorinated Benzene..... | 16 |
| 1.5 General Mechanism of the Formation of PCDD/F from Polychlorinated phenoxy radicals.. | 17 |
| 1.6 Formation of Naphthalene from CPD-CPD Interaction Pathway..... | 19 |
| 1.7 Proposed Mechanism of the formation of 1-Hydroxynaphthalene..... | 22 |
| 1.8 Proposed Mechanism of the Formation of Naphthalene diol-1-8 followed by 1H-Inden-7-ol formation by elimination of CO..... | 23 |
| | |
| 4.1 Thermal Degradation of the Model HQ: Mechanism of the Formation of Various Radical..... | 105 |
| 4.2 Mechanism of the Formation of the OHCPD Followed by the Generation of the Cyclopentadienone Molecule..... | 110 |

ABSTRACT

Catechol, hydroquinone and Phenol are major constituents of the mainstream tobacco smoke. The toxicity of tobacco has been attributed to the ability of catechol and hydroquinone to undergo endogenous or exogenous redox cycling to form semiquinone type radicals responsible of Reactive Oxygen Species (ROS) formation. ROS such as hydroxyl radicals can cause severe oxidative stress on biological tissues and can provoke severe signaling pathways leading to cardiovascular and pulmonary dysfunctions and carcinogenesis. Given that semiquinone type radicals are organic radicals, characterized by their high instability and reactivity; it is somewhat surprising that they can live long enough mostly when associated with atmospheric fine particles to induce the biological damages reported in the literature. Thus identification of the exact nature of the free radicals, their origin, the reason for their stability and persistency, and their health impacts appear to be an increasing environmental issue.

Consequently, we have performed studies of the thermal degradation of catechol, hydroquinone and phenol and structurally similar derivatives that have been proposed as progenitors of semiquinone type radicals. Tobacco pyrolysis has also been investigated. We have employed in conjunction with the Electron Paramagnetic Resonance (EPR), the technique of Low Temperature Matrix Isolation in which catechol, hydroquinone, phenols and Tobacco were pyrolyzed in both low and atmospheric pressures reactor that was directly connected to a liquid nitrogen-cooled cold finger located in the EPR cavity of a Bruker EPR spectrometer.

Comprehensive potentially persistent free radicals identification associating additional experimental and mathematical tools has led to the acquisition of the EPR spectra of p-Semiquinone, o-Semiquinone, cyclopentadienyl and phenoxy radicals. The hydroxycyclohexadienyl radical, one of the unexpected radicals according to the decomposition mechanism developed earlier, was found during the atmospheric pyrolysis of phenol. The

supposedly very labile radical identified was the hydroxycyclopentadienyl. The methylperoxide type radicals were found when trace of oxygen was used during the pyrolysis experiments.

The precursors pyrolysis product analysis employing GC-MS revealed the formation of naphthalene, indenol, indene, benzofuran-2-methyl, indenone, fluorene, and acenaphthylene, thus giving additional evidence of the formation of both labile and potentially persistent free radicals.

CHAPTER 1: INTRODUCTION

1.1 General Introduction

The goal of the present study is to characterize the potentially environmentally persistent free radicals formed from the thermal degradation of basic precursors such as catechol, hydroquinone, and phenols found in mainstream tobacco smoke¹⁻⁴. Catechol, hydroquinone and phenol supposedly form semiquinone and phenoxy types radicals detected in Particulate Matter (PM) which toxicity has been reported in the literature⁵⁻⁷.

Semiquinone radicals are highly active in oxidative stress that can lead to cancer, mutations, and alteration of DNA⁸⁻¹⁰. Phenoxy radicals can also combine to form polychlorinated dibenzo-p-dioxins / dibenzofurans (PCDD/F), the most potent toxic environmental pollutants¹¹. Cyclopentadienyl radical toxicity is not clearly and solely established. However, cyclopentadienyl type radicals are known to be environmentally persistent¹² and are precursors to Polycyclic Aromatic Hydrocarbons (PAHs) formation^{13,14}. Semiquinone type radicals have been found in tobacco^{15,8} and thought to be the causes of tobacco toxicity¹⁶.

However, for organic radicals such as semiquinone, known to be very reactive, to be stable enough to cause damage in living tissue is quite surprising. Thus the determination of the exact nature of radicals formed during the pyrolysis of precursors found in the mainstream tobacco smoke is important to establish the link. The combustion sources that generate the semiquinone containing PM are numerous. The following paragraph will present a summary of those sources.

1.2 Combustion Sources of Particulate Matter

One of the greatest of mankind's achievements is the ability to make fire. Fire making produces heat used in variety of ways. Over the time, people have used combustion to generate energy needed to sustain life. Archaeological research holds evidence that control fire had been a humankind reality 1 to 1.8millions years ago (UNESCO-Fossil Hominid Sites) where the

primary sole source of energy was wood. Wood remains a viable energy source worldwide. However, the need of diversification of energy sources has led to the search for fossil fuels, such as petroleum, natural gas and coal.

Power plants use those sources to supply the vast majority of the world's electricity today; the International Energy Agency states that nearly 80% of the world's power comes from these sources. The burning of fuels of any kind not only provides human with certain welfare, but also generates by-products which by polluting the environment can harm people.

Combustion-generated harmful PM has been extensively investigated and reported in the literature. The combustion of wood in residential fireplaces and wood stoves accounted from 10 to 20% of the total fine particle emissions in United States according to U.S. Environmental Protection Agency data for 1995¹⁷. Wood species grown in Northeastern United States revealed that the fine particulate mass emission rates from their combustion ranged from 2.7 to 11.4g per Kg of wood burned¹⁸, while those grown in the Southern United States PM mass emission ranged from 4.3 to 6.8g per Kg of wood burned¹⁹. Even higher rates have been reported²⁰. Polychlorinated dibenzo-p-dioxins and polychlorinated furans (PCDD/F) are the most toxic environmental pollutants. Combustion and thermal processes are the primary source of their formation²¹⁻²⁶. Fine particulate matters are also formed from motor vehicles, power plants, meat charbroiling, and cigarette smoke^{27,28}.

The mechanism by which free radicals are formed is under intensive scientific scrutiny. Several researches have shown that combustion sources are primary causes of radical formation. The hydrocarbon fuel, coal and wood burning are combustion processes by which energy is released for the human welfare. The sustainability of the combustion process is radicals driven. The concentration of free radicals that a given material can release strongly determines the

flammability of the material. This speeds up initiation and propagation reactions, leading to the combustion of the material. Given that fuels contain significant amount of Catechol (CT) hydroquinone (HQ), and phenols²⁹⁻³³, the link between fuels burning and environmental pollution has been well established. Phenol, HQ, and CT are found in the thermal degradation of lignin and other polymeric plant materials that usually contain aryl ether and aryl alcohol linkages^{29, 30, 34, 35}.

Biomass burning also releases significant quantity of CT, HQ and phenols^{18, 36, 37}. CT, HQ and phenols are also formed from coal burning^{32, 33, 38}. Their derivatives including quinones and PAHs have been reported in both atmospheric aerosols and combustion-generated particulate matter (PM). In 2004, a report gave evidence of their occurrence in atmospheric total suspended particulate (TSP) at concentrations of 5.0-730 $\mu\text{g}/\text{m}^3$ ³⁹.

The emissions of HQ and CT from wood-burning fireplaces were reported to be 0.3-10 mg/g and 1.7-9.8 mg/g of organic carbon, respectively^{18,19}. The emissions of CT from open burning of agricultural biomass were reported to be 0.060-1.2 mg/g of organic carbon and 0.11-4.0 mg/g for other quinones³¹. Methoxyhydroquinones and methoxyphenols (e.g. syringols) are frequently reported in biomass combustion emissions as partial decomposition products of lignin^{34,40}.

Methoxyhydroquinones have been reported to be 0.50-3.0 % of total biomass burned⁴¹. Methoxyphenol concentrations were reported in airborne PM at concentrations of 0.10-22 ng/m³⁴². From 900 up to 4200 mg of methoxyphenol is released per Kg of burnt wood and biomass⁴³⁻⁴⁵. The burning of tobacco generates major organic components such as phenol, CT and HQ⁴⁶⁻⁵³. Refineries, power plants and motor vehicles contribute significantly to CT, HQ and

phenol emission. The huge effort put in vehicle designs and gasoline formulations has somehow reduced the emissions of air pollutants. However, combustion-generated air pollutants are still of major concern mostly in cities with high population densities.

The emissions of quinone from catalyst-equipped gasoline-powered motor vehicle are reported to be 0.849 $\mu\text{g}/\text{km}$ versus 25.4 $\mu\text{g}/\text{km}$ for no catalyst-equipped gasoline-powered motor vehicle⁵⁴. Also, emissions of quinones were reported to be 15-140 $\mu\text{g}/\text{g}$ in gasoline exhaust particles⁵⁵ and 7.90-40.4 $\mu\text{g}/\text{g}$ in diesel exhaust particles³⁹. Light-duty gasoline vehicles technology classes reported the emission of benzoquinone in low emission vehicles, three-way catalyst equipped vehicles, and smoking vehicles to be 2.0 $\mu\text{g}/\text{L}$, 85 $\mu\text{g}/\text{L}$, 3200 $\mu\text{g}/\text{L}$ of fuel consumed respectively in gas-phase and 1.8 $\mu\text{g}/\text{L}$, 46 $\mu\text{g}/\text{L}$, 1500 $\mu\text{g}/\text{L}$ of fuel consumed respectively in particle-phase⁵⁶. Significant reduction of benzoquinone emission from heavy-duty diesel vehicles has been achieved. In 1995, the benzoquinone emission was estimated to be 28000 $\mu\text{g}/\text{L}$ versus 510 $\mu\text{g}/\text{L}$ in 1999 of fuel consumed in gas-phase and 1600 $\mu\text{g}/\text{L}$ versus 230 $\mu\text{g}/\text{L}$ in particle-phase⁵⁶.

From the presentation of those data, it is obvious that combustion of fuels is the cause of major environmental pollution, leading to necessarily regulatory action. For example, the United States Environmental Protection Agency has adopted a new health effects-based Ambient Air Quality Standard that limits the maximum allowable ambient concentrations of fine particulates⁵⁷. An estimate of 30 billion US dollars per year will be needed to meet these standards and require the development of new control technology⁵⁸. **Table 1.1** summarizes the sources of the environmentally Persistent Free Radical (PFRs) precursors.

Table 1.1 Sources of Environmentally Persistent Free Radicals

| Categories | PFR Precursors | | | | Comment | References |
|----------------------------|---------------------------------|-----------------------|-------------------|---------------------|--|--|
| Wood Smoke | Phenols | | | | Fine Particle emissions from combustion of Woods grown in the southern ¹ , north-eastern ² of United States Measured in mg/g of Organic Carbon OC, and San Joaquin Valley (CA) ³ in µg/g of wood (na: not in the original source) | (1) (2002) Fine, P.; Cass, G.; Simoneit, B.; <i>Env & Tech.</i> (2) (2001) Fine, P.; Cass, G.; Simoneit, B.; <i>Environ.Sci. Technol.</i> (3) (2001) Nolte, C.; Schauwer, J.; Cass, G.; Simoneit, B.; <i>Environ.Sci. Technol.</i> |
| | Type of Woods | CT | HQ | Phenol | | |
| | Yellow poplar ¹ | 4.127 | 7.609 | na | | |
| | White ash ¹ | 1.741 | 1.621 | na | | |
| | Sweet-gum ¹ | 1.383 | 1.435 | na | | |
| | Mochemut hickory ¹ | 9.865 | 10.119 | na | | |
| | Loblolly pine ¹ | 2.600 | 0.763 | na | | |
| | Slash pine ¹ | 1.711 | 0.295 | na | | |
| | Red maple ² | 0.799 | 0.625 | na | | |
| | Northern red oak ² | 5.434 | 5.570 | na | | |
| | Paper birch ² | 1.110 | 0.919 | na | | |
| | Eastern white pine ² | 1.512 | 0.356 | na | | |
| | Eastern hemlock ² | 0.952 | 1.146 | na | | |
| | Balsam fir ² | 7.11 | 4.793 | na | | |
| | Oak ³ | na | na | 0.3-68 | | |
| | Eucalyptus ³ | na | na | 0.1-106 | | |
| | Pine ³ | na | na | 0.1-125 | | |
| | Oxy-PAH | | | | | |
| | | 1,4 naphthalene dione | 1H-phenalen-1-one | Benzanthrone | | |
| | Yellow poplar ¹ | 0.110 | 0.474 | 0.164 | | |
| | White ash ¹ | 0.008 | 0.299 | 0.205 | | |
| | Sweet-gum ¹ | 0.006 | 0.163 | 0.088 | | |
| | Mochemut hickory ¹ | 0.017 | 0.379 | 0.173 | | |
| Loblolly pine ¹ | 0.018 | 0.244 | 0.108 | | | |
| Slash pine ¹ | 0.016 | 0.280 | 0.094 | | | |
| Red maple ² | 0.010 | very low | 0.117 | | | |
| N. red oak ² | 0.007 | 0.046 | 0.066 | | | |
| Tobacco Smoke | Phenols | | | | a: µg/mg of TPM of mainstream tobacco smoke | 1- (2006) Wooten, J.; Chouchane, S.; McGrath, T. E. |
| | | CT ^a | HQ ^a | Phenol ^a | | |
| | Bright ¹ | 5.8-6.0 | 4.1-4.5 | 2.2-2.4 | | |
| | Burley ¹ | 3.1-3.2 | 3.5-3.7 | 2.0-2.2 | | |
| | Oriental ¹ | 5.9-6.0 | 3.6-3.8 | 1.4-1.6 | | |
| | Mix | | | | | |
| | Polyphenols | | | | | |
| | | Chlorogenic acid | Quinic acid | Caffeic acid | | |
| | Bright ¹ | 9.7 | 1.9 | 0.19 | | |
| | Burley ¹ | 0.4 | 1.4 | ~ 0.01 | | |
| Oriental ¹ | 9.0 | 1.2 | 0.15 | | | |
| Mix | | | | | | |
| | 1-Phenols | | | Open burning of | (2005) Hays, M.; Fine, P.; Geron, C.; Kleeman, M.; | |
| | CT | HQ | Phenol | | | |

| | | | | | | | |
|---------------------|------------------------------------|--|--|---|---|--|---|
| Biomass Burning | Rice straw | 1.179 | 0.710 (methylbeze nediol) | 0.371 (methoxybeze nediol) | agricultural biomass (mg/g of OC) ND: Not Detected | Gullett, B; <i>Atmosp. Env.</i> | |
| | Wheat straw | 0.060 | 0.104 (methylbenz enediol) | 0.095 (methoxybeze nediol) | | | |
| | 2- Oxy-PAHs | | | | | | |
| | | Anthracene-9,10 dione | | | | | |
| | Rice straw | ND | | | | | |
| | Wheat straw | 0.033 | | | | | |
| Municipal Waste | Phenols | | | | Semivolatile compounds $\mu\text{g}/\text{cm}^3$ of waste | (1998) 1-Trenholm, A.; <i>Waste Management</i> | |
| | | CT | HQ | Phenol | | | |
| | | na ¹ | na ¹ | ¹ 5-25 $\mu\text{g}/\text{cm}^3$ | | | |
| | | | | | | | |
| | PAHs, Oxy-PAHs | | | | | | |
| | Bezoquinon e | 1,4 naphthaquin one | | | | | |
| | | ¹ 1-5 $\mu\text{g}/\text{cm}^3$ | ¹ 1-5 $\mu\text{g}/\text{cm}^3$ | | | | |
| Motor Vehicles | Oxy-PAHs | | | | a catalyst- equipped- non catalyst equipped motor vehicles | 1-(2002) Schauer, J.; Kleeman, M.; Simoneit, B. <i>Environ.Sci. Technol</i> 2-(2002) Zheng, M.; Cass, G.; Edgerton, E. <i>Environ.Sci. Technol</i> 3-(1998) Trenholm, A. <i>Waste Mangement</i> | |
| | | Benzoqui none ³ | Anthrace -9,10- dione ¹ | 1,4 Naphtho quinone ³ | | | Benz(a) anthracene -7,12-dione ² |
| | | 1-5 $\mu\text{g}/\text{cm}^3$ | 0.849- 25.4 μg /km ^a | 1-5 $\mu\text{g}/\text{cm}^3$ | | | 0.02-0.26 ng/m ³ |
| Fuels Burning | Phenols | | | | Mass of methoxy Phenol of total PM2.5 mass emission from wax and beeswax (paraffin) | 1-(2002) Hays, M.; Geron, C.; Linna, K.;Smith, D. <i>Environ.Sci. Technol</i> 2- (1999) Fine, P.; Cass, G. <i>Environ.Sci. Technol</i> . . 3- (2004) Jefford, A. <i>London</i> 4- (2004) Yingjun, C.;Xinhui, B.; Jiamo, F. <i>Fuel</i> | |
| | | CT | HQ | Phenol | | | |
| | Foliar Fuels ¹ | na | Na | 0.5 -3% of PM2.5 mass | | | |
| | Coal | | | | | | |
| | Peat ³ | | | 29.6-46.4ppm | | | |
| | Candle | | | | | | |
| | OxyPAHs | | | | | | |
| | | Anthracened ione/ anthracene | Benz(a)anth racene 7,12- dione | Corocene/pyre ne(PAH) | | | |
| | Foliar Fuels ¹ | | | | | | |
| | Coal ⁴ | /0.002- 4.691mg/g | 0.073-0.217 g/mg | 1.119mg/g 0.075-4.3 | | | |
| Peat ³ | | | | | | | |
| Candle ² | 0.09- 0.05mg/g of wax/beeswa | 0.007- 0.02mg/g of wax/beeswa | | | | | |

1.3 Health Effects of Fine Particles

Fine particles are known to be very toxic and their health related effects are well documented. Several epidemiological studies in both the United States and Europe, have concluded that exposure to fine particulates increases mortality due to heart and lung disease⁵⁹⁻⁶⁴. The magnitude of their health impact is potentially enormous: fine particle toxicity may cause up to 450,000-600,000 deaths per year in the United States⁶⁵. Ambient air pollution is the result of complex mixture of volatiles and particulates from various sources including vehicle exhaust pipes, flaring of hydrocarbons at refineries sites, coal burning at power plants, burning trash or crops after harvest still in use in many developed countries⁶⁶. The size and composition distribution of fine particulate matter from motor vehicles, wood burning, and cigarette smoke^{27,28,67-69} significantly impact human health.

Particles which sizes are greater than 10 μm , once inhaled, can pass through nose or mouth to penetrate the larynx. They can eventually be exhaled. The ones which sizes are between 10 μm and 2.5 μm , can follow air stream through the larynx and enter the trachea and the bronchial regions of the lung. They can also be removed. However, those particles with sizes less than 2.5 μm deposit deep into the alveolar regions of the lung and even diffuse directly into the blood stream.

It is well established that fine particulate matters produce acute cardiovascular malfunction indirectly through the induction and perpetuation of inflammatory responses in the lung⁶⁶. Worse, particles with the sizes of 0.1 μm can penetrate deep into the lower respiratory tract and diffuse into the blood stream then get to the heart where they may cause many heart diseases including the influences of the cardiac myocytes and cardiovascular functioning⁷⁰⁻⁷². Exposure to fine particulate matter causes acute inflammatory response⁷³ asthma and chronic obstructive pulmonary disease⁷⁴.

It has been reported that the number of deaths due to respiratory viral infections is increased on high concentration of ambient air pollution days ⁷⁵. Cardiac myocyte degeneration ⁷⁶ and changes in heart rate ⁷⁷ when exposed to environmental pollutants for even a short period of time have been shown.

Fine particles toxicity has been attributed to their association with free radicals ⁷⁸⁻⁸⁰. PFRs are chemical compounds with one or more unpaired electrons, sufficiently stable towards decomposition and resistant to further reaction and can exist for long period of time in the atmosphere.

Those PFRs that potentially include semiquinone-type and phenoxy-type radicals are highly resonance stabilized and are formed in combustion systems or thermal processes such as burning of cigarette, biomass fuels, fossil fuels, coal, and hazardous materials ⁸¹⁻⁸³. Recent studies have reported that semiquinone and phenoxy radicals are persistent when they are associated with combustion generated fly-ash. Thus they can exist for long period of time and be transported over considerable atmospheric distances ⁵⁻⁷. Semiquinone radicals are highly active in oxidative stress that can lead to cancer, mutations, and alteration of DNA ⁸⁻¹⁰. Phenoxy radicals can also combine to form polychlorinated dibenzo-p-dioxin / dibenzofuran (PCDD/F) which is the most potent toxic environmental pollutants ¹¹. Cyclopentadienyl radical toxicity is not clearly and solely established.

However, cyclopentadienyl type radicals are known to be environmentally persistent.¹² and is precursor to PAHs formation ^{13,14}. Due to the structural similarity of semiquinone and phenoxy radicals; and possible further decomposition of semiquinone and phenoxy radicals to form cyclopentadienyl radical, Hydroquinone, Catechol, chlorinated benzenes, phenol, and chlorinated phenols are chosen as their precursors in the present study. The main reason of this

choice is that Hydroquinone, Catechol, and phenols occur naturally in all type of fuels and are used in a variety of ways that can have serious health impacts.

1.4 Occurrence, Use and Health Impacts of Phenols, Hydroquinone, and Catechol

Phenols, Catechol and Hydroquinone natural occurrence has been reported in the literature. Phenol is found in variety of biological substances such as leaves, plants, hardwoods, fish tissue animal waste, and water⁸⁴⁻⁸⁷. Likewise, Catechol (CT) and Hydroquinone (HQ) are found in a variety of forms as natural products from plants and animals. The hazardous substances data bank (HSDB, 1993) reported that CT is found in onions, apples, and even in the leaves or branches of oak and willow trees. CT and HQ have been identified in roasted coffee beans⁸⁸ and in the leaves of blueberry, cranberry, cowberry and bearberry plants⁸⁹. HQ is also contained in tea at concentration up to 1% of total ingredients⁹⁰. HQ was observed in the tissue cultures of *Antennaria-microphylla* and *Euphorbia-esula*^{91, 92} and in the explosion chamber of beetle^{93,94}. The natural occurrence of phenol, catechol and hydroquinone that implies their daily use in variety of ways can lead to serious health issues.

The usefulness of phenol, catechol (CT) and hydroquinone (HQ) has been fully investigated. Cosmetic and hygienic products employ phenol. Variety of indoor products ranking from mouth washes, shaves, creams, to throat lozenges contain phenol⁹⁵. Phenol is also employed in the manufacture of synthetic products such as plastics, fibers, adhesives, resins, and rubber (HSDB, 1991).

HQ and CT are used in many fields including graphic arts, photographic developers; antioxidants, polymerization inhibitors, and pharmaceuticals. In medicine, CT and HQ are used both for cosmetics and medical skin preparations. They serve as de-pigmenting agent to lighten small areas of hyper-pigmented skin⁸⁹ or in ingredient of permanent hair dyes and color preparations^{96,97}. HQ and CT are used in medical and industrial X-ray films⁹⁸ as well as

developer in black-and-white photography or related graphic arts such as lithography and rotogravure^{89,98-100}. They are widely used in the manufacture of rubber antioxidants, monomer inhibitors, and food antioxidants to prevent deterioration in many oxidizable products^{89,101}. Application of a CT antioxidant protocatechuic acid on 12-Otetradecanoylphorbol- 13-acetate induces inflammatory responses in mouse skin¹⁰². The hypochlorous acid, a powerful pro-inflammatory oxidant produced by activated neutrophils, to protect liposomes against iron-ascorbate-induced oxidation is scavenged by abietic acid-derived CT¹⁰³. It is obvious that catechol, phenol and hydroquinone contribute to human welfare. However, they become very harmful and toxic at a given dose as it is known, dose makes toxicity.

When inhaled, phenol, HQ or CT can induce coughing, burning sensations, labored breathing in humans¹⁰⁴⁻¹⁰⁷ as well as reduced bone marrow and corneal damage in mice¹⁰⁷⁻¹¹¹. Cigarette smoking is the leading cause of preventable death in the United States. More than 400,000 deaths per year (clinnimmune-immunotoxicology report, 2003) is tobacco toxicity related. A typical smoker inhales more than 100 µg of HQ or CT per cigarette¹⁶ and ~280 µg of phenol per cigarette¹¹². In studies of repeated-dose toxicity of phenol, "slight" changes in the liver and "slight to moderate" kidney damage were observed in rats receiving 50 (liver) or 50 and 100 (kidney) mg phenol/kg-body weight per day (gavage in 1% water solution) over six months^{113,114}, followed by considerate weight loss due to less consumption of water by the exposed animals^{115, 116}. Even though their toxicity level in human is not well established, those values seem enough to cause diseases given that heavy smokers smoke at least 20 cigarettes per day. It is also reported that the use of phenol in the surgical procedure of skin peeling produces cardiac arrhythmias¹¹⁷.

Toxicological studies of Hydroquinone showed that Hydroquinone has reproducibly to induce benign neoplasms in the kidneys of male F344 rats dosed orally either by gavage (25 and

50 mg/kg body weight) or diet (0.8%)¹¹⁸. Inhibitions of ribo-nucleotide reductase that cause immediate cessation of DNA synthesis in proliferating lymphocytes^{46,119} is due to HQ or CT concentration as low as 10µM. 50µM of HQ or CT is reported to instantaneously block more than 90% DNA synthesis¹²⁰.

The potency of HQ and CT is attributed to their capability to exist as semiquinone radical form causing cancer, mutations, and many health issues. Semiquinone radical has been reported in cigarette smoke^{5,9} and demonstrated to be highly redox-active toward producing reactive oxygen species (ROS) in biological systems^{9,121,122}.

ROS induces oxidative stress in living organisms which is currently considered to be significant causes of the health impacts of airborne fine particulate matter^{66,78,121, 123,124}. Cigarette smoke enhances tumor cell invasions and metastasis, thus spreading cancer in the whole body¹²⁵. Semiquinone type radicals and ROS from cigarette smoking have been shown to cause oxidative DNA damage, stress on lung tissues¹²⁶⁻¹²⁹.

Semiquinone radical also has been reported in wood smoke and other combustion sources. A study of wood burning indicates the generation of radicals and ROS that break cellular DNA strands in cultured raw 264.7 mouse macrophage cells¹³⁰. Even if the initial DNA cell is damaged, human immune system has the ability to repair it. However, the reparation can be stopped or delayed by the presence of radical in the bloodstream. Phenol significantly contributes to health damage.

By losing the hydrogen atom of its hydroxyl group, phenol may exist in form of phenoxy radicals. Phenoxy radical toxicity is well documented. In 1999, a study on the oxidation of the fluorescent dye 2',7'-dichlorofluorescein (DCF) by horseradish peroxidase was reported suggesting that DCF could be oxidized either by horseradish peroxidase-compound I or -compound II with the obligate generation of the DCF phenoxy radical (DCF[•]). In turn, DCF

oxidizes GSH, generating the glutathione thiyl radical (GS[•]). Similarly, DCF[•] oxidized NADH, generating the NAD[•] radical that reduced oxygen to superoxide¹³¹, confirming the belief that phenoxy radical may also have a major impact on human health to the same extent of the semiquinone radicals. Furthermore, studies have shown the direct implication of phenoxy radicals in tobacco toxicity¹³², glutathione depletion¹³³, DNA adduction^{134, 135} generation of reactive oxygen species¹³⁶ and its contribution to the anti oxidant mechanism of myricetin.

1.5 Formation of Cyclopentadienyl, Phenoxy, and Semiquinone Radicals

The toxicity of the PM has been attributed to their association with environmentally persistent free radicals⁷⁸. Combustion-generated radicals have been extensively investigated^{6, 7, 67, 81-83, 137-148}. Several attempts have been explored to draw the mechanisms of cyclopentadienyl, phenoxy and semiquinone type radicals formation based on products distribution of the combustion of suitable precursors. However, few studies have really focussed attention on the environmentally Persistent Free Radicals (PFRs) formation in gas-phase^{12,7}. The most representative precursors used in the understanding of persistent free radicals formation were Catechol and Hydroquinone not only because of their structural similarity, but also because of their common aromatic properties and their natural occurrence.

Phenol, a likely reaction intermediate in the decomposition of hydroquinone and catechol, is also used as precursor of the environmentally persistent free radicals. **Figure 1.1** depicts the molecular structures of Hydroquinone, Catechol, phenol, para-semiquinone, ortho-semiquinone, parabenzoquinone, phenoxy and cyclopentadienyl radicals. Free Radicals formation from precursors can occur either in pure gas phase or on surface mediated radical formation.

In the gas-phase, endothermic dissociation of the oxygen-hydrogen bond of HQ, CT or phenol forms semiquinone¹⁴⁰ or phenoxy radicals¹⁴⁹. Radical-molecule interaction can also, in gas phase lead to the abstraction of hydrogen atom of the hydroxyl group of HQ, CT or phenol.

In the presence of high concentration of initiated radicals the radical-molecule interaction forms

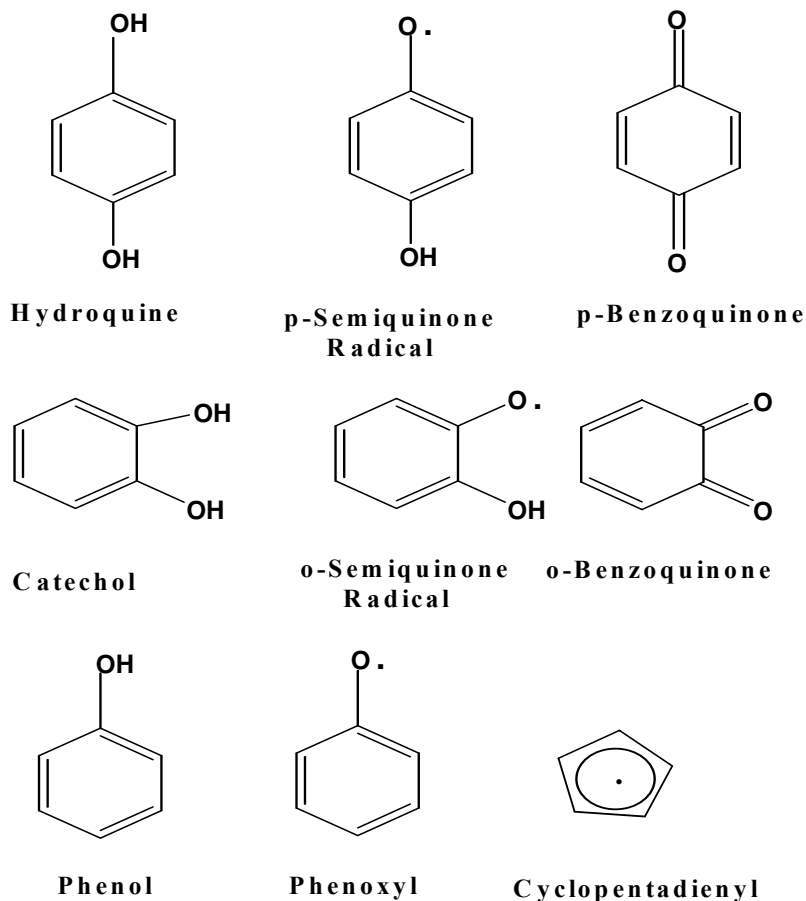
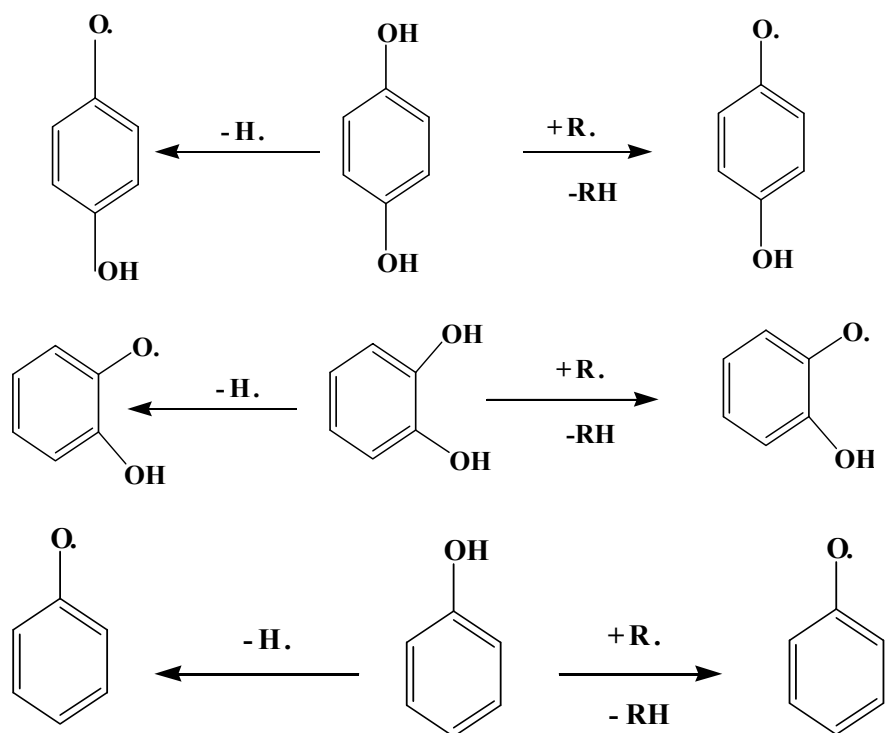


Figure 1.1 Formula structure of Hydroquinone, Catechol, phenol, para-semiquinone, ortho-semiquinone, p-Benzoquinone, o-Benzoquinone, phenoxy and cyclopentadienyl radicals.

semiquinone or phenoxy^{140,142-144,150}.

Scheme 1.1 displays possible routes of formation of semiquinone radical from HQ and CT molecules and phenoxy radical from phenol in gas-phase.

Likewise, the chemisorption onto particulate matters of molecules of similar structure as phenol, catechol and hydroquinone such as monochlorobenzene (MCBz), 1,2-dichlorobenzene (1,2-DCBz), 2-monochlorophenol (2-MCP), 4-chlorophenol (4-MCP) and 1,4 dichlorobenzene can lead to the formation of substituted or non-substituted phenoxy radical. Chlorinated



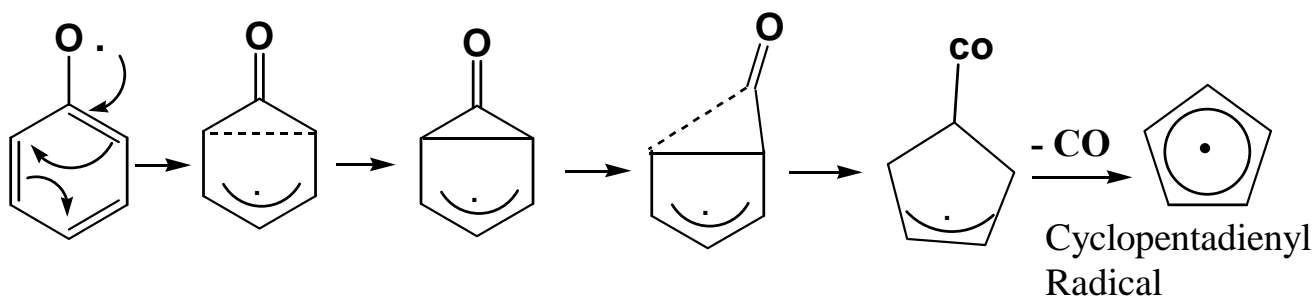
Scheme 1.1: General Formation of Semiquinone and phenoxy Radicals in Gas-Phase

benzenes such as MCBz and 1,2-DCBz may bind to the surface of particulate matter and form phenoxy radical or chlorinated phenoxy radical through hydrogen chloride

Heterogeneous reaction of precursors at surfaces can lead to surface-generated radical formation.

Semiquinone radicals may form on the surface of combustion generated fly-ash through the elimination of water and electron transfer to the metal surface in chemisorption

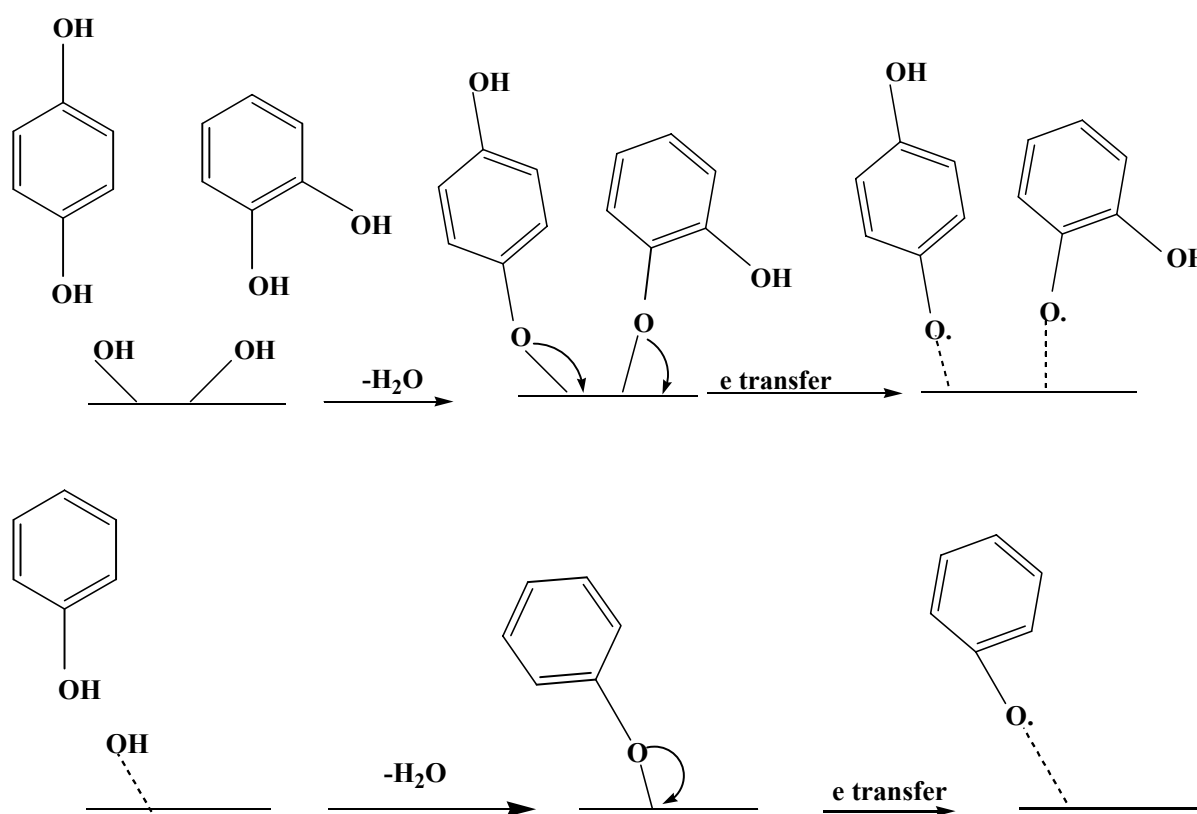
Process^{6, 151, 152}. **Scheme 1.3** depicts possible routes of formation of semiquinone radical from HQ or CT and phenoxy radical from phenol (on a metal surface).



Scheme 1.2 Gas-Phase Formation of CPD from Phenoxy Radical (adapted from reference 142)

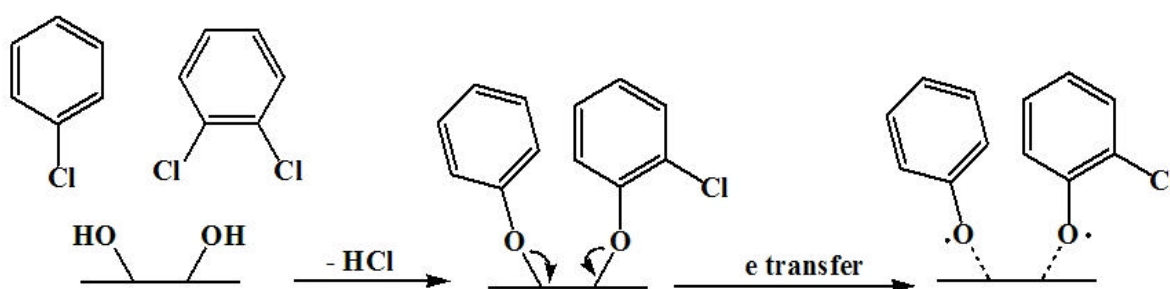
elimination and electron transfer^{152, 153} as shown in **scheme 1.4**. 2-MCP and 4-MCP can proceed to the formation of substituted chlorophenoxy radical either by water or hydrogen chloride elimination.

The mechanism of phenyl type radical formation either in gas phase or onto metal surface seems straightforward. However, cyclopentadienyl radical formation may be very complex because of the possibility of the existence of several routes leading to the radical. The simpler route, as depicted in **Scheme 1.2** is through phenoxy radical with elimination of carbon monoxide^{142-144, 150, 154, 155}.



Scheme 1.3: Semiquinone and Phenoxy Radicals Formation Respectively from HQ or CT and Phenol on a Metal Surface (adapted from 156).

CT and HQ thermally degrade to yield CPD as major product in given temperature domain¹². It has been shown that phenol is one of major products of CT pyrolysis¹⁵⁶, and an important reaction intermediate for catechol, hydroquinone and resorcinol^{157, 140}. It therefore can be suggested that the simplest route for CT or HQ thermal decomposition is through phenol formation that generates phenoxy radical which by elimination of carbon dioxide lead to CPD formation. See reference¹² for the scheme of the reaction. The presence of CPD radical in all



Scheme 1.4: Formation of Phenoxy Radical and Chlorinated Phenoxy Radical on a Metal Surface from Chlorinated Benzene (adapted from reference 156)

temperature domain of the Pyrolysis of CT and HQ suggests that some heterogeneous reactions with the wall are occurring which favour its formation even at low temperature¹².

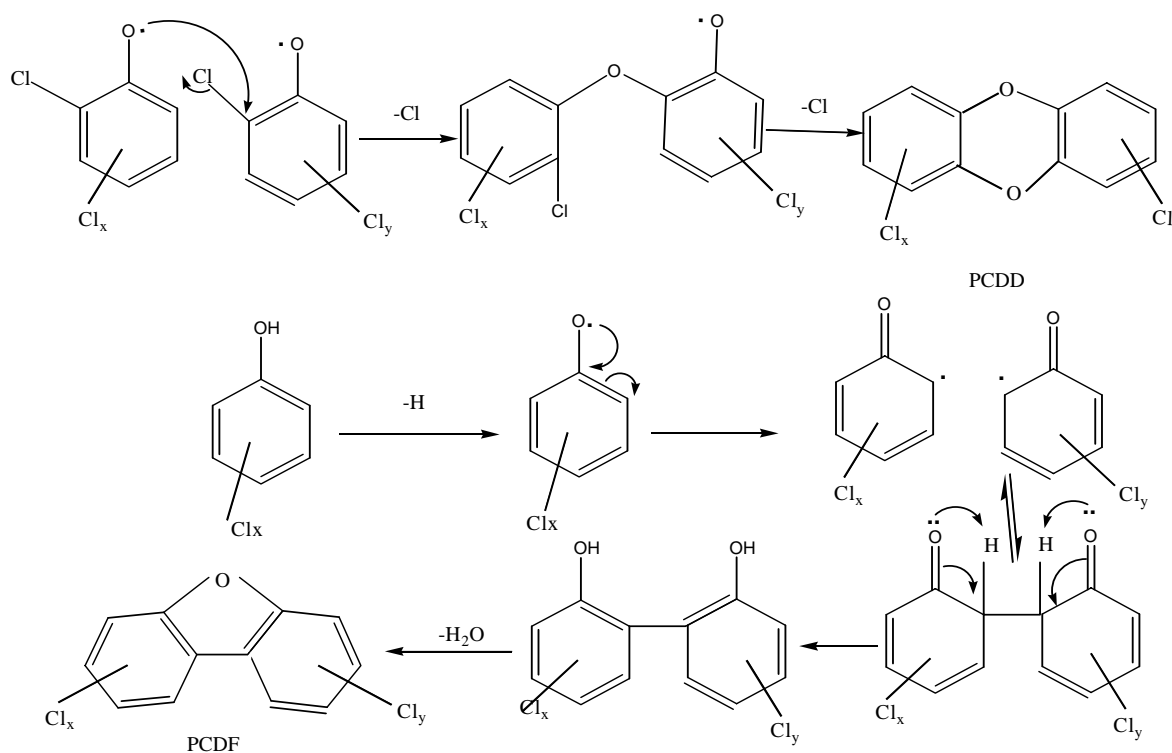
Radicals exhibit very short lifetime in the gas-phase or in solution^{158, 146, 147}; however, they can be stabilized and exist for a very long period of time when they associate with surface of some particulate matter that contain transition metals^{6, 7, 138, 139, 78}. Fine particles of fly ash are normally generated from combustion sources that contain transition metals and persistent radicals^{81, 82, 67}. The interaction between phenoxy-type radicals may result in the formation of hazardous pollutants such PCDD/F and PAHs.

1.6 Hazardous Pollutant Formation from Radicals

It has been demonstrated that free organic radicals are precursors to the formation of hazardous pollutants such as naphthalene, dioxins/furans and their congeners^{26, 159-161}. Even though only combustion products distribution analysis was the key element in implicating radicals in the formation of hazardous pollutants, those studies gave good understanding of the mechanisms of the formation of naphthalene and its derivatives, the dichlorodibenzo-dioxins and furans.

1.6.1 Formation of PCDD/Fs

PCDD/Fs are found as trace products from many combustion and other thermal processes;



Scheme 1.5 General mechanism of the formation of aPCDD/Fs from polychlorinated phenoxy

they are also found in fish, sediment, and soil ¹⁶². Extremely toxic, research focuses have been on PCDD/Fs for decades. The most toxic among PCDD/F is the 2,3,7,8-tetrachlorodibenzo-p-dioxin (TCDD). TCDD, even at ppb level, bio-accumulates in living tissues and causes birth defects, cancer, skin disorder, liver damage, and suppression of the immune system ¹⁶³. In combustion processes, radical-radical interaction of phenoxy and/or chlorophenoxy radicals is the main mechanism pathway to the formation of PCDD/Fs ^{159, 164-166}

1.6.2 Formation of Naphthalene, Hydroxynaphthalene, Dihydroxynaphthalene, 1H-Indenol and 1H-Indene

The formation of Naphthalene and its chlorinated congeners from combustion of phenol and chlorinated phenols has been reported in the literature ^{143, 155, 167-171}. In this radicals identification study, the atmospheric pyrolysis of phenol and chlorinated phenols, catechol and hydroquinone yielded, in addition to radicals identified by EPR, products that have been identified as naphthalene, hydroxynaphthalene, dihydroxynaphthalene, 1H-Indenol, and 1H-Indene by GC-MS ¹⁴

PAHs formation has been explained by the combination of the propargyl radical to give non radical species or radical species that subsequently undergo rearrangement to non-radical species ^{167, 172, 173}. In 1975, Naphthalene formation from phenol was first reported ¹⁷⁴. However, Naphthalene is thought to be formed from the condensation of two CPD radicals ¹⁷⁵, or the condensation of two molecules of Cyclopentadiene ¹⁵⁵. Scheme 1.6 depicts the naphthalene formation mechanism as in reference ¹⁷⁵

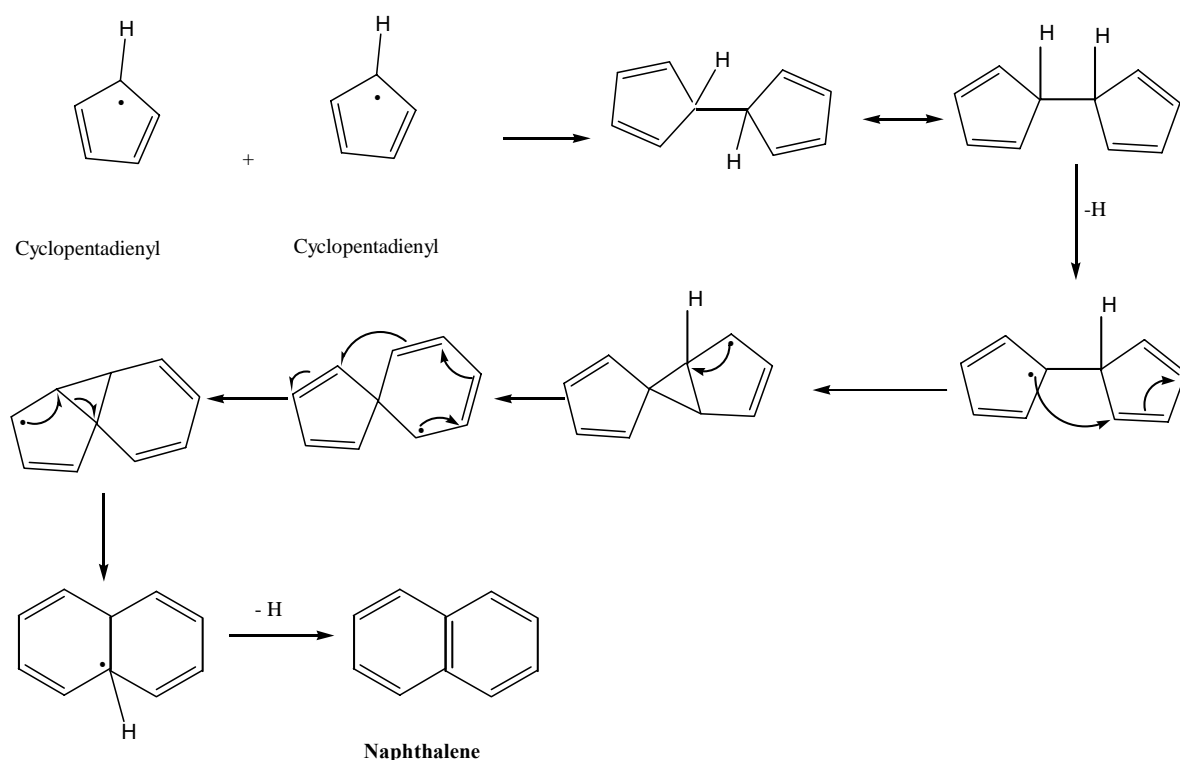
The formation of 1-Hydroxynaphthalene proceeds by the condensation of one molecule of CPD and one molecule of HydroxyCyclopentadienyl radical as proposed in reference ¹⁴. The formation of 1H-Indene, reported in the literature ^{176, 167, 14}, is thought to proceed in this study by carbon monoxide elimination from 1- Hydroxynaphthalene as depicted by **Scheme 1.7**

Likewise, the formation of Naphthalene diol-1-8 resulted from the condensation of two HydroxyCyclopentadienyl radicals. By elimination of CO, the 1H-Inden-7-ol is formed as shown in **Scheme 1.8**

1.7 Rationale for the Current Study

Over decades, intensive scrutiny of radical basically in medicine and biology has been achieved¹⁷⁷⁻¹⁷⁹. Radical formation has been investigated primarily in liquid-phase^{8, 180, 181}. Given that radicals are short live, spin trapping was used to stabilise them for study purposes¹⁸²⁻¹⁸⁴

Catechol, hydroquinone and phenols, being major components of cigarette smoke mainstream⁴⁶⁻⁵³, they supposedly form, during combustion processes, semiquinone type radicals whose deadly actions have been reported in the literature^{132, 134, 135, 121}



Scheme 1.6 Formation of naphthalene from CPD-CPD interaction pathway as predicted in reference 175

Semiquinone type radicals are organic radicals and supposed to be very unstable. It is somewhat surprising that they can be very stable to cause tissues damage. Therefore, it is of utmost importance that the exact nature of radicals formed during the gas-phase pyrolysis of catechol, hydroquinone, phenols and tobacco, their persistency and reason of their stability be investigated.

. To our knowledge, no such study is reported in the literature at the present time. We have therefore employed precursors that are more likely to generate the environmentally persistent and deadly free radicals. Catechol, hydroquinone and phenol are the primary precursors used in this study followed by compounds with structural similarity to the formers such as anisole, para-chlorophenol, ortho-chlorophenol, benzene, and chlorobenzene.

Radicals' identification has been rendered possible by employing compounds that can directly deliver specific radicals. We employed the tricarbonylcyclopentadienylmanganese (η^5 - $C_5H_5Mn(CO)_3$)¹⁸⁵ to generate pure CPD radical. The di-tert-butylperoxide¹⁸⁶⁻¹⁸⁸ at low temperature was used along with phenol to get pure phenoxy radical. Photolysis of the main precursors yielded semiquinone type radicals. Low pressure and atmospheric experiments were carried out alongside with GC-MS to characterize persistent free radicals

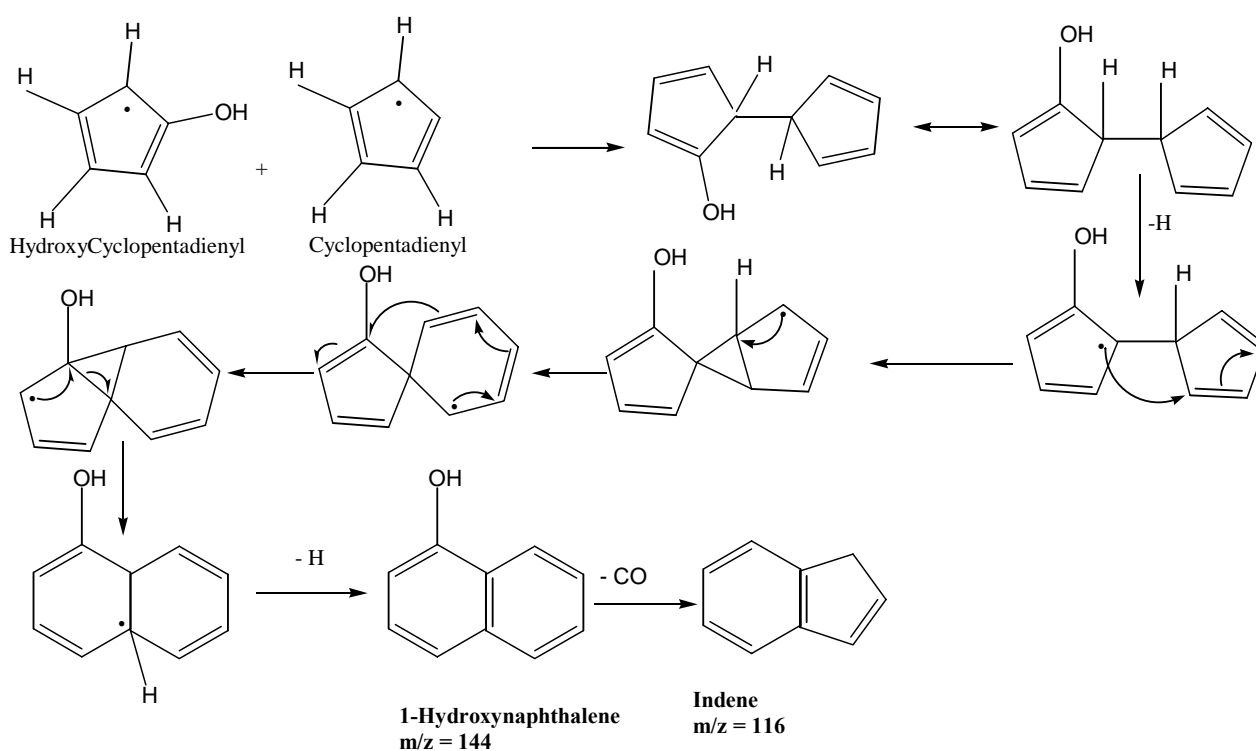
GC-MS analysis of pyrolysis products was useful in determining the very unstable radicals formed but whose spectra could not be acquired due to their low steady concentration corroborated by their strong reactivity. We have also had strong look on how the presence of traces of oxygen affected the radical nature. **Table 1.2** summarizes previous works that studied Persistent Free Radicals in various aqueous and solids media.

Table 1.2 EPR Spectral Characteristics of PFRs

| Radical | Media | T, °C | # of Lines | g .center | hfsc ^a (G) | ΔH p-p, (G) | ΔH_{Total} (G) | Ref. |
|------------------------------|------------------------------------|-------|-------------------------------|----------------------|-------------------------------|---------------------------|------------------------|------|
| p-SQ ^b | Methanol | -95 | 5 | 2.00468 ^c | 2.368 | | 15 | 189 |
| p-SQ | Methanol | -110 | 5 | 2.00468 ^c | 2.368 | | 21 | 189 |
| p-SQ | Methanol | -160 | Unres. singlet | 2.00468 ^c | 2.368 | | 25 | 189 |
| p-SQ | Dimethoxyethane | 22 | 5 | NA | NA | 0.45(single line) | 8.5 | 190 |
| p-SQ | Powder | -196 | singlet | NA | - | 5.55 | 25 | 190 |
| o-SQ | Liquid | room | 9 | | 3.68 0.76 | 0.15 (individual line) | 8 | 9 |
| o-SQ | Liquid ^d | room | singlet | NA | - | 5.2 | 27 | 191 |
| p-SQ anion | Ethanol | 19 | 5 | 2.00466 | 2.368 | | 9 | 192 |
| p-SQ protonated ^e | Ethanol | 19 | triple double-triplets | NA | 0.29 5.09 1.86 | | 13 | 192 |
| Phenoxy | CCl ₄ Photooxidation | 22 | multi lines | 2.00530 | 7.01 2.05 10.13 | | 27 | 193 |
| p-Cl Phenoxy | CCl ₄ Photooxidation | 22 | 14 | 2.00630 | 6.56, 1.99 | | 27 | 193 |
| Phenoxy | Phenol aqueous sol., radiolysis | room | multi lines | 2.00461 | 6.61(2), 1.85(2), 10.22 | | | 194 |
| Phenoxy/bulk ^f | Polyradical, in benzene | room | Poorly resolved singlet | 2.00450 | | | 13 | 195 |

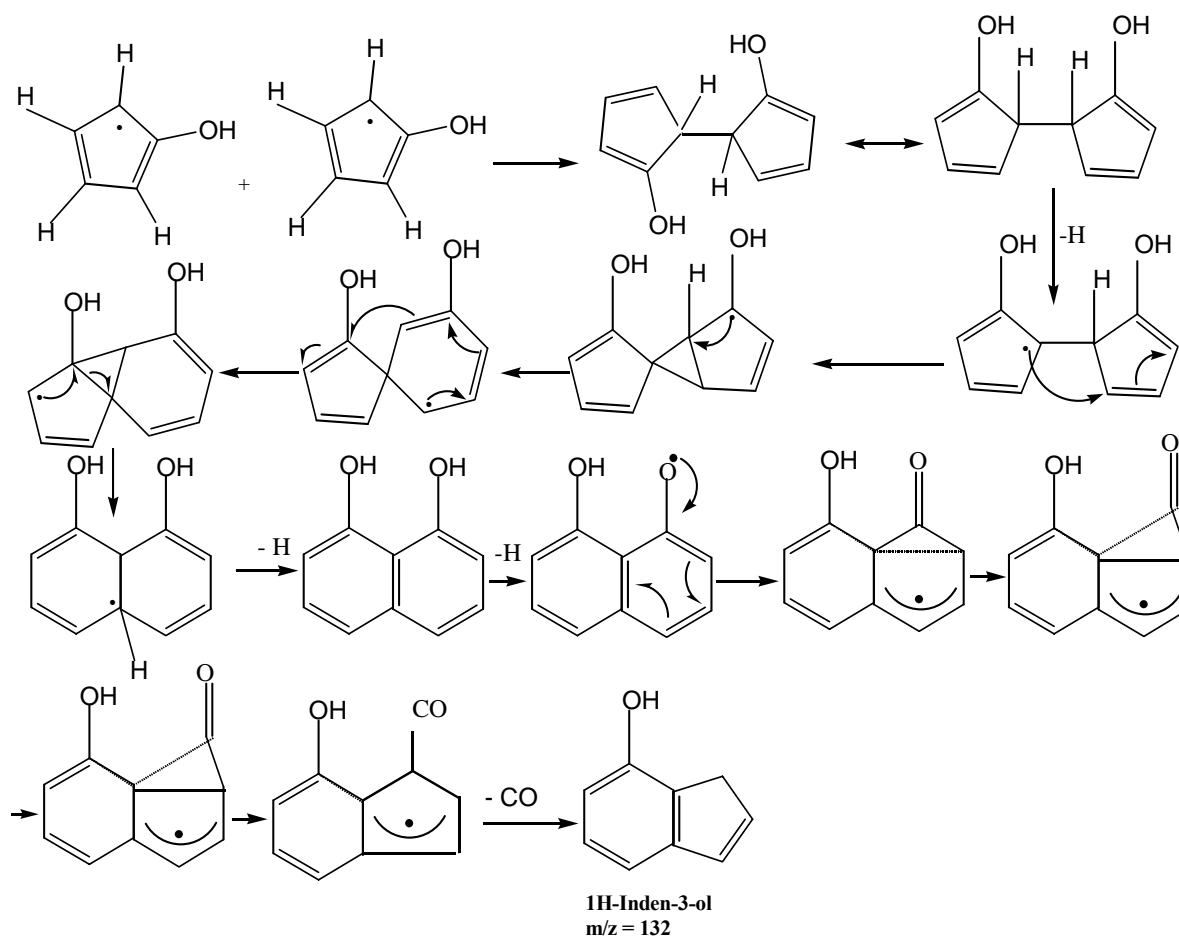
| | | | | | | | | |
|---------------------------------|-------------------------------|---------|---|----------------------|------|-----|------|----------------|
| CPD ^a | Toluene | -37 | 6 | NA | 6.05 | | 33 | ¹⁹⁶ |
| CPD | Solid matrix | -196 | 6 | NA | 5.6 | | 46 | ¹⁹⁷ |
| CPD | Crystal | 70-120K | 6 | 2.0044 | 6.2 | 3.5 | 31.3 | ¹⁹⁸ |
| CPD | Solid matrix, CO ₂ | -196 | 6 | 2.00508 ^b | 6.06 | | 44 | ¹² |
| Tyrosil radical in protein R2F | Frozen Solution | 15 K | 5 | 2.00517 | | | 52 | ¹⁹⁹ |
| Tyrosil radical in protein R2-2 | Frozen Solution | 10 K | 5 | 2.0053 | | | 48 | ²⁰⁰ |

^a hfsc- hyperfine splitting constant, ^b SQ – semiquinone, ^c measured at room temperature, NA - not available in the original source, ^d the protein derived radical by one-electron oxidation



Scheme 1.7 Proposed mechanism of the formation of 1-hydroxynaphthalene from the condensation of one molecule of CPD and one molecule of hydroxyCPD followed by the formation of 1H-indene by elimination of CO from the formed Hydroxynaphthalene.

of immobilized L- DOPA, $P^H = 7.4$, ϵ photolysis of p-benzoquinone solution in acidic solution of ethanol (mono protonated p-benzoquinone neutral radical, triple double-triplets), $h\nu$ values; 0.29 (3,5 ring proton), 5.09 (2,6 ring proton), 1,86 (hydroxyl proton), f poly(phenylenevinylene)-attached phenoxyl radicals, ferromagnetic interaction through planarized and π -conjugated skeletons, g cyclopentadienyl radical, h high value.



Scheme 1.8 Proposed mechanism of naphthalene diol¹⁻⁸ formation followed by 1H-inden-7-ol formation by elimination of CO
inhomogeneous broadening.

1.8 References

1. E. Roemer, Stabbert, R., Rustemeier, K., Veltel, D. J., Meisgen, T. J., Reininghaus, W., Carchman, R. A., Gaworski, C. L., Podraza, K. F., "Chemical composition, cytotoxicity and mutagenicity of smoke from US commercial and reference cigarettes smoked under sets of machine.," *Toxicology*, 195 (2004), 31-52.
2. W.S. Scholtzhauer, Martin, R. M., Snook, M. E., Williamson, R. E., "Pyrolytic studies on the contribution of tobacco leaf constituents to be formation of smoke catechols," *J. Agric. Food Chem.*, 30 (1982), 372-74.
3. S.G. Carmella, Hecht, S.S., Tso, T.C., Hoffman, D., "Roles of tobacco cellulose, sugars, and chlorogenic acid as precursors to catechol in cigarette smoke," *Journal of Agricultural and Food Chemistry*, 32 (1984), 267-73.
4. M.E. Counts, Morton, M.J., Laffoon, S.W., Cox, R.H., Lipowicz, P.J., "Smoke composition and predicting relationships for international commercial cigarettes smoked with three machine-smoking conditions," *Regulatory Toxicology and Pharmacology*, 41 (2005), 185–227.
- 5 .B. Dellinger, W.A. Pryor, R. Cueto, G.L. Squadrito and W.A. Deutsch, "The role of combustion-generated radicals in the toxicity of PM2.5," *Proceedings of the Combustion Institute*, 28 (2000), 2675-81.
- 6 .S. Lomnicki and B. Dellinger, "A Detailed Mechanism of The Surface-Mediated Formation of PCDD/F from the Oxidation of 2-Chlorophenol on CuO/ Silica Surface," *Journal of Physical Chemistry A*, 107 (2003), 4387-95.
- 7.B. Dellinger, S.Lomnicki; Khachatryan, L.; Maskos, Z.; Hall, R., W.; Adoukpe, J.;McFerrin, C.; Truong, H., "Formation and stabilization of persistent free radicals," *Proceedings of the Combustion Institute* 31 (2007), 521-28.
8. W.A. Pryor, Hales, B.J., Premovic, P.I., Church, D.F., "The radicals in cigarette tar: Their nature and suggested physiological implications," *Science*, 220 (1983), 425-27.
9. W.A. Pryor, Stone, K., Zang, L-Y., and Bermudez, E., "Fractionation of Aqueous Cigarette Tar Extracts: Fractions that Contain the Tar Radical Cause DNA Damage," *Chem.Res. Toxicol.*, 11 (1998), 441-48.
10. B. Dellinger, W.A. Pryor, R. Cueto, G.L. Squadrito, V. Hedge and W.A. Deutsch, "Role of free radicals in the toxicity of airborne fine particulate matter," *Chemical Research in Toxicology*, 14 (2001), 1371-77.
11. F.L. Berho, R., "The phenoxy radical: UV spectrum and kinetics of gasphase reactions with itself and with oxygen. ," *Chemical Physics Letters*, 279 (1997), 289-96.
12. L. Khachatryan, Adoukpe, J., Maskos, M., and Dellinger, B., "Formation of Cyclopentadienyl Radicals from the Gas-Phase Pyrolysis of Hydroquinone, Catechol, and Phenol," *Environ. Sci. Technol.*, 40, 5071-5076 (2006).

13. C.F. Melius, M.E. Colvin, N.M. Marinov, W.J. Pitz and S.M. Senkan, "Reaction mechanisms in aromatic hydrocarbon formation involving the C₅H₅ cyclopentadienyl moiety," *26th Symposium (International) on Combustion; The Combustion Institute: Pittsburgh, PA.*, 26 (1996), 685-92.
14. J. Adoukpe, L. Khachatryan, Dellinger B., "Radicals from the Gas-Phase Pyrolysis of Hydroquinone 1. Temperature dependence of the total radical yield.," *Fuels and Energy Submitted*, (2008).
15. W.A. Pryor, Prier, D.G., and Church, D.F., "ESR Study of mainstream and sidestream cigarette smoke:Nature of free radicals in gas-phase smoke and in cigarette tar.," *Environmental Health Perspectives*, 47 (1983), 345-55.
16. S.S.C. Hecht, S.; Mori, H.; Hoffmann, D., , "A Study of Tobacco Carcinogenesis .Role of Catechol as a Major Cocarcinogen in the Weakly Acidic Fraction of Smoke Condensate. ," *Journal of the National Cancer Institute* 66 (1981), 163-69.
17. U.S. EPA, "National Emission Trends (NET) database; Emission Faactor & Inventory Group:," *Research Triangle Park, NC, 2000*, (2000).
18. P.M.C. Fine, G. R.; Simoneit, B. R. T., "Chemical characterization of fine particle emissions from fireplace combustion of woods grown in the northeastern United States," *Environmental Science & Technology* 35 (2001), 2665-75.
19. P.M.C. Fine, G. R.; Simoneit, B. R. T., "Chemical characterization of fine particle emissions from the fireplace combustion of woods grown in the southern United States," *Environmental Science & Technology* 2002, 36, (7), 1442-1451., 36 (2002), 1442-51.
20. U.S. EPA, "Compilation of Air Pollutant Emission Factors: Stationary Point and Aera Sources," *5th ed. AP-42; Office of Air Quality Planning and Standards, Research Triangle Park, NC, 1* (1996).
21. V.H. Thomas and T.G. Spiro, "The U.S dioxin inventory: are there missing sources?," *Environmental Science and Technology*, 30 (1996), 82-85.
22. L.P. Brzuzy and R.A. Hites, "Global mass balance for polychlorinated dibenzo-p-dioxins and dibenzofurans," *Environmental Science and Technology*, 30 (1996), 1797-804.
23. H. Fiedler, "Thermal formation of PCDD/PCDF: a survey," *Environ.Eng.Sci.*, 15 (1998), 49-58.
24. B. Dellinger, P.H. Taylor, D.A. Tirey and C.C. Lee, "Pathways of formation of chlorinated PICs [products of incomplete combustion] from the thermal degradation of simple chlorinated hydrocarbons," *Journal of Hazardous Materials*, 22 (1989), 175-85.
25. S. Sidhu, N. Kasti, P. Edwards and B. Dellinger, "Hazardous air pollutants formation from reactions of raw meal organics in cement kilns," *Chemosphere*, 42 (2001), 499-506.

26. C.E. Evans, and Dellinger, B., "Mechanisms of Dioxin Formation from the High-Temperature Pyrolysis of 2-Chlorophenol," *Environ. Sci.&Technol.*, 37 (2003), 1325-30.
27. M. Kleeman, J.J. Schauer and G.R. Cass, "Size and Composition Distribution of Fine Particulate Matter Emitted from Motor Vehicles," *Environmental Science & Technology*, 34 (2000), 1132-42.
28. M.J.S. Kleeman, J.J.; Cass, G.R.;; "Size and Composition Distribution of Fine Particulate Matter Emitted from wood burning, meat carbroiling, and cigarettes" *Environmental Science and Technology*, 33 (1999), 3516-23.
29. R.E. Font, M.; Garcia, A. N., , "Toxic by-products from the combustion of Kraft lignin. Chemosphere 2003, 52, (6), 1047-1058," *Chemosphere*, 52 (2003), 1047-58.
30. B.R.T. Simoneit, Biomass burning - "A review of organic tracers for smoke from incomplete combustion. ," *Applied Geochemistry*, 17 (2002), 129-62.
31. M.D.F. Hays, P. M.; Geron, C. D.; Kleeman, M. J.; Gullett, B. K, "Open burning of agricultural biomass: Physical and chemical properties of particle-phase emissions. ." *Atmospheric Environment* 39 (2005), 6747-64.
32. A.E.L. Wroblewski, C.; Markuszewski, R.; Verkade, J. G., "P-31 Nmr Spectroscopic Analysis of Coal Pyrolysis Condensates and Extracts for Heteroatom Functionalities Possessing Labile Hydrogen. ," *Energy & Fuels* 2(1988), 765-74.
33. S.G.G. Gagarin, T. G., "Evaluation of the formation enthalpy of the organic matter of brown coals.," *Khimiya Tverdogo Topliva (Moscow, Russian Federation)*, 5 (2002), 11-21.
34. C.G.S. Nolte, J. J.; Cass, G. R.; Simoneit, B. R. T., "Highly polar organic compounds present in wood smoke and in the ambient atmosphere. ," *Environmental Science & Technology* 35 (2001), 1912-19.
35. G.E.M. Troughton, J. F.; Chow, S. Z., " Lignin utilization. II. Resin properties of 4-alkyl-substituted catechol compounds. ," *Forest Products Journal* 22 (1972), 108-10.
36. R.H. Visser, A. A. M.; Hovestad, A.; Stevens, T. W., "Identification of organic compounds in waste water of wood gasifiers with capillary gas chromatography," *Proc. Int. Symp. Capillary Chromatogr*, 6 (1985), 281-87.
37. P.M.C. Fine, G. R.; Simoneit, B. R. T., "Chemical characterization of fine particle emissions from the fireplace combustion of wood types grown in the Midwestern and Western United States," *Environmental Engineering Science* 21 (2004), 387-409.
38. S.S.K. Rayalu, P.; Rao, K. S. M. , "Chemical transformation of phenolics in coal carbonization wastewater. ," *Indian Journal of Environmental Protection* 12 (1992), 210-18.

39. A.K.D.S. Cho, E.; You, Y.; Rodriguez, C. E.; Schmitz, D. A.; Kumagai, Y.; and A.H.E.-F. Miguel, A.; Kobayashi, T.; Avol, E.; Froines, J. R., "Determination of four quinones in diesel exhaust particles, SRM 1649a, an atmospheric PM_{2.5}," *Aerosol Science and Technology* 38 (2004).
40. F. Britt, P.; Buchaanan III, A., C.; Thomas, B., K.; and Lee, S-K, "Pyrolysis mechanisms of lignin:surface-immobilized model compound investigation of acid-catalyzed and free-radical reaction pathways. ," *Journal of Analytical and Applied Pyrolysis*, 33 (1995), 1-19.
41. M.D.G. Hays, C. D.; Linna, K. J.; Smith, N. D.; Schauer, J. J., "Speciation of gas-phase and fine particle emissions from burning of foliar fuels " *Environmental Science & Technology*, 36 (2002), 2281-95.
42. C.D.P. Simpson, M.; Dills, R. L.; Liu, L. J. S.; Kalman, D. A., "Determination of methoxyphenols in ambient atmospheric particulate matter: Tracers for wood combustion " *Environmental Science & Technology* 39 (2005), 631-37.
43. J.J.K. Schauer, M. J.; Cass, G. R.; Simoneit, B. R. T., "Measurement of emissions from air pollution sources. 3. C-1-C-29 organic compounds from fireplace combustion of wood. ," *Environmental Science & Technology* 35 (2001), 1716-28.
44. S.B.K. Hawthorne, M. S.; Miller, D. J.; Mathiason, M. B., "Collection and Quantitation of Methoxylated Phenol Tracers for Atmospheric-Pollution from Residential Wood Stoves," *Environmental Science & Technology*, 23 (1989), 470-75.
45. W.F.H. Rogge, L. M.; Mazurek, M. A.; Cass, G. R.; Simoneit, B. R. T., "Sources of fine organic aerosol. 9. Pine, oak and synthetic log combustion in residential fireplaces. ," *Environmental Science & Technology* 32 (1998), 13-23.
46. J.M.L. McCue, K. L.; Eaton, S. S.; Freed, B. M., , "Exposure to cigarette tar inhibits ribonucleotide reductase and blocks lymphocyte proliferation. ," *Journal of Immunology* 165 (2000), 6771-75.
47. M.R.J. Lee, J. E.; Hsiang, W. S.; Hwang, B. H., "Determination of pyrolysis products of smoked methamphetamine mixed with tobacco by tandem mass spectrometry.," *Journal of Analytical Toxicology* 23 (1999), 41-45.
48. W.S.W. Schlotzhauer, D. B.; Snook, M. E.; Higman, H. C., "Characterization of Catechols, Resorcinols, and Hydroquinones in an Acidic Fraction of Cigarette-Smoke Condensate. ," *Journal of Agricultural and Food Chemistry* 26 (1978), 1277-88.
49. S.G.H. Carmella, S. S.; Tso, T. C.; Hoffmann, D., "Chemical Studies on Tobacco-Smoke .77. Roles of Tobacco Cellulose, Sugars, and Chlorogenic Acid as Precursors to Catechol in Cigarette-Smoke," *Journal of Agricultural and Food Chemistry*, 32 (1984), 267-73.
50. A.G.M. Kallianos, R. E.; Mold, J. D. , "Effect of nitrates in tobacco on the catechol yield in cigaret smoke. ," *Tobacco Science* 12 (1968), 125-29.

51. W.S.M. Schlotzhauer, R. M.; Snook, M. E.; Williamson, R. E. , "Pyrolytic Studies on the Contribution of Tobacco Leaf Constituents to the Formation of Smoke Catechols," *Journal of Agricultural and Food Chemistry* 30 (1982), 372-74.
52. P.D. Talbot, G.; Knoll, M.; Gomez, C., "Identification of cigarette smoke components that alter functioning of hamster (*Mesocricetus auratus*) oviducts in vitro," *Biology of Reproduction* 58 (1998), 1047-53.
53. K.R. Riveles, R.; Talbot, P., "Phenols, quinolines, indoles, benzene, and 2-cyclopenten-1-ones are oviductal toxicants in cigarette smoke," *Toxicological Sciences* 86 (2005), 141-51.
54. J.J.K. Schauer, M. J.; Cass, G. R.; Simoneit, B. R. T., "Measurement of emissions from air pollution sources. 5. C-1-C-32 organic compounds from gasolinepowered motor vehicles," *Environmental Science & Technology* 36 (2002), 1169-80.
55. A.F. Valavanidis, K.; Vlahogianni, T.; Papadimitriou, V.; Pantikaki, V., "Determination of selective quinones and quinoid radicals in airborne particulate matter and vehicular exhaust particles (vol 3, pg 118, 2006) " *Environmental Chemistry* 3 (2006), 233-U12.
56. C.A.R. Jakober, S. G.; Robert, M. A.; Destailats, H.; Charles, M. J.; Green, P. G.; Kleeman, M. J., , "Quinone Emissions from Gasoline and Diesel Motor Vehicles.," *Environmental Science & Technology* (2007), 41(13), 4548-4554. .
57. M.D. Avakian, B. Dellinger, H. Fiedler, B. Gullet, C. Koshland, S. Marklund, G. Oberdorster, S. Safe, A. Sarofim, K.R. Smith, D. Schwartz and W.A. Suk, "The origin, fate, and health effects of combustion by-products: A research framework," *Environmental Health Perspectives*, 110 (2002), 1155-62.
58. US-EPA, Regulatory impact analyses for the particulate matter and ozone national ambient air quality standards and proposed regional haze rule. ed. D. Washington (US Environmental Protection Agency; , 1997).
59. J.M.D. Samet, F. ; Curriero, F.C.;Coursac,I.; and Zeger, S.L., "Fine particulate air pollution and mortality in 20 US cities, 1987–1994, ," *N Engl J Med* 343 343 (2000), 1742-49.
60. D.W.P.I. Dockery, C.A.; Xu, X.;Spengler, J.D.; Ware, J.H.; and Fay , M.A. , "An association between air pollution and mortality in six US cities," *N Engl J Med* 329 (1993), 1753-59.
61. K.T. Katsouyanni, G.; Samoli, E.; Gryparis, A; Le Tertre, A.; and Monopolis Y. , "Confounding and effect modification in the short-term effects of ambient particles on total mortality: results from 29 European cities within the APHEA2 project, ," *Epidemiology* 12 (2001), 521-31.
62. C.A. Pope III, R.T. Burnett, M.J. Thun, E.E. Calle, D. Krewski, K. Ito and G.D. Thurston, "Lung Cancer, Cardiopulmonary Mortality, and Long-term Exposure to Fine Particulate Air Pollution," *JAMA*, 287 (2002), 1132-41.
63. J. Kaiser, "Evidence mounts that tiny particles can kill " *Science*, 289 (2000), 422-23.

64. J. Schwartz, "Assessing confounding, effect modification, and thresholds in the association between ambient particles and daily deaths," *Environ Health Perspect* 108 (2000), 563-68.
65. J. Kaiser, "Showdown over clean air science, ," *Science* 277 (1997), 466-69.
66. S.A.L. Cormier, S.; Backes, W.; Dellinger, B. , "Origin and health impacts of emissions of toxic by-products and fine particles from combustion and thermal treatment of hazardous wastes and materials," *Environmental Health Perspectives*, 144 (2006), 810-17.
67. C.D.R. Okeson, M. R.; Fernandez, A.; Wendt, J. O. L. , "Impact of the composition of combustion generated fine particles on epithelial cell toxicity: influences of metals on metabolism," *Chemosphere* 51 (2003), 1121-28.
68. Y.Z.S. Chen, N.; Huggins, F. E.; Huffman, G. P., , "Investigation of the microcharacteristics of PM_{2.5} in residual oil fly ash by analytical transmission electron microscopy," *Environmental Science & Technology* 38 (2004,), 6553-60.
69. W.P.M. Linak, C. A., , "Comparison of particle size distributions and elemental partitioning from the combustion of pulverized coal and residual fuel oil. ," *Journal of the Air & Waste Management Association* . 50 (2000), 1532-44.
70. A.V. Nemmar, H.; Hoylaerts, M. F.; Hoet, P. H. M.; Verbruggen, A.; Nemery, B. , " Passage of intratracheally instilled ultrafine particles from the lung into the systemic circulation in hamster. ," *American Journal of Respiratory and Critical Care Medicine* 164 (2001), 1665-68.
71. L.M.-T. Calderon-Garciduenas, A.; Fordham, L. A.; Chung, C. J.; R.O. Garcia, N.; Hernandez, J.; Acuna, H.; Gambling, T. M.; Villarreal-Calderon, A.; and J.K. Carson, H. S.; Devlin, B. , "Canines as sentinel species for assessing chronic exposures to air pollutants: Part 1. Respiratory pathology.," *Toxicological Sciences* 61 (2001), 342-55.
72. L.G. Calderon-Garciduenas, T. M.; Acuna, H.; Garcia, R.; Osnaya, N.; and S.V.-C. Monroy, A.; Carson, J.; Koren, H. S.; Devlin, R. B., "Canines as sentinel species for assessing chronic exposures to air pollutants: Part 2. cardiac pathology ." *Toxicological Sciences*, 61 (2001), 356-67.
73. J.D.G. Carter, A. J.; Samet, J. M.; Devlin, R. B., " Cytokine production by human airway epithelial cells after exposure to an air pollution particle is metal-dependent.," *Toxicology and Applied Pharmacology* 146 (1997), 180-88.
74. M.S. Boezen, J.; Rijcken, B.; Vonk, J.; Gerritsen, J.; van der Zee, S.; Hoek, G.; Brunekreef, B.; Postma, D., "Peak expiratory flow variability, bronchial responsiveness, and susceptibility to ambient air pollution in adults. ," *American Journal of Respiratory and Critical Care Medicine* 158 (1998), 1848-54.
75. J. Schwartz, "What Are People Dying of on High Air-Pollution Days. ," *Environmental Research* 64 (1994.), 26-35.

76. U.P.M. Kodavanti, C. F.; Ledbetter, A. D.; Schladweiler, M. C.; Costa, D. L.; and R.C. Hauser, D. C.; Nyska, A., " Inhaled environmental combustion particles cause myocardial injury in the Wistar Kyoto rat. ," *Toxicological Sciences* . 71 (2003), 237-45.
77. T.N. Gordon, C.; Schlesinger, R.; Chen, L. C., "Pulmonary and cardiovascular effects of acute exposure to concentrated ambient particulate matter in rats. ," *Toxicology Letters* 96 (1998), 285-88
- 78.B. Dellinger, W. A.Pryor; Cueto, R.; Squadrito, G. L.; Hedge,V.; Deutsch, W. A. 2001, 14, 1371-1377., "Role of free radicals in the toxicity of airborne fine particulate matter.," *Chem. Res. Toxicol.*, 14 (2001), 1371-77.
79. Z.a.Z. Meng, Q., "Oxidative damage of dust storm fine particles instillation on lungs, hearts and livers of rats " *Environmental Toxicology and Pharmacology* 22 (2006), 277-82.
80. K.B. Donaldson, D. M.; Mitchell,C.; Dineva, M.; Beswick, P.; Gilmour,P.; MacNee, W., "Free Radical Activity of PM10: Iron-mediated Generation of Hydroxyl Radicals," *Environ Health Perspect*, 105 (1997), 1285-89.
81. G.P.H. Huffman, F. E.; Shah, N.; Huggins, R.; Linak, W. P.; Miller, C. A.; and R.J.M. Pugmire, H. L. C.; Seehra, M. S.; Manivannan, A., " Characterization of fine particulate matter produced by combustion of residual fuel oil. ," *Journal of the Air & Waste Management Association* . 50 (2000), 1106-14.
82. L.G. Yan, R. P.; Wall, T. F., , "The implication of mineral coalescence behaviour on ash formation and ash deposition during pulverised coal combustion. ," *Fuel* 80 (2001), 1333-40.
83. Y.Z.S. Chen, N.; Huggins, F. E.; Huffman, G. P.,, "Transmission electron microscopy investigation of ultrafine coal fly ash particles. ," *Environmental Science & Technology* 39 (2005), 1144-51.
84. S.U. Amlathe, S.; Gupta, V. K. , "Spectrophotometric Determination of Trace Amounts of Phenol in Waste-Water and Biological-Fluids," *Analyst*, 112 (1987), 1463-65.
85. A.J.L. Shariff, R. W.; Berthiaume, D.; Bryce, J. R. G.; Mclean, R. A. N., "Unexpected Source of Phenol in the Sulfur-Free Semichemical Pulping of Hardwood. ," *Tappi Journal* 72 (1989), 177-83.
86. J.B.R. Luten, J. M.; Weseman, J. M., " Determination of Phenol, Guaiacol and 4-Methylguaiacol in Wood Smoke and Smoked Fish-Products by Gas-Liquid-Chromatography," *Zeitschrift Fur Lebensmittel-Untersuchung Und-Forschung* 168 (1979), 289-92.
87. J.D. Michalowicz, R. O. W., "Analysis of chlorophenols, chlorocatechols, chlorinated methoxyphenols and monoterpenes in communal sewage of Lodz and in the Ner River in 1999-2000. ," *Water Air and Soil Pollution* 2005, 164, (1-4), 205-222., 164 (2005), 205-22.
88. O. Hogl, "Some nonvolatile extracts of coffee. Mitteilungen aus dem Gebiete der " *Lebensmitteluntersuchung und Hygiene* 49 (1958), 433-41.

89. J. Varagnat, " Hydroquinone, resorcinol, and catechol. ," *Kirk-Othmer Encycl. Chem.Technol.*, , 3rd Ed. (1981), 39-69.
90. W.B.K. Deichmann, M. L., " Industrial toxicology. Phenols and phenolic compounds. ," *Patty's Ind. Hyg. Toxicol.* , 3rd Revis. Ed (1981), 2567-627.
91. M.E.M. Hogan, G. D., "Allelopathy of Small Everlasting (Antennaria-Microphylla) Phytotoxicity to Leafy Spurge (Euphorbia-Esula) in Tissue-Culture. ," *Journal of Chemical Ecology* 16 (1990), 931-39.
92. M.E.M. Hogan, G. D., "Differential Allelochemical Detoxification Mechanism in Tissue-Cultures of Antennaria-Microphylla and Euphorbia-Esula," *Journal of Chemical Ecology* 17 (1991), 167-74.
93. T.J. Eisner, T. H.; Hicks, K.; Silberglied, R. E.; Meinwald, J., "Defense-Mechanisms of Arthropods .53. Quinones and Phenols in Defensive Secretions of Neotropical Opilionids. ," *Journal of Chemical Ecology* 3(1977), 321-29.
94. J.J. Meinwald, T. H.; Eisner, T.; Hicks, K., , "Defense-Mechanisms of Arthropods .56. New Methylcyclopentanoid Terpenes from Larval Defensive Secretion of a Chrysomelid Beetle (Plagioderia-Versicolora). ," *Proceedings of the National Academy of Sciences of the United States of America* 74 (1977), 2189-93.
95. A.T.W. Hodgson, J. D. , *Assessment of indoor concentrations, indoor sources and source emissions of selected volatile organic compounds* (Yorktown Heights: IBM, 1991), Pages.
96. C.T.W. Jung, R. R.; Desai, P. B.; Bronaugh, R. L. , " In vitro and in vivo percutaneous absorption of catechol. ," *Food and Chemical Toxicology* 41 (2003), 885-95.
97. A. Meybeck, "Pharmaceuticals or cosmetics containing hydroquinone - kojic acid mixtures encapsulated in liposomes or in lamellar lipid phases. ," *88-FR295, 8809659,19880610.* (1988).
98. J.C. Loblaw, "High contrast photographic elements exhibiting reduced stresssensitivity," *86-109090, 209010, 19860703.*, (1987).
99. K.N. Yamane, T. , "Support for photography. ," *95-111745, 08304961, 19950510.*, (1996).
100. H.W. Yurow, "Photographic developer for direct production of equal density images on a high contrast film. ," *99-356536,6083671, 19990719.*,, (2000).
101. H.A.C. Mattill, B., , "Autoxidation of corn oil as related to its unsaponifiable constituents.," *Industrial and Engineering Chemistry* 22 (1990), 341-44.
102. Y.T. Nakamura, K.; Ohigashi, H., , "A catechol antioxidant protocatechuic acid potentiates inflammatory leukocyte-derived oxidative stress in mouse skin via a tyrosinase bioactivation pathway. ," *Free Radical in Biology and Medicine* 30 (2001), 967-78.

103. G.C.C. Justino, C. F.; Mira, L.; Dos Santos, R. M. B.; Simoes, J. A. M.; Silva, A. M.; Santos, C.; Gigante, B., " Antioxidant activity of a catechol derived from abietic acid. ," *Journal of Agricultural and Food Chemistry* 2006, 54, (2), 342-348., 54 (2006), 342-48.
104. R.M.S. Bruce, J.; Neal, M. W., "Summary Review of the Health-Effects Associated with Phenol. ," *Toxicology and Industrial Health* 3(1987), 535-68.
105. C.W. Flickinger, "Benzenediols - Catechol, Resorcinol and Hydroquinone - Review of Industrial Toxicology and Current Industrial Exposure Limits. ," *American Industrial Hygiene Association Journal* 37 (1976), 596-606.
106. P.T. Leanderson, C., , "Cigarette Smoke-Induced DNA-Damage - Role of Hydroquinone and Catechol in the Formation of the Oxidative DNA-Adduct, 8-Hydroxydeoxyguanosine. ." *Chemico-Biological Interactions* 1990, 75 (1990), 71-81.
107. M.H. Bilimoria, "Detection of Mutagenic Activity of Chemicals and Tobacco-Smoke in a Bacterial System," *Mutation Research*, 31 (1975), 328-38.
108. P.T. Leanderson, C., , "Cigarette Smoke-Induced DNA Damage in Cultured Human Lung-Cells - Role of Hydroxyl Radicals and Endonuclease Activation. ," *Chemico-Biological Interactions* 81 (1992), 197-208.
109. D.I. Wierda, R. D., , "Hydroquinone and Catechol Reduce the Frequency of Progenitor Lymphocytes-B in Mouse Spleen and Bone-Marrow. ," *Immunopharmacology* 4(1982), 41-54.
110. K.W.W. Gaido, D., , "Suppression of Bone-Marrow Stromal Cell-Function by Benzene and Hydroquinone Is Ameliorated by Indomethacin. ," *Toxicology and Applied Pharmacology* 89 (1987), 378-90.
111. A.G.L. King, K. S.; Wierda, D., , "Hydroquinone Inhibits Bone-Marrow Pre-B Cell Maturation Invitro.," *Molecular Pharmacology* 32 (1987), 807-12.
112. J.M.M. Daisey, K. R. R.; Hodgson, A. T., "Toxic volatile organic compounds in simulated environmental tobacco smoke: Emission factors for exposure assessment. ," *Journal of Exposure Analysis and Environmental Epidemiology* 8(1998), 313-34.
113. E.M. Adams, The toxicity of phenol. (Biochemical Research Laboratory, Dow Chemical Company, 1944).
114. E.S. Berman, M.; Moser, V. C.; MacPhail, R.C., " A multidisciplinary approach to toxicological screening: I. Systemic toxicity. ," *J Toxicol Environ Health* 45 (1995), 127-43.
115. N.N.C. Institute), Bioassay of phenol for possible carcinogenicity ed. U.S.D.o.H.a.H. Services (Carcinogenesis Testing Program, National Cancer Institute/National Toxicology Program, 1980).
116. A.R. Laboratories., Oral (gavage) developmental toxicity study of phenol in rats. (Horsham, PA. 1997), Protocol number: 916-011.

117. M.A.H. Warner, J. V., , "Cardiac Dysrhythmias Associated with Chemical Peeling with Phenol. ." *Anesthesiology* 62 (1985), 366-67.
118. D. McGregor, " Hydroquinone: an evaluation of the human risks from its carcinogenic and mutagenic properties. ," *Crit Rev Toxicol.* , 37 (2007), 887-914.
119. J.M.L. McCue, S.; Cohen, J. J.; Modiano, J. F.; Freed, B. M., "Hydroquinone and catechol interfere with T cell cycle entry and progression through the G(1) phase.," *Molecular Immunology* 39 (2003), 995-1001.
120. Q.A. Li, M. T.; Christian, T.; Freed, B. M., , "Differential inhibition of DNA synthesis in human T cells by the cigarette tar components hydroquinone and catechol." *Fundamental and Applied Toxicology* 38 (1997), 158-65.
121. G.L. Squadrito, B. Dellinger, R. Cueto, W.A. Deutsch and W.A. Pryor, "Quinoid Redox Cycling as a Mechanism for Sustained Free Radical Generation by Inhaled Airborne Particulate matter," *Free Radical Biology & Medicine*, 31 (2001), 1132-38.
122. K. Hirakawa, Oikawa, S., Hiraku, Y., Hirosawa, I., and Kawanishi, S., "Catechol and hydroquinone have different redox properties responsible for their differential DNA-damaging ability," *Chem.Res. Toxicol.*, 15 (2002), 76-82.
123. B. Dellinger, W.A. Pryor, R. Cueto, G.L. Squadrito and W.A. Deutsch, The role of combustion-generated radicals in the toxicity of PM2.5 In *Proceedings of the 28th International Symposium on Combustion*, (2000).
124. Z. Maskos, Khachatryan, L., and Dellinger, B, "Precursors of radicals in tobacco smoke and the role of particulate matter in forming and stabilizing radicals," *Energy & Fuels*, 19 (2005), 2466-73.
125. R.C. Gopalakrishna, Z. H.; Gundimeda, U., , "Tobacco-Smoke Tumor Promoters, Catechol and Hydroquinone, Induce Oxidative Regulation of Protein-Kinase-C and Influence Invasion and Metastasis of Lung-Carcinoma Cells. ," *Proceedings of the National Academy of Sciences of the United States of America* 91 (1994), 12233-37.
126. J.P.M. Marsh, B. T., , "Role of Asbestos and Active Oxygen Species in Activation and Expression of Ornithine Decarboxylase in Hamster Tracheal Epithelial-Cells.," *Cancer Research* 51 (1991), 167-73.
127. T.W.T. Kensler, M. A., , "Role of Oxygen Radicals in Tumor Promotion.," *Environmental Mutagenesis* 6(1984), 593-616.
128. P.A. Cerutti, "Prooxidant States and Tumor Promotion. ," *Science* 227 (1985), 375-81.
129. S.M. Asami, H.; Miyake, J.; Tsurudome, Y.; Hirano, T.; Yamaguchi, R.; Itoh, and H. H.; Kasai, "Cigarette smoking induces an increase in oxidative DNA damage, 8-hydroxydeoxyguanosine, in a central site of the human lung. ," *Carcinogenesis* 18 (1997), 1763-66.

130. S.S.W. Leonard, S. W.; Shi, X. L.; Jordan, B. S.; Castranova, V.; Dubick, M. and A., "Wood smoke particles generate free radicals and cause lipid peroxidation, DNA damage, NF kappa B activation and TNF-alpha release in macrophages. ," *Toxicology* 150 (2000), 147-157.
131. C.F. Rota, Y, C.; Mason, P. R., "Phenoxy Free Radical Formation during the Oxidation of the Fluorescent Dye 2',7'-Dichlorofluorescein by Horseradish Peroxidase Possible Consequences for Oxidative Stress Measurements. ," *Journ. of Biol Chem.* , 274 (1999), 28161-68.
132. S.T. Carr, Perfetti; Michael, Morton ; Alan, Rodgman ; Rajni, Garg; Cynthia, Selassie; Corwin, Hansch; Gray, Bowman Gray "The relative toxicity of substituted phenols reported in cigarette mainstream smoke," *Toxicological sciences*, 69 (2002), 265-78.
133. T.G.H. Gantchev, Darel J. , "Enhancement of etoposide (VP-16) cytotoxicity by enzymic and photodynamically induced oxidative stress," *Anti Cancer Drugs*, 8 (1997), 164-73.
134. J.S. Dai, Amy L.; Wright, Marcus W.; Manderville, Richard A. , "Role of Phenoxy Radicals in DNA Adduction by Chlorophenol Xenobiotics Following Peroxidase Activation," *Chemical Research in Toxicology* 18 (2005), 771-79.
135. J.W. Dai, Marcus W.; Manderville, Richard A. , "An Oxygen-Bonded C8-Deoxyguanosine Nucleoside Adduct of Pentachlorophenol by Peroxidase Activation: Evidence for Ambident C8 Reactivity by Phenoxy Radicals," *Chemical Research in Toxicology* 16 (2003), 817-21.
136. D.A.G. Stoyanovsky, Radoslav; Claycamp, H. Gregg; Kagan, Valerian E. , "Phenoxy radical-induced thiol-dependent generation of reactive oxygen species: implications for benzene toxicity," *Archives of Biochemistry and Biophysics* 317 (1995), 315-23.
137. B. Dellinger, W. A.; Cueto, R.; Squadrito, G.; Deutsch, W. A. Pryor, "The role of combustion-generated radicals in the toxicity of PM2.5. ," *Proceedings of the Combustion Institute* 28 (2000), 2675-81.
138. M.A.B. Rodrigues, M. P.; Tada, D. B.; Bastos, E. L.; Baptista, M. S.; Politi, M. J. , "Synthesis and characterization of silica gel particles functionalized with bioactive materials. ." *Adsorption* 11 (2005), 595-602.
139. L.J. Hurrell, L. J.; Mathivanan, N.; Vong, D., "Photochemistry of Lignin Model Compounds on Solid Supports," *Canadian Journal of Chemistry-Revue Canadienne De Chimie* 71 (1993), 1340-48.
140. E.B. Ledesma, Marsh, N.D., Sandrowitz, A.K., and Wornat, M.J, "An Experimental Study on the Thermal Decomposition of Catechol," *Proc. Combust. Inst.*, 29 (2002), 2299-306.
141. S.L. Alderman, Farquar, G.R., Poliakoff, E.D., Dellinger, B., "FTIR Investigation of 2-chlorophenol Chemisorption on Cu(II)O/SiO₂," *Environ. Sci. Technol.*, 37 (2003), 935.
142. C.Y.L. Lin, M. C. , "Unimolecular Decomposition of the Phenoxy Radical in Shock-Waves.," *International Journal of Chemical Kinetics* 17 (1985), 1025-28.

143. K. Brezinsky, Pecullan, M., Glassman, I., "Pyrolysis and oxidation of phenol," *Journal of Physical Chemistry A*, 102 (1998), 8614-19.
144. S. Cooke, and Lares, M.M., "Destruction of environmentally hazardous monochlorinated phenols via pyrolysis in an inert atmosphere," *Carbon*, 32 (1994), 1055-58.
145. G.J. Black, L. E., " Radiative Lifetimes of the $V'3 = 0, 1, \text{ and } 2$ Levels of Ch3s(A2a1) . ," *Journal of Chemical Physics* 85 (1986), 5379-80.
146. D.E.S. Falvey, G. B., "Picosecond Time Scale Dynamics of Perester Photodecomposition - Evidence for an Acyloxy Radical Intermediate in the Photolysis of Tert-Butyl 9-Methylfluorene-9-Pericarboxylate. ," *Journal of the American Chemical Society*" 108 (1986), 7419-20.
147. T.T. Okamura, I., "Radiative Lifetimes of Benzyl, Deuterated Benzyl, and Methyl-Substituted Benzyl Radicals. ," *Journal of Physical Chemistry* 79 (1975), 2728-31.
148. R.R. Mohapatra, J. R., . , "Some aspects of characterisation, utilisation and environmental effects of fly ash," *Journal of Chemical Technology and Biotechnology* 76 (2001), 9-26.
149. B. Dellinger, S. Lomnicki, L. Khachatryan, Z. Maskos, R. Hall, J. Adoukpe, McFerrin. C. and H. Truong, "Formation and stabilization of persistent free radicals " *ScienceDirect, Proceedings of the Combustion Institute*, 31 (2007), 521-28.
150. A.B. Lovell, Brezinsky, K., and Glassman, I., "The gas phase pyrolysis of phenol," *Int.J.Chem.Kin.*, 21 (1989), 547-60.
151. G.R. Farquar, Alderman, S. L., Poliakoff, E. D., Dellinger, B., "X-Ray Spectroscopic studies of the high temperature reduction of Cu(II)O by 2-Chlorophenol on a simulated fly ash surface," *Environ. Sci. Technol.*, 37 (2003), 931-35.
152. B. Dellinger, Lomnicki, S., Khachatryan, L., Maskos, Z., Hall R., Adoukpe, J., McFerrin. C., Truong, H., "Formation and stabilization of persistent free radicals," *31st Intern. Symp. on Combustion, University of Heidelberg, Germany, Abstracts* (2006), 88.
153. G. Farquar, Alderman, S., Poliakoff, E., Dellinger, B., "X-Ray spectroscopic studies of the high-temperature reduction of Cu(II)O by 2-chlorophenol on a simulation fly-ash surface.," *Environmental Science and Technology*, (2003), 931-35.
154. R. Cypres, Bettens, B., "Mecanismes de fragmentation pyrolitique du phenol et des cresols," *Tetrahedron*, 30 (1974), 1253 -60.
155. J.A. Manion, and Louw, R., "Rates, products, and mechanisms in the gas-phase hydrogenolysis of phenol between 922 and 1175 K," *J.Phys. Chem.*, 93 (1989), 3563-74.
156. H. Truong, S. Lomicki; Dellinger, B., "Mechanism of Product Formation from the Pyrolysis of Hydroquinone," *Environmental Science and Technology*, Submitted (2006).

157. T. Sakai, and Hattori, M., "Thermal Decomposition of Catechol, Hydroquinone and Resorsinol.," *Chemistry Letters*, (1976), 1153-56.
158. G.J. Black, L. E., " Radiative Lifetimes of the $V'3 = 0, 1,$ and 2 Levels of $Ch3s(A2a1).$," *Journal of Chemical Physics* 85 (1986), 5379.
159. J.G.P. Born, R. Louw and P. Mulder, "Formation of dibenzodioxins and dibenzofurans in homogenous gas-phase reactions of phenols," *Chemosphere*, 19 (1989), 401-06.
160. L. Khachatryan, Asatryan R., Dellinger B., "Development of an expanded and core kinetic model for the gas phase formation of dioxins from chlorinated phenols.," *Chemosphere*, 52 (2003), 695-708.
161. R. Louw and S.I. Ahonkhai, "Radical/radical vs radical/molecule reactions in the formation of PCDD/Fs from (chloro)phenols in incinerators," *Chemosphere*, 46 (2002), 1273-78.
162. S. Safe and O. Hutzinger, "PCDDs and PCDFs: sources and environmental impact," *Environ.Toxin Ser.*, 3 (1990), 1-20.
163. E.K.M. Silbergeld, D. R., " Experimental and Clinical-Studies on the Reproductive Toxicology of 2,3,7,8-Tetrachlorodibenzo-P-Dioxin. ," *American Journal of Industrial Medicine* 11 (1987), 131-44.
164. S.S. Sidhu, L. Maqsd, B. Dellinger and G. Mascolo, "The homogeneous, gas-phase formation of chlorinated and brominated dibenzo-p-dioxin from 2,4,6-trichloro- and 2,4,6-tribromophenols," *Combustion and Flame*, 100 (1995), 11-20.
165. R. Weber and H. Hagenmaier, "Mechanisms of the Formation of Polychlorinated Dibenzo-p-dioxins and dibenzofurans from Chlorophenols in Gas Phase Reactions," *Chemosphere*, 38 (1999), 529-49.
166. I.L. Wiater-Protas, R., "Gas-phase chemistry of chlorinated phenols - Formation of dibenzofurans and dibenzodioxins in slow combustion.," *European Journal of Organic Chemistry* 20 (2001), 3945-52.
167. A.M. Herring, J.T. Kinnon, D.E. Petrick, K.W. Gneshin, J.a. Filley and B.D. McCloskey, "Detection of reactive intermediates during laser pyrolysis of cellulose char by molecular beam mass-spectrometry, implication for the formation of polycyclic aromatic hydrocabons," *J. Anal. Appl. Pyrolysis*, 66 (2003), 165-82.
168. D.H.M. Kim, J. A.; Ryu,J-Y, "Gas-phase Polychlorinated Naphthalene formation from chlorophenols," *Organohalogen Comounds*, 66 (2004), 1043-49.
169. L. Khachatryan, Asatryan, R., Dellinger, B., "An Elementary Reaction Kinetic Model of The Gas-Phase Formation of Polychlorinated Dibenzofurans from Chlorinated Phenols," *J. Chem. Phys.*, A, 108 (2004), 9567-72.

170. D.H.M. Kim, J. A., "Temperature-Dependent Formation of Polychlorinated Naphthalenes and Dibenzofurans from Chlorophenols," *Environmental Science & Technology*, 39 (2005), 5831-36.
171. D.V. Wang, A.; Kim, D. H.; Mullholland, J.A., "Formation of Naphthalene, Indene, and Benzene from Cyclopentadiene Pyrolysis: A DFT Study," *J. Phys. Chem. A*, 110 (2006), 4719-25.
172. H. Richter, O.A. Mazyar, R. Sumathi, W.H. Green, J.B. Howard and J.W. Bozzelli, "Detailed kinetic study of the growth of small polycyclic aromatic hydrocarbons. 1. 1-naphthyl plus ethyne," *Journal of Physical Chemistry A*, 105 (2001), 1561-73.
173. M. Herring, M.; McKinnon, J., T.; Petrick, E., D.; Gneshin, W., K.; Filley, J.; and McCloskey D., B., "Detection of reactive intermediates during laser pyrolysis of cellulose char by molecular beam mass spectroscopy, implications for the formation of polycyclic aromatic hydrocarbons.," *Journal of Analytical and Applied Pyrolysis*, 66 (2003), 165-82.
174. R.B. Cypres, B., "Formation of most of the aromatic compounds produced by the pyrolysis of phenol does not involve the carbon bearing the hydroxyl function.," *Tetrahedron* 31 (1975), 359-65.
175. C.F. Melius, Colvin, M.E., Marinov, N.M., Pitz, W.J., Senkan, S.M., "Reaction mechanisms in aromatic hydrocarbon formation involving the C₅H₅ cyclopentadienyl moiety," *Proc. Combust. Inst.*, 26 (1996), 685-92.
176. E.-J.S.M.R.H.F. Rasouli, "Heterogeneous cracking of catechol under partially oxidative conditions," *Fuel*, 83 (2004), 1445-53.
177. S. Fujiwara, *Recent DevelopmentS of magnetic Resonance in Biological systems* (Hirokawa, Tokyo: 1968), Pages.
178. M.A. Foster, *Magnetic Resonance in Medecine and Biology* (Oxford: Pergamon Press, 1984), Pages.
179. G.R.E. Eaton, S. S.; Ohno, K., *EPR Imaging and In Vivo EPR* (Boca Raton: CRC Press, 1991), Pages.
180. H. Truong, Copper II Oxide Mediated Formation and Stabilization of Combustion Generated Persistent Free Radicals In *Department of Chemistry*, (Baton Rouge: Louisiana State University, 2007), 157.
181. L.-Y. Zang, Stone, K., Pryor, W.A., "Detection of free radicals in aqueous extracts of cigarette tar by electron spin resonance," *Free Radicals in Biology and Medicine*, 19 (1995), 161-67.
182. W.A. Pryor, Tamura, A., Church, D.F., "ESR spin-trapping study of the radicals produced in NO_x/Olefin reactions: A mechanism for the production of the apparently long-lived radical in the gas-phase cigarette smoke," *J.Am.Chem.Soc.*, 106 (1984), 5073-79.

183. E.G. Janzen, *A critical look at spin trapping in biological systems. In: Free radicals in biology*, W.A.Pryor (Ed.), Ac.Press, NY 1980), Pages.
184. L.R.C. Barclay, Cromwell, G.R., Hilborn, J.W., "Photochemistry of a model lignin comound. Spin trapping of primary products and properties of an oligomer," *Can.J.Chem.*, 72 (1994), 35-41.
185. D.K. Russell, Davidson, I.M.T., Ellis, A.M., Mills, G.P., Pennington, M., Povey, I.M., Raynor, J.B., Saydam, S., Workman, A.D., "Mechanicm of pyrolysis of tricarbonyl(cyclopentadienyl)manganese and tricarbonyl(methylcyclopentadienyl)manganese," *Organometallics*, 14 (1995), 3717-23.
186. L. Batt, Benson, S.W., "Pyrolysis of Di-tertiary butyl peroxide: Temperature gradients and chain contribution to the rate," *J.Chem.Phys*, 36 (1962), 895-901.
187. M.F.R. Mulcahy, Williams, D.J., and Wilmshurst, J.R., "Reactions of free radicals with aromatic compounds in the gaseous phase " *Aust.J.Chem.*, 17 (1964), 1329-41.
188. Yip. C.K. and H.O. Pritchard, "Thermal decomposition of di-tert-butyl peroxide in binary mixtures near the critical point," *Canadian Journal of Chemistry*, 49 (1971), 2290-96.
189. B.J. Hales, "Immobilized Radicals. I. Principal Electron Spin Resonance Parameters of the Benzosemiquinone Radical," *Journal of the American Chemical society*, 97 (1975), 5993-97.
190. B.J. Hales, "Immobilized Radicals. 3. Anisotropic saturation of Semiquinones in Protic Solvents," *The Journal of Chemical Physics*, 65 (1976), 3767-72.
191. Y.-R. Chen, Chen, C-L., Chen, W., Zweier, J.L., Augusto, O., Radi, R., and Mason, R.P., "Formation of Protein Tyrosine ortho-Semiquinone Radical and Nitrotyrosine from Cytochrome c-derived Tyrosyl Radical," *Journal of Biological Chemistry*, 279 (2004), 18054-62.
192. H. Yoshida, Hayashi, K., and Warashina, T., "ESR during Photolysis of p-Benzoquinone and Its Derivatives in Ethanol," *Bull. Chem. Soc. Jpn.*, 45 (1972), 3515-20.
193. F. Graf, Loth, K., and Gunthard, H-H., "Chlorine hyperfine splittings and spin density distribution of peroxy radicals. An ESR and Quantum chemical study.," *Helvetica Chimica Acta.*, 60 (1977), 710-21.
194. P. Neta, and Fessenden, R.W., "Hydroxyl radical reactions with phenols and anilines as studied by ESR.," *J.Phys. Chem.*, 78 (1974), 523-29.
195. H. Hiroyuki Nishide, Kaneko, T., Nii, T., Katoh, K., Tsuchida, E., and Lahti, P.M., "Poly(phenylenevinylene)-Attached Phenoxy Radicals: Ferromagnetic Interaction through Planarized and δ -Conjugated Skeletons," *J.Am.Chem.Soc.*, 118 (1996), 9695-704.
196. P.J. Barker, Davies, A.G., and Tse, M-W., "The photolysis of cycklopentadienyl compounds of Tin and mercury. ESR spectra and electronic configuration of the cycklopentadienyl, deuterocycklopentadienyl, and alkylcycklopentadienyl radicals," *J.Chem.Soc., Perkin Transaction 2*, (1980), 941-48.

197. S.-I. Ohnishi, Tanei, T., and Nitta, I, "ESR study of free radicals produced by irradiation in benzene and its derivatives," *J.Chem.Phys.*, 37 (1962), 2402-07.
198. G.R. Liebling, and McConnell, H.M., "Study of molecular orbital degeneracy in C₅H₅," *J.Chem.Phys*, 42 (1965), 3931-34.
199. P. Allard, Barra, A.L., Andersson, K. K., Schmidt, P. P., Atta, M., and Graˆslund, A., "Characterization of a New Tyrosyl Free Radical in Salmonella typhimurium Ribonucleotide Reductase with EPR at 9.45 and 245 GHz," *J.Am.Chem.Soc.*, 118 (1996), 895-96.
200. A. Liu, Poˆtsch, S., Davydov, A., Barra, A-L., Rubin, H., and Graˆslund, A., "The Tyrosyl Free Radical of Recombinant Ribonucleotide Reductase from *Mycobacterium tuberculosis* Is Located in a Rigid Hydrophobic Pocket," *Biochemistry*, 37 (1998), 16369-77.

CHAPTER 2: EXPERIMENTAL

2.1 Introduction

The main goal of the current research is to detect and characterize potentially environmentally persistent free radicals occurring during the pyrolysis of suitable precursors and tobacco. Tobacco samples used in this study derived from cigarette packages obtained from Philip Morris USA and British American Tobacco Companies. Catechol, hydroquinone and phenol samples were obtained from Aldrich, 99.5% purity.

The major component of the experimental set up for this study is the Electron Paramagnetic Resonance part to which different samplings set up are connected to, depending on the type of experiments. Basically, two sets of experiments were run: the low pressure and the atmospheric pressure radicals' identification. The Low Temperature Matrix Isolation technique was employed to trap formed radicals arising from the gas-phase pyrolysis/photolysis of precursors and tobacco. All EPR spectra were recorded on a Bruker EMX-20/2.7 EPR spectrometer (Bruker Instruments, Billerica MA) with dual cavities, X-band, 100 kHz, and microwave frequency, 9.53 GHz. The typical parameters for all radicals' identification were: sweep width set to 200 G, microwave power was varied from 0.1 to 20 mW, modulation amplitude set ≤ 4 G, the time constant is variable. Values of g-factors were calculated using Bruker's WINEPR program. Gas Chromatography- Mass Spectroscopy was employed to do mass analysis of the products of the pyrolysis.

2.2 The Electron Paramagnetic Resonance Spectroscopy

The capture and identification of radicals has been in used for decades to characterize foods, drugs, and environmental samples. Electron Paramagnetic Resonance (EPR) or Electron Spin Resonance (ESR) spectroscopy is suitable for radicals study. It is an analytical technique that permits to detect and characterize molecules with unpaired electrons. Its great advantage

compared to other analytical tools is that it does not destroy, alter or interfere with the molecules in the sample under investigation. EPR has a variety of applications.

In chemistry, kinetics of radical reactions, polymerization reactions, spin trapping¹, organo-metallic compounds, catalysis, petroleum research², oxidation and reduction processes, and biradicals and triplet states of molecules are studied using EPR³⁻⁵. Physics and materials research has intensively employed EPR.

In physics, measurement of magnetic susceptibility, transition metal⁶, lanthanide, and actinide ions, conduction electrons in conductors have received EPR application⁷. In materials research of degradation of paints and polymers by light, polymer properties⁸, defect in diamond, optical fibers, laser materials, organic conductors, influence of impurities and defects in semiconductors⁹, properties of novel magnetic materials¹⁰, high T_c superconductors, and behavior of free radicals in corrosion¹⁰, EPR has been employed.

Ionization radiation that studies alanine radiation dosimetry¹¹, controlled of irradiated foods, archeological dating¹¹, short-live behavior of organic free radicals produced by radiation, radiation effect and damage, and radiation effects on biological compounds¹, EPR has been an important analytical tool. The most important application of EPR is in medicine and biology¹²⁻¹⁴.

The study of the free radicals in living tissues and fluids, antioxidants, radical scavengers, drug detection, metabolism and toxicity, enzyme reactions, photosynthesis, oxygen based radicals, nitric oxide in biological systems¹⁵, carcinogenic reactions are studied employing EPR technique¹⁶. Most of biological reactions proceed from reduced and energy-rich carbohydrates to oxidized, energy-poor carbon dioxide. The one electron steps in redox reactions imply that in biological tissues, free radical intermediates are formed even though they may be too short-lived to observe. Thus applications of electron paramagnetic resonance to study those reactions have

received considerable scientific scrutiny. Given the importance of EPR, it is fundamental to have some understanding of the basic theory behind the big applications cited above.

2.2.1 EPR Theory

The EPR theory is based on Zeeman Effect. In an atom, different electrons may have same energy level. In the presence of a magnetic field, the degeneracy is broken due to at least the electron spin number. Pauli Exclusion Principle states that two electrons in an atom can not have all four same quantum numbers; they will differ at least by their spin number. Thus, the spin number is the key point in Zeeman Effect. The total Hamiltonian for an atom can be divided into three parts:

$$\hat{H} = \hat{H}^0 + \hat{H}_{rep} + \hat{H}_{s.o} \quad (1)$$

Where \hat{H}^0 is the sum of hydrogenlike Hamiltonians,

$$\hat{H}^0 = -\frac{1}{2} \sum_j \frac{\hbar^2}{2m_e} \nabla_j^2 - \sum_j \frac{Ze^2}{r_j} \quad (2)$$

\hat{H}_{rep} represents the interelectronic repulsions,

$$\hat{H}_{rep} = \sum_i \sum_{j>i} \frac{e^2}{r_{ij}} \quad (3)$$

and $\hat{H}_{s.o}$ is the spin-orbit interaction

$$\hat{H}_{s.o} = \sum_{i=1}^n \xi_i \hat{L}_i \cdot \hat{S}_i \quad (4)$$

where L and S are respectively the electron orbital angular momentum, and the electron angular spin and

$$\xi_i = \frac{1}{2m_e c^2} \frac{1}{r_i} \frac{dV_i(r_i)}{dr_i} \quad (5)$$

V_i is the potential energy experienced by the electron i of mass m_e in the atom, r_{ij} is the distance between two electrons, r_i is the distance between the electron and the nucleus, and e' is the reduced electron charge. C is the speed of light.

$$C \sim 3 \times 10^8 \text{ m/s}; m_e = 9.1 \times 10^{-31} \text{ Kg.}; e' = e/2\pi.$$

Considering only \mathbf{H}^0 , all atomic states corresponding to the same electronic configuration are degenerate. If \mathbf{H}_{rep} is added, the degeneracy between states with different \mathbf{L} and \mathbf{S} or both is

lifted, thus splitting each configuration into *terms*. If finally $\mathbf{H}_{S,O}$ is added, this splits each term into *levels*. Each level is composed of *states* with the same value of \mathbf{J} and is $(2J+1)$ -fold degenerate¹⁷. The degeneracy of each level can be removed by applying an external magnetic field: the Zeeman Effect. That is when the use of EPR is utmost fundamental where fine structure of radicals can be investigated. The g-factors are important data in EPR spectra analysis. Their values arise from the perturbation due to the magnetic field that is applied to resolve the degeneracy of each electronic level.

Suppose \mathbf{B} is the external applied magnetic field, the magnetic potential energy of the atom in the applied external field is

$$\mathbf{V}_M = -\vec{\mu} \cdot \vec{B} \quad (6)$$

where $\vec{\mu}$, the magnetic moment of the atom, consists of the electronic and the nuclear parts. However, the nuclear part is many orders of magnitude smaller and will be neglected in this presentation. Therefore,

$$\vec{\mu} = -\mu_\beta g \vec{J}, \quad (7)$$

where μ_β is the Bohr magneton, \vec{J} is the total electronic angular momentum, and g is the gyro magnetic ratio (g-factor). The operator of the magnetic moment of an electron is the sum of the contributions of the orbital angular momentum \vec{l} and the spin angular momentum \vec{s} , with each multiply by the appropriate related gyro magnetic ratio:

$$\vec{\mu} = -\mu_\beta (g_l \vec{l} + g_s \vec{s}), \quad (8)$$

In the case of L-S coupling, one sums over all the electrons in the atom to obtain

$$g \vec{J} = \left\langle \sum_i (g_l \vec{l}_i + g_s \vec{s}_i) \right\rangle = \langle g_l \vec{L} + g_s \vec{S} \rangle, \quad (9)$$

where \vec{L} and \vec{S} are the total orbital momentum and spin of the atom. Averaging is done over a state with given value of the total angular momentum. When the spin-orbit interaction dominates over the effect of the external magnetic field, \vec{L} and \vec{S} are not separately conserved, but the total angular momentum $\vec{J} = \vec{L} + \vec{S}$ is. The time “averaged” orbital vector and spin vector are respectively the projection of orbital and spin vectors onto the direction of \vec{J} .

$$\vec{L}_{avg} = \frac{\vec{L} \cdot \vec{J}}{J^2} \vec{J} \quad \text{and} \quad \vec{S}_{avg} = \frac{\vec{S} \cdot \vec{J}}{J^2} \vec{J}. \quad (10)$$

$$\text{Thus, } \langle V_M \rangle = \frac{\mu_\beta}{\hbar} \vec{J} \left(g_L \frac{\vec{L} \cdot \vec{J}}{J^2} + g_S \frac{\vec{S} \cdot \vec{J}}{J^2} \right) \cdot \vec{B}. \quad (11)$$

We need now to evaluate the scalar products $\vec{S} \cdot \vec{J}$, $\vec{L} \cdot \vec{J}$ and $\vec{J} \cdot \vec{B}$ that appear in equation 11 to get the value of $\langle V_M \rangle$.

Using $\vec{L} = \vec{J} - \vec{S}$ and squaring both sides, $(\vec{L})^2 = (\vec{J} - \vec{S})^2$ we get

$$\vec{S} \cdot \vec{J} = \frac{1}{2} (J^2 + S^2 - L^2) = \frac{\hbar^2}{2} [j(j+1) - l(l+1) + s(s+1)], \quad (12)$$

and using $\vec{S} = \vec{J} - \vec{L}$ and squaring both sides, $(\vec{S})^2 = (\vec{J} - \vec{L})^2$ we get

$$\vec{L} \cdot \vec{J} = \frac{1}{2} (J^2 - S^2 + L^2) = \frac{\hbar^2}{2} [j(j+1) + l(l+1) - s(s+1)] \quad (13)$$

Assuming that \vec{B} is oriented along the Z-axis, $\vec{J} \cdot \vec{B} = m_j B$ (14), m_j being the Z-component of the total angular momentum.

Plugging equations (12), (13), and (14) into (11), we get:

$$V_M = \mu_\beta B m_j \left[g_L \frac{j(j+1) + l(l+1) - s(s+1)}{2j(j+1)} + g_S \frac{j(j+1) - l(l+1) + s(s+1)}{2j(j+1)} \right] \quad (15)$$

The quantity in square bracket of equation 15 represents the Lande g-factor g_J of the atom.

$$g_J = g_L \frac{j(j+1) + l(l+1) - s(s+1)}{2j(j+1)} + g_s \frac{j(j+1) - l(l+1) + s(s+1)}{2j(j+1)} \quad (16)$$

where $g_L = 1$ and $g_s = 2.0023192$ (the anomalous gyro magnetic ratio where the deviation of the value from 2 is due to the relativistic effects, also the g-value of a free electron). When we take $g_s \approx 2$, then equation 16 becomes the most known g-value expression: ¹⁷⁻¹⁹

$$g = 1 + \frac{j(j+1) - l(l+1) + s(s+1)}{2j(j+1)} \quad (17)$$

This is the result of weak-field application that splits each level into $2J+1$ states, each state having different value of m_j .

Through the energy level diagram, it is clear that the application of external magnetic field will split the energy levels to states. However, if the atom's nucleus has a non zero spin, the nuclear spin magnetic moment interacts with the electronic spin and orbital moments to give rise to the hyperfine splitting very important in organic radicals identification. Physically, the nuclear spin angular momentum \mathbf{I} adds vectorially to the total electronic angular momentum \mathbf{J} , giving the total angular momentum \mathbf{F} of the atom: $\mathbf{F} = \mathbf{I} + \mathbf{J}$. To illustrate the hyperfine structure theory, let's take example on the hydrogen atom. The ground state of hydrogen has $\mathbf{I} = 1/2$ for the proton and $\mathbf{J} = 1/2$. Therefore the quantum number F can be 0 or 1, corresponding to the proton and the electron spins being antiparallel or parallel. The transition $F = 1 \rightarrow 0$ gives a line at 1420MHz, the 21-cm line emitted by hydrogen atoms in the outer space discovered in 1951 ¹⁷.

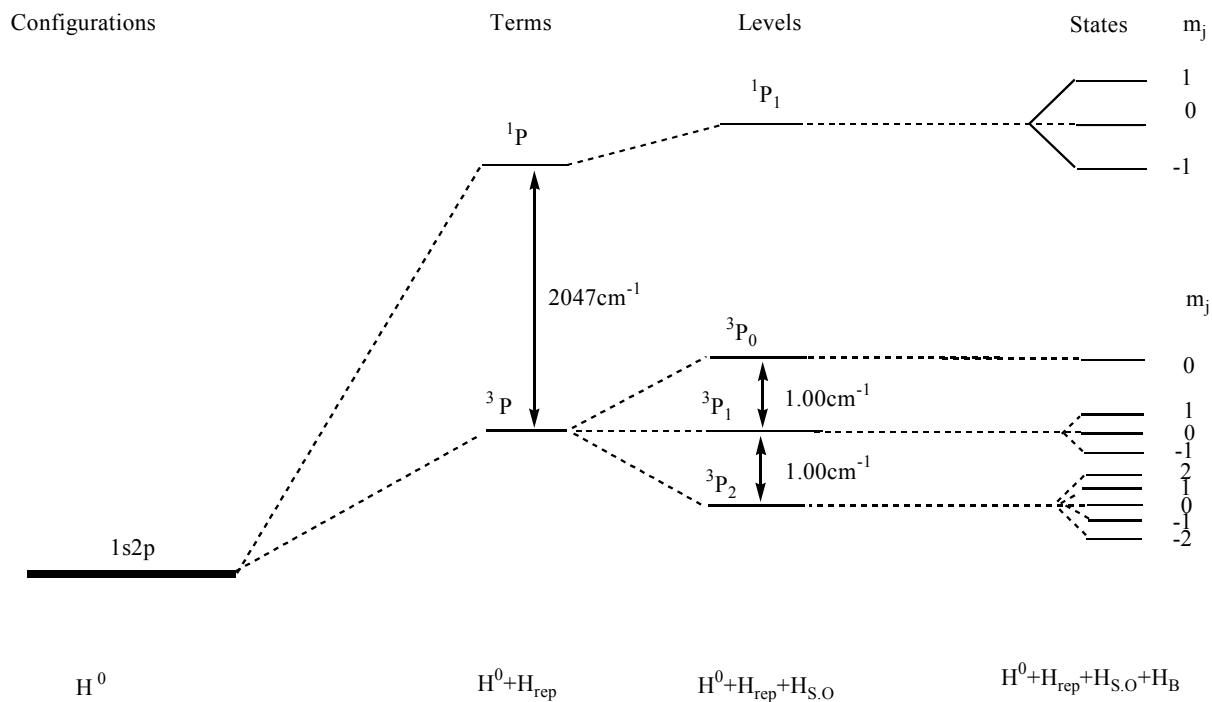


Figure 2.1 Effect of inclusion of successive terms in the atomic Hamiltonian for $1s2p$ helium configuration. H_B is not part of the atomic Hamiltonian but is due to an applied external magnetic field. Adapted with permission from reference ¹⁷.

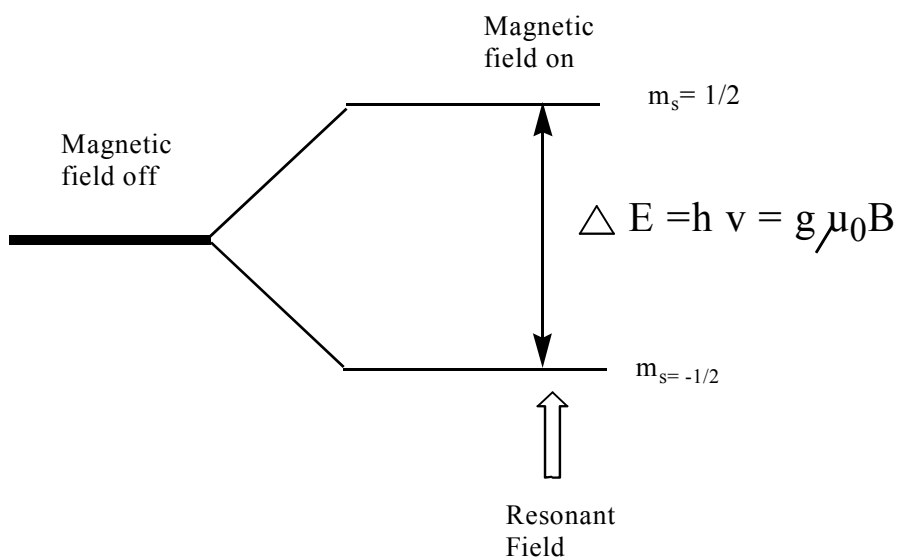


Figure 2.2. Resonance Condition

EPR is the spectroscopic technique that is employed to detect species having one or more unpaired electrons. When an external magnetic field is applied, the paramagnetic electrons either orient in a direction parallel or anti-parallel to the direction of the magnetic field. This phenomenon creates two different energy levels for the unpaired electrons and making it possible for absorption of electron-magnetic radiation to occur when electrons are driven between the two energy levels. The condition where the magnetic field and the microwave frequency are “just right” to produce an absorption is known as the resonance condition.

$$\Delta E = h\nu = g\mu_0 B . \quad (18)$$

where ν is the radiation frequency (Hz) that meets the resonance condition.

h is Planck's constant value ($h = 6.64 \times 10^{-34}$ J.S), μ_0 is the Bohr magnetron constant value ($\mu_0 = 9.27 \times 10^{-24}$ J/T).

However, in equation (18) at a fix radiation value, the resonance phenomenon occurs by varying the intensity of the applied magnetic field. In this study, the latter option was employed to register the absorption curves. The spectra registered on a Bruker spectrometer model EMX 10/2.7 (Bruker Instruments, Billerica, MA) are the first derivative of the absorption spectra.

2.2.2 Importance and Physical Significance of the EPR g-values

One of radical characteristic parameters is the g-factor or g-value. The g-factor can be a complex tensor depending on the molecular environment that it characterises. The g-value, along with the hyperfine splitting, usually represents a complex number that tells of the radical nature. It represents the extent to which the external magnetic field splits the energy levels of the radicals under investigation and accounts for both the Orbital-Spin coupling and Orbital-perturbation of the wave function of the unpaired electrons. Simply put, the g-value measures how the magnetic environment of the unpaired electrons differ from that of a free, gas-phase electron ($g = 2.0023$). The g-values of EPR spectra usually measured at the center of the EPR

spectra in principle are indicative of the types of radicals present. When the EPR spectrum arises from only one radical, only one g-value is obtained. In principle, the g-values of EPR spectra can be used to determine whether a radical is carbon-centered or oxygen-centered.

In general, the closer the unpaired electron is to an oxygen atom, the greater the g-value due to higher electron density that leads to strong spin-orbital coupling: for carbon-centered radicals, $g < 2.0030$ (e.g., graphitic carbon $g = 2.0028$)²⁰; PAH radicals, $g \sim 2.0026$ ²¹; aryl radicals, $g < 2.0024$, (e.g., phenyl, 1- and 2-naphthyl, 1- and 9-anthracyl, and 1-pyrenyl)²²; for carbon-centered radicals near an oxygen, $g = 2.0030-2.0040$ ²³; and for oxygen-centered radicals, $g > 2.0040$ ²⁴⁻²⁷. However, these values can be shifted by matrix interactions or other substituents such as chlorine²⁵. In addition, if the unpaired electron is not exclusively centered on a single atom (viz. through delocalization or complex formation) the EPR spectrum can broaden. The presence of multiple radicals can also result in an apparently broadened EPR spectrum making it impossible to use the g-values to identify the radicals.

2.2.3 Low Temperature Matrix Isolation

Radicals are known to be very reactive due to the presence of unpaired electrons in their structure. Thus their study requires an environment that will keep them “alive” for the duration of the study. Given that the concentrations of reactive free radicals in biological systems are usually too low for direct EPR detection, the spin trapping method was developed to allow immobilization, detection and analysis of free radicals²⁸⁻³⁰. The method consists of using a “trap” to catch the radical. The trap can be stable radical molecule in either liquid or solid phase. The most spin traps used are 2-methyl-2-nitrosopropane³¹, tertiary nitrosobutane³², N-t-butyl-alpha-phenylnitron^{33, 34}, the well studied 5,5-dimethyl-1-pyrroline 1-oxide (DMPO)³⁵. Among the nitrones used as spin trap, DMPO has received the most attention²⁹. This method has been very successful trapping radicals in liquid and solid phases to identify them by EPR

spectrometry. However, by trapping radicals, the electronic density of their unpaired electrons is modified, and one can even assist to what in the literature is termed inverted trapping where the spin adduct is formed by electron transfer without the reaction of a radical, leading to wrong conclusions.

The EPR g-values of complexed radicals are usually lower than those of un-complexed radicals due to the transfer of electron density from the radicals to the complexing agent^{36, 37}. Unfortunately, such problems arise from the most used nitrones such as DMPO, N-phenyl-Alpha-ter-butylnitron (PBN), and 2-methyl-2-nitrosopropane (MNP, tBuNO)³⁸ exposing some of the spin-trapping technique limitations. The use of some liquids (DMSO, ethanol) interferes in radicals EPR spectra because of their electron attracting nature, making their interpretation even more complicated. The gas-phase spin trapping is even more complicated because of radical-radical fast interaction.

The technique referred to in the literature as low temperature matrix isolation is suitable in isolating and keeping the gas-phase formed radicals as long as their EPR characterization will last. The huge advantage of this technique is that the radicals are not electronically influenced by the trap structure as in the case of spin trap. With the LTMI-EPR, real radicals are directly identified. The LTMI-EPR technique is well known in the literature³⁹⁻⁴³. LTMI EPR allows accumulation and detection of trace quantities of radicals from the gas-phase as well as the determination of the reaction kinetic behavior of gas-phase reactions³⁹. We have successfully employed this technique in this study. It consists of freezing gas-phase formed radicals at liquid nitrogen temperature (77K) in a gas matrix which characteristics allow the radicals' survival. The matrix should be inert. Thus it does not react with the radicals. The matrix should also be rigid to cryogenically block radical diffusion by keeping them at isolated sites in the matrix. Finally,

the matrix should be volatile so that during annealing process, very reactive radicals will be annihilated, leaving behind the more persistent ones.

2.2.4 Pyrolysis Experiments

2.2.4.1 Experimental Set-Up

The main and unchangeable part of the experimental set up is the liquid nitrogen-cooled Dewar which cooled finger is located in the cavity of the EPR spectrometer. Upon exiting the flow reactor the pyrolysis/photolysis products are cryogenically trapped onto the cold finger of the cold Dewar at 77K (-196°C). This allows detection and identification of the gas-phase formed radicals arising from the reactor. A rotary pump was used to pump the gas effluent through the cold finger of the Dewar, thus maintaining the total working pressure at ~ 0.1 Torr.

The variable experimental part of the experimental set up is the sampling system which depends on experimental conditions. For low pressure Pyrolysis of catechol, hydroquinone and phenols, a flow reactor was used and its outlet connected to the Dewar through a transfer line.

The atmospheric pyrolysis of catechol, hydroquinone and phenol uses a different sampling set up. The homemade tubular flow reactor additionally to its outlet connected to the flow transfer line that hooks it up to the Dewar has another outlet open up to the atmosphere. However, a gas trap at liquid nitrogen temperature was used on the atmospheric line to collect part of the pyrolysis products for GC-MS mass analysis purpose. A quartz diaphragm of appropriate pinhole diameter of 10 μ m is used to reduce the pressure from atmospheric pressure to ~ 0.1 torr to allow easy pyrolysis products pumping towards the cold finger of the Dewar. An electrically heated furnace hosts the pyrolysis reactor.

The reactor is a homemade tubular flow quartz reactor which dimensions allow variable vaporized compounds residence time. Its inner diameter and length are respectively 12mm and 40mm and it can stand temperature up to 1200C. An independent thermo-controller connected

to the flow reactor through a high temperature thermocouple is employed to set and vary the vaporized gas pyrolysis temperature.

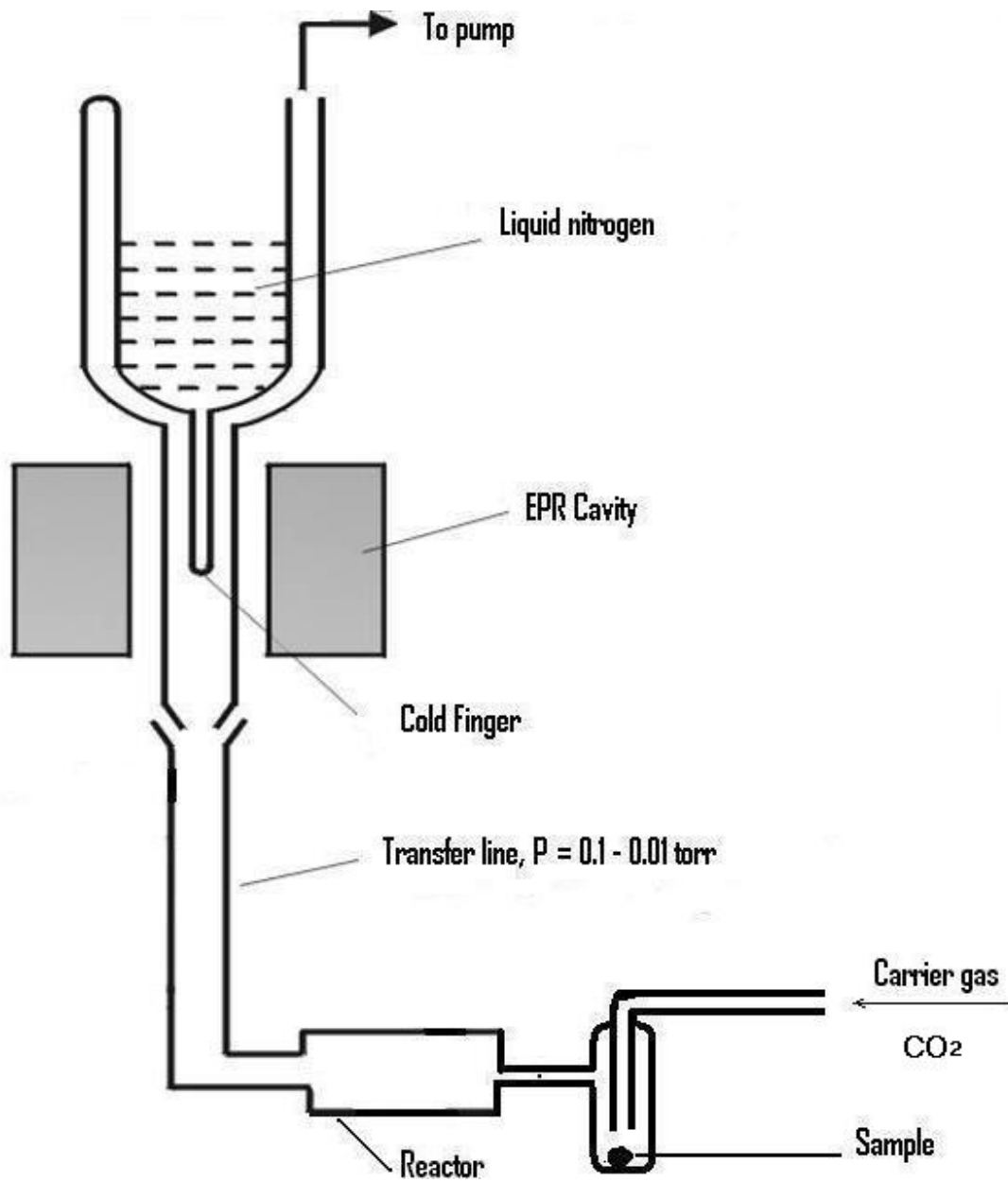


Figure.2.3 Cold Dewar Assembly

The samples of CT, HQ, and phenol are vaporized in an electrical furnace (vaporizer in the photograph taken from the rear side) which temperature is independently controlled by a thermo-controller by the means of a thermocouple.

In the CT and HQ experiments, all transfer lines between the vaporizer and the cold finger of the Dewar were maintained at temperature $\sim 80\text{-}90^\circ\text{C}$ to avoid condensation of sample and products in the lines.

A turbo, two stage pump DCU Pfeiffer Vacuum was employed to pump the reagent through a gas manifold directly connected to the Cold Dewar outlet. The pump maintain the desired working pressure to 0.1 to 0.3Torr. It pumps when needed the vaporized samples through the reactor to the cold finger of the Dewar. It is also used while flushing the equipment line and the samples

A homemade gas manifold is used to monitor the working pressures readable through the pressure gauges in the system. Between the gas manifold and the pump, a liquid nitrogen trap

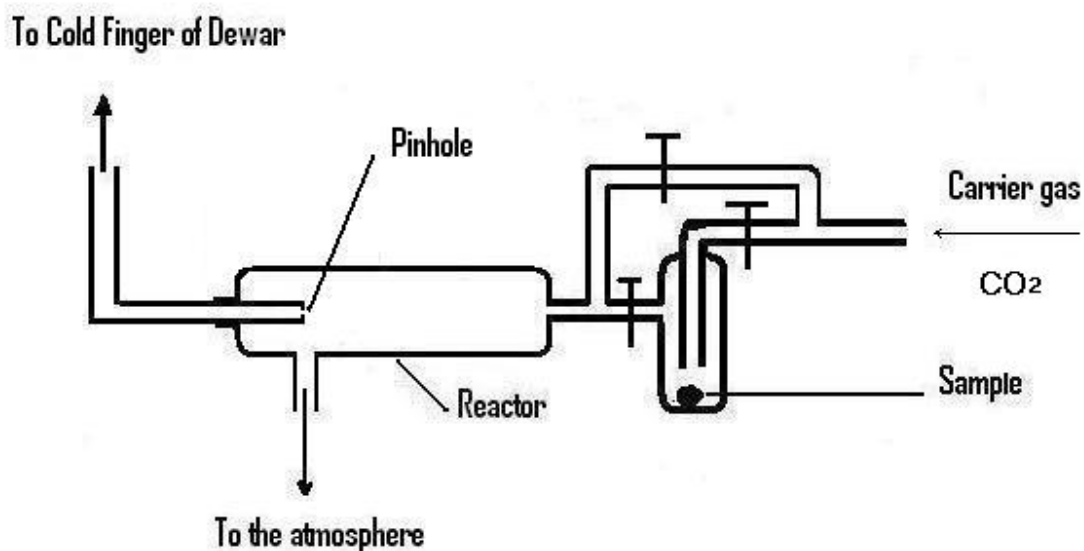


Figure 2.4 Assembly for atmospheric pyrolysis experiments

was employed to avoid excessive chemical getting into the pump.

A rough (first stage) part of the turbo pump is initially used to clean the samples and the transfer lines by removing basically the air (oxygen) from the system.



Figure 2.5 Photograph of the Experimental layout

2.2.4.2 Experimental Procedure

2.2.4.2.1 Pyrolysis of Catechol, Hydroquinone and Phenol

For the pyrolysis of catechol, hydroquinone and phenol, almost same experimental procedure is followed except for some minor differences due to their vapor pressures. Catechol and hydroquinone have very low vapor pressures. Thus they needed to be vaporized prior to their Pyrolysis. Experiments were carried out by loading HQ, CT, or phenol (>99.5 % pure) into a

Pyrex container-vaporizer in a constant temperature oven held at 50-75 °C for the vaporization of the sample of CT and HQ and at 15 °C.

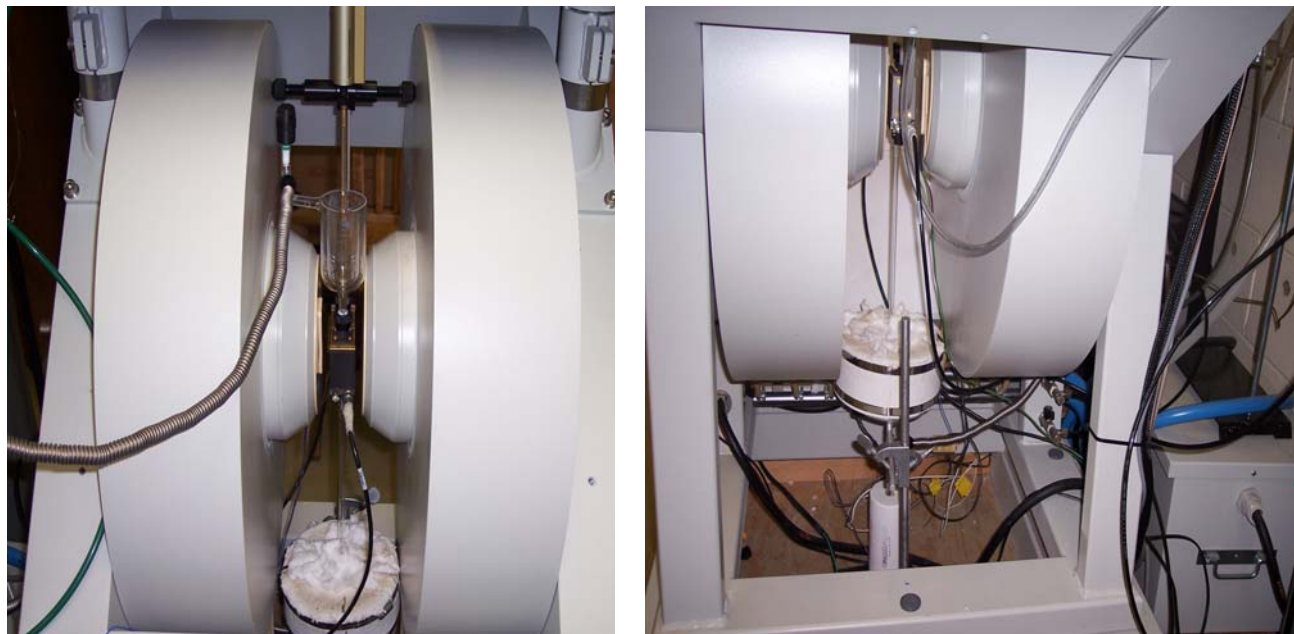


Figure 2.6 Cold Dewar in EPR cavity-Front view Cold Dewar connected to the vaporizer-Rear view

To avoid condensation of the vaporized CT and HQ samples on the transfer line to the cold Finger of the Dewar, the transfer line was insulated and held at a temperature of 80-90 °C employing heating tapes and blankets. Phenol's high vapor pressure allows experiments at either room temperature or 0°C. All samples were at a total pressure of carrier gas of ~ 0.1 - 0.3 Torr for the low pressure pyrolysis of the precursors, and 760 Torr for the atmospheric pyrolysis measured by the on-line pressure gauges in the system. The experimental set-up for the atmospheric conditions pyrolysis is depicted in **figure 2.3**. The carrier gases used for this research are nitrogen and carbon dioxide. The pressure of the test compound was maintained at ≤ 0.1 torr. Upon exiting the vaporizer, the vaporized sample entered the tubular-flow quartz reactor (i.d. = 12 mm, length = 40 mm) located in an electrically heated furnace. Radical

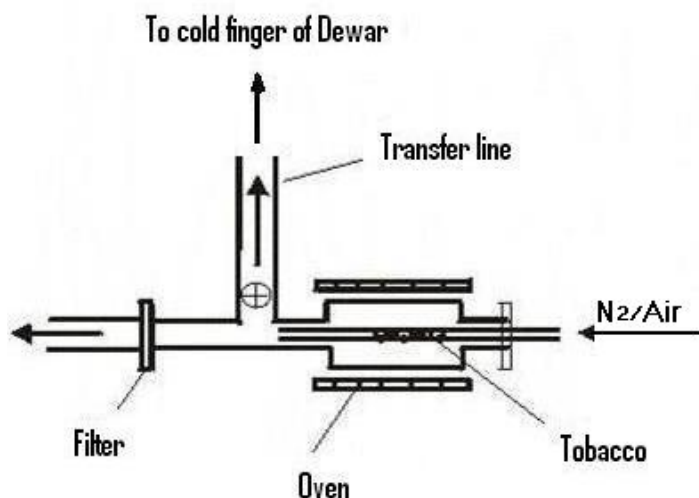


Figure 2.7 Tobacco Atmospheric Pyrolysis Assembly

accumulation time ranged from 10 to 12 minutes, starting point of the saturation. Reagents are pumped by means of rotary pumps at a pressure of 0.1 Torr through the electrically heated pyrolysis zone. Pyrolysis products are condensed onto the cold finger of the Dewar placed in the EPR cavity and cooled by liquid nitrogen. Carbon dioxide (or other gases that can be used to generate an appropriate matrix) can be introduced at a given flow as a main carrier gas into the pyrolysis zone. Once the sample is loaded in the vaporizer, the sample, the transfer line and the Dewar were flushed long enough under the carrier gas flow (CO_2 or N_2) to remove oxygen from the sample and the system. The flushing is done by the rough pump at a rate of 60 cc/min. Given that Catechol and Hydroquinone have very low vapour pressure, slightly heating their samples during the flushing period helps to get rid of absorbed/adsorbed oxygen. Phenol's samples do not need the pre-heating because of phenol's high vapour pressure. After sufficient flushing, the vaporizer hosted by a furnace was set at the sample vaporizing temperatures, 50 or 75 ° C for Catechol and Hydroquinone, 15 ° C for phenol. The flow meters in the system allow monitoring the time of residence of the vaporized sample in the pyrolysing reactor held at the experimental temperature by a thermo-electric furnace. The radical accumulation starts when the Dewar is filled with liquid nitrogen. A rotary pump is used to pump the pyrolyzed products through the liquid nitrogen cooled Dewar. Freezing of radical onto the cooled finger of the

Dewar can be observed by the dropping of the total reagent pressure (from 0.1 Torr to 10^{-3} Torr) and most of the time by the slight change of cold finger color. The accumulation lasts generally 10 to 12 minutes during which EPR spectra of frozen radicals are acquired every minute. The end of the accumulation time is marked by the non increasing EPR signal intensity of the radicals. At the end of the accumulation, the carrier gas flow was stopped, and the sample vaporizer closed. More EPR spectra of total radical were then registered in the absence of thermal noise generated by the interaction of the hot gas flow with the cooled finger of the Dewar. This is the time in the experiment where the power dependence of radical accumulation is performed to get the microwave power saturation curve. The annealing experiment is performed to allow the most reactive radicals to terminate, living behind the most persistent ones

2.2.4.2.2 Pyrolysis of Tobacco

Tobacco sample is loaded in a Pyrex tube (i.d =6mm, Length= 5cm) to mimic actual cigarette seize. The qualitative tobacco pyrolysis experiments were undertaken to characterize free radicals formed during the gas-phase pyrolysis of three tobacco blends obtained from Phillips Moris USA tobacco company. For the quantitative tobacco pyrolysis generated radicals, four tobacco blends from British American Tobacco (BAT) were used. Each time, 0.25gram of tobacco was employed. To keep the sample from flying during flushing, quartz woods was put at the two ends of tobacco sample in the experimental tube. The sample is flushed with nitrogen gas for 30 minutes to remove absorbed/adsorbed oxygen. Thereafter, the sample is dried at 100 °C for 10 minutes by a thermo-electric furnace. During the drying up of tobacco, heavy smoke is observed showing vaporization of water and some very volatile tobacco components.

2.2.4.2.3 The Time of Residence of the Vaporized Samples in the Reactor

The residence time is a very crucial part of any chemical reaction. In the case of the pyrolysis/photolysis of Catechol, Hydroquinone and Phenol the residence time allows the

formation and the survival of radicals. The flow meters in the system permit the monitoring of the residence time. In general, in our experiments, a residence time of 4ms was used. The residence time in the tubular flow reactor was calculated employing the formula:

$$\bar{t}_r = \frac{\pi R^2 L}{W} \left(\frac{T_a}{T_{\text{exp}}} \right) \text{ where } R = \text{radius of the reactor, } L \text{ its length, } W \text{ the carrier gas flow, } T_a \text{ the}$$

ambient Temperature and T_{exp} the experimental Temperature.

Table 2.1 depicts the variation of the flow W in terms of T_{exp} , the ambient temperature being the EPR Spectroscopy's room temperature held at 15 ° C at a residence time of 4ms

Table 2.1 Temperature Dependence Variation of Gas Flow for a Constant Residence time

| T_{exp} (° C) | T_{exp} (K) | Flow Rate (mL/min) |
|------------------------|----------------------|--------------------|
| 400 | 673 | 483.7 |
| 450 | 723 | 450.3 |
| 500 | 773 | 421.1 |
| 550 | 823 | 395.6 |
| 600 | 873 | 373.0 |
| 650 | 923 | 352.7 |
| 700 | 973 | 334.6 |
| 725 | 998 | 326.2 |
| 750 | 1023 | 318.2 |
| 775 | 1048 | 310.6 |
| 800 | 1073 | 303.4 |
| 825 | 1098 | 296.5 |
| 850 | 1123 | 290.0 |

| | | |
|------|------|-------|
| 875 | 1148 | 283.6 |
| 900 | 1173 | 277.5 |
| 925 | 1198 | 271.7 |
| 950 | 1223 | 266.2 |
| 975 | 1248 | 260.8 |
| 1000 | 1273 | 255.7 |

2.2.5 Photolysis Experiments

In this study, the UV photolysis experiments of Catechol, Hydroquinone and phenol were carried out in the gas phase using the same experimental equipment of LTIM EPR discussed elsewhere ⁴⁴. The aim of these experiments was to generate oxygen centered semiquinone and phenoxy type of radicals directly from the gas phase photolysis of suitable precursors at lower temperatures and freeze them at liquid nitrogen temperature. The huge advantage of photolysis is that it is possible to prevent thermal degradation and transformation of formed radicals and transfer them at low pressure to the cold zone.

The photolytic cell, a simple suprasil 1 quartz tube was used to load the sample in lieu of the reactor. The sample was irradiated by UV light at 253.7nm from the side. The 253.7 nm light was emitted by conventional mercury vapor ozone free lamp (pencil type), Jelight Company, Inc. This double bore lamp, with a 9mm OD, has a 4 inch lighted length with a capable power of about 9mW/cm² at 254nm measured at a distance of 0.75 inch from the lamp.

2.2.6 Annealing Experiments

The annealing experiments consist of fractional elimination of the most reactive radicals. Gradual warming of the Dewar resulted in the matrix annealing and selective annihilation of the more reactive radicals such that the spectra of the more persistent, individual radicals in the mixture could be discerned. The cold finger of Dewar was slowly warmed by removing liquid nitrogen with a bubbling stream of nitrogen gas. Annealing of the matrix by warming the cold finger resulted in some reactive radicals, being annihilated by radical-radical recombination. On the other hand it is known that radical diffusion in cold matrix occurs at a temperature well below the melting point of the matrix ⁴⁵. Usually the radicals begin to disappear when the temperature rises to between one-tenth and one-third of the melting point. In the present study where CO₂ is the most used both as carrier gas and isolation matrix, the temperature at which the radicals are annihilated varies between ~ 176 - 130 K.

2.3 Gas Chromatography-Mass Spectroscopy

Toxic organic compounds such as Dioxins/ Furans and PAHs gas-phase formation has been demonstrated through radical formation. Phenols, chlorinated benzene and chlorinated phenols are the precursors to the formation of PCDD/Fs through phenoxy/semiquinone types radicals intermediates ⁴⁶⁻⁴⁸. Those conclusions on radical intermediate PCDD/Fs and PAHs formation were drawn based on combustion products distribution. The present study's goal is to demonstrate the formation of the persistent radicals at low and atmospheric pressures. The atmospheric conditions were one golden opportunity to collecting products formed from the pyrolysis of Phenols, Catechol and Hydroquinone and do their GC-MS analysis while acquiring the EPR spectra of formed radicals. To do this, a gas trap was put on the atmospheric line of the system at 2 inches from the center of the homemade quartz reactor. Pyrolysis products collection was done under liquid nitrogen and Carbon dioxide flow. After the accumulation of pyrolysis

products, CO₂ was evacuated with ethanol under hoods and the ethanol evaporated to permit concentration of products for GC-MS analysis. 1 µl of the substrate was injected in the GC-MS for the pyrolysis products analysis. The products were analyzed using an Agilent Technologies 6890N GC system coupled with a 5973 Mass Selective Detector. Products separation was completed employing a 30m, 0.25mm i.d., 0.25 µm film thickness column (Restek Rts 5mx) with a temperature program ramp from -60 to 300 °C at 15 °C/min. Detection of products was obtained on the Agilent 5973 Mass Selective Detector operating in full-scan mode from 15 to 350 amu. The GC/MS software, an Automated Mass Spectral Deconvolution and Identification System (AMDIS-DSWA NIST, 1997), was used to identify the products of the atmospheric pyrolysis of all precursors.

2.4 References

1. Y.N.S. Molin, K. M.; Zamaraev, K. I., *Spin Exchange-Principles and Applications in Chemistry and Biology* (New York: Berlin, 1980), Pages.
2. L.F. Petrakis, J.P., *Magnetic resonance: Introduction, Advanced Topics and Applications to Fossil Energy* (Reidel, Dordrecht: NATO ASI, 1984), Pages.
3. P.B. Ayscough, *Electron Spin Resonance in Chemistry* (New York: 1967).
4. L.J. Berliner, *Spin Labeling: Theory and Applications* (New York: Academic Press, 1976),
5. I.B.B.A.J. Goldberg, *Electron Spin Resonance Spectroscopy in treatise of Analytical Chemistry* (New York: 1983).
6. J.B. Peisach, W. E., *Electron Spin Resonance of Metal Complexes* (New York: Plenum Press, 1969).
7. D.J.E. Ingram, *Spectroscopy at Radio and Microwave Spectroscopy Frequencies* (London: Butterworths, 1967).
8. B.R. Ranby, J.F. , *ESR Spectroscopy in Polymer Research* (New York: Springer, 1977).
9. G. Lancaster, *Electron Spin Resonance in Semiconductors:* (London: Hilger and Watts, 1966).
10. F.E.C. Mabbs, D., *Electron Paramagnetic Resonance of d-transition Metal Compounds, in Study in Inorganic Chemistry* (Amsterdam: Elsevier Science, 1992).

11. M. Ikeya, *New Application of Electron Spin Resonance, Dating, Dosimetry, and Microscopy* (Singapore: 1993).
12. S. Fujiwara, *Recent DevelopmentS of magnetic Resonance in Biological systems* (Hirokawa, Tokyo: 1968).
13. M.A. Foster, *Magnetic Resonace in Medecine and Biology* (Oxford: Pergamon Press, 1984).
14. G.R.E. Eaton, S. S.; Ohno, K., *EPR Imaging and In Vivo EPR* (Boca Raton: CRC Press, 1991).
15. E.G.S. Rozantsev, V. D., "Synthesis and Reactions of Stable Nitroxyl Radicals," *Synthesis*, (1971), 190-202.
16. J.S. Hyde, *Saturation Transfer Spectroscopy in Methods in Enzymology: Enzyme Structure* (New York: Academic Press, 1978).
17. I.N. Levine, *Quantum Chemistry* (New Jersey: Prentice-Hall, Inc, 2000).
18. H.A.J. Bethe, R.W., *Intermediate Quantum Mechanics* Benjamin-Cummings, 1985).
19. P. Forman, "Alfred Landé and the anomalous Zeeman Effect, 1919-1921. Historical Studies.," *Physical Sciences*, (1970), 153-261.
20. P. Delhaes, and Marchand, A.A., "Analyze de la forme et de la position de signaux RPE observes sur des carbons graphitiques pulverulents," *Carbon*, 6 (1968), 257.
21. A. Szent-Gyorgyi, Isenberg, I., Baird, S., "On the electron donating properties of carcinogens," *Proc.Natl.Acad.Sci, USA*, 46 (1960), 1444.
22. P.H. Kasai, Clark, P.A., and Whipple, E.B., "The electronic ground states of aryl radicals," *J.Am.Chem.Soc.*, 92 (1969), 2640-44.
23. L.R.C. Barclay, Cromwell, G. R., Hilborn, J. W., "Photochemistry of a model lignin compound. Spin trapping of primary products and properties of an oligomer.," *Canadian Journal of Chemistry*, 72 (1994), 35-41.
- 24.P. Neta, and Fessenden, R.W., "Hydroxyl radical reactions with phenols and anilines as studied by ESR.," *J.Phys. Chem.*, 78 (1974), 523-29.
25. F. Graf, Loth, K., and Gunthard, H-H., "Chlorine hyperfine splittings and spin density distribution of peroxy radicals. An ESR and Quantum chemical study.," *Helvetica Chimica Acta.*, 60 (1977), 710-21.
26. P. Allard, Barra, A.L., Andersson, K. K., Schmidt, P. P., Atta, M., and Graˆslund, A., "Characterization of a New Tyrosyl Free Radical in Salmonella typhimurium Ribonucleotide Reductase with EPR at 9.45 and 245 GHz," *J.Am.Chem.Soc.*, 118 (1996), 895-96.

27. B.J. Hales, "Immobilized radicals I. Principal Electron Spin Resonance parameters of the benzoquinone radicals.," *J. Am. Chem. SOC.*, 97 (1975), 5993-97.
28. W.A. Janzen, and Blackburn, B.J., "Detection and identification of short-lived free radicals by ESR trapping technique.," *J.Am.Chem.Soc.*, 91 (1969), 4481-93.
- 29.E.G. Janzen, *A critical look at spin trapping in biological systems. In:Free radicals in biology*, W.A.Pryor (Ed.), Ac.Press, NY 1980), Pages.
30. E.D.S. Janzen, H. J.; Dubose, C. M.; Poyer, J. L.; McCay, P. B., "Chemistry and Biology of Spin-Trapping Radicals Associated with Halocarbon Metabolism in Vitro and in Vivo," *Environmental Health Perspectives*, 64 (1985), 151-70.
31. K.S.R.S.H. H., "Studies of short-lived radicals in the gamma-irradiated aqueous solution of uridine-5'-monophosphate by the spin-trapping method and the liquid chromatography.," *International journal of radiation biology and related studies in physics, chemistry, and medicine* 30 (1976), 525-34.
32. S.J. Rustgi, A.; Riesz P.; Friedberg F., "E.s.r. of spin-trapped radicals in aqueous solutions of amino acids. Reactions of the hydrated electron," *International journal of radiation biology and related studies in physics, chemistry, and medicine*, 32 (1977), 533-52.
33. K.Y.S. Y, "Electron spin resonance studies on the oxidation of rifamycin SV catalyzed by metal ions," *Journal of biochemistry* 91 (1982), 397-401.
34. S.K.N.H.N.M.T.-K.S.I. Y, "Generation of hydroxyl radicals during the enzymatic reductions of the Fe³⁺-ADP-phosphate-adriamycin and Fe³⁺-ADP-EDTA systems. Less involvement of hydroxyl radical and a great importance of proposed perferryl ion complexes in lipid peroxidation. ," *Biochimica et biophysica acta* 753 (1983), 411-21.
35. J.-M.C.-E. Richard, D.; Jeunet, A., "First electron spin resonance evidence for the production of semiquinone and oxygen free radicals from orellanine, a mushroom nephrotoxin. ," *Free Radical Biology & Medicine* 19 (1995), 417-29.
- 36.C.C. Felix, Sealy, R. C., "o-Benzoquinone and its metal chelates. Electron spin resonance investigation of radicals from the photolysis of catechol in the presence of complexing metal ions.," *J. Am. Chem. SOC.*, 104 (1982), 1555-60.
- 37.C.C. Felix, Sealy, R. C., "Electron spin resonance characterization of radicals from 3,4-dihydroxyphenylalanine: semiquinone anions and their metal chelates," *J. Am. Chem. SOC.*, 103 (1981), 2831-36.
38. L.P. Ebersson, O., "Generation of acyloxyl spin adducts from N-tert-butyl- Alpha-phenylnitron (PBN) and 4,5-dihydro-5,5-dimethylpyrrole 1-oxide (DMPO) via non conventional mechanisms," *Journal of the Chemical Society, Perkin Transactions*, 2 (1997), 1689-96.

39. A.B. Nalbandyan and A.H. Mantashyan, "The elementary processes in slow gas-phase reactions " *Inst. Chem.Phys. NA of Armenia*, (1975), Yerevan, Armenia.
40. L. Khachatryan, Niazyan, O., Mantashyan, A.H., Vedeneev, V.I., Teitel'boim, M.A., "Experimental determination of the equilibrium constant of the reaction $\text{CH}_3 + \text{O}_2 \rightleftharpoons \text{CH}_3\text{O}_2$ during the gas-phase oxidation of methane.," *Int.J.Chem.Kin.*, 14 (1982), 1231-41.
41. M. Carlier, Pauwels, J.P., and Sochet, L-R., "Application of ESR techniques to the study of gas-phase oxidation and combustion phenomena," *Oxidation Communication*, 6 (1984), 141-56.
42. I.M.T.E. Davidson, A. M.; Mills, G. P.; Pennington, M.; I.M.R. Povey, J. B.; Russell, D. K.; Saydam, S.; Workman, and A. D. . . 1994, 13., "Mechanism of pyrolysis of organometallic deposition precursors," *J. Mater. Chem*, 4 (1994).
43. K. Mach, Mills, G.P., Raynor, J.B., " Low pressure pyrolysis of hexamethyldisilane:ESR identification of radical intermediates.," *J.Organometallic Chemistry*, 532 (1997), 229-33.
44. L. Khachatryan, Adoukpe, J., Maskos, M., and Dellinger, B., "Formation of Cyclopentadienyl Radicals from the Gas-Phase Pyrolysis of Hydroquinone, Catechol, and Phenol," *Environ. Sci. Technol.*, 40, 5071-5076 (2006).
45. B. Mile, "Free radical studies at low temperatures," *Angew. Chem., International Edition*, 7 (1968), 507-19.
46. J.G.P. Born, R. Louw and P. Mulder, "Formation of dibenzodioxins and dibenzofurans in homogenous gas-phase reactions of phenols," *Chemosphere*, 19 (1989), 401-06.
47. R. Weber and H. Hagenmaier, "Mechanisms of the Formation of Polychlorinated Dibenzo-p-dioxins and dibenzofurans from Chlorophenols in Gas Phase Reactions," *Chemosphere*, 38 (1999), 529-49.
48. R. Louw and S.I. Ahonkhai, "Radical/radical vs radical/molecule reactions in the formation of PCDD/Fs from (chloro)phenols in incinerators," *Chemosphere*, 46 (2002), 1273-78.

CHAPTER 3: RESULTS *

This section presents the results of low pressure pyrolysis of catechol (CT), hydroquinone (HQ), and phenol at various temperatures. It shows temperature dependence of radical signal EPR intensity and radical shape. The photolysis of CT, HQ, and phenol yielded pure semiquinone types radical that were compared to those of their pyrolysis at low temperature region. The atmospheric pressure pyrolysis of CT, HQ, and phenol at 750°C gave additional insights to the understanding of radical behavior, alongside with the effects of trace of oxygen on radical shape.

Positive identification of spectra of radicals formed from the gas-phase pyrolysis of CT, HQ, and phenol was complicated because the spectra were the convolution of more than two radicals most of the times. Thus additional experiments to generate spectra of unique radical employing pure compounds were undertaken. The results of mathematical manipulations of spectra employing the Simfonia software were additional and necessarily data in the identification of radicals.

The preliminary pyrolysis of the precursors was undertaken to establish the basic understanding of the research, the experimental optimum conditions that pertain radicals' isolation and identification, and the assembly of the necessarily sampling equipment and precursors purchasing. Experimental conditions are very important in any scientific work.

Initially, we have generally set the residence time to 10 ms, the vaporization of solid state precursors at 50 °C for all precursors, and varied the EPR spectrometer parameters. As can be seen in the detailed pyrolysis experiment of each precursor, the residence time, and the vaporization temperatures depend on the physical properties of each precursor. For instance, Catechol and Hydroquinone have very low vapour pressures (~0.001mmHg). Not only we found

that the optimum vaporization temperature was 75 °C, but also the residence time change from 10 ms to 4 ms was important for radical survival. Phenol whose vapour pressure is higher (0.03mmHg) was set at a vaporization temperature of 15 °C, and even at 0 °C. While all the transfer line in Catechol and Hydroquinone pyrolysis experiments was thermally insulated and held at 80-90 °C, phenol pyrolysis did not need this additional care. Overall, the first step in this research had focused on the qualitative observation of radicals.

3.1 Low Pressure Pyrolysis of Phenol

Phenol vaporized at 15 °C was pyrolyzed from 400 to 1000 °C. The time and temperature dependence radical accumulation from phenol pyrolysis show pattern different from catechol and hydroquinone. The following paragraphs report interesting results from detailed phenol study.

The pyrolysis of Phenol at low pressure was conducted employing the flow reactor which temperature was varied from 400 to 1000°C. The pyrolysis products were pumped by the means of a turbo pump through the cold finger of the Dewar.

We employed the technique of the Low Temperature Matrix Isolation (LTMI) EPR¹, in which phenol vaporized at 15 °C was pyrolyzed in a low pressure reactor (0.01- 0.1 torr) which was directly connected to a liquid nitrogen-cooled cold finger situated within the EPR cavity of a Bruker EPR spectrometer **Figure 2.3**

3.1.1 Total Radical Yield

Phenol at 15 °C was pyrolyzed from 400 to 1000 °C. At a given temperature, radicals accumulation was performed for 12 min, and the radicals EPR spectra registered every minute. This has the double advantage to follow on screen both the change in radicals' shape and intensity and to correlate radicals' accumulation to time for kinetic study purpose. Unlike

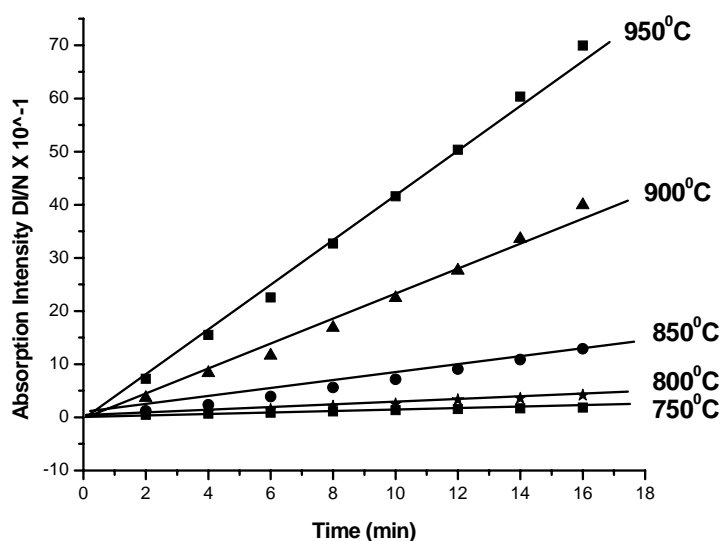


Figure 3.1 Time Dependence of Radical EPR Intensity From the Pyrolysis of Phenol. A linear trend with excellent correlation Intensity vs. radical accumulation time was observed in all temperature domain. DI/N value is the double integrated (DI) intensity of the EPR spectrum that has been normalized (N) to account for the conversion time, receiver gain, number of data points and sweep width

catechol and hydroquinone, the radicals from the pyrolysis of phenol EPR signal intensities at various temperatures exhibit a linear correlation with the accumulation time.

The radical accumulation time dependence of radicals EPR intensity depicted in **figure 3.1** was obtained from considering the radical EPR intensities at 6 minutes for various temperatures. We have decided to draw the temperature dependence of radical EPR intensities at 6min, the half time of our radical accumulation lapse to avoid the saturation region that was observed in the cases of CT and HQ.

3.1.2 Temperature Dependence of Radical Yield

Figure 3.2 depicts the variation of the radical EPR intensity vs. temperature. It shows that with increase temperature from 400 to 1000 °C, the radical intensity increases as well. It will be interesting to go beyond 1000 °C to see the curve behavior. It is noteworthy to see the sharp increase of radical yield starting from 800 °C giving the proof of enormous yields of radical from the pyrolysis of phenol beyond 800 °C.

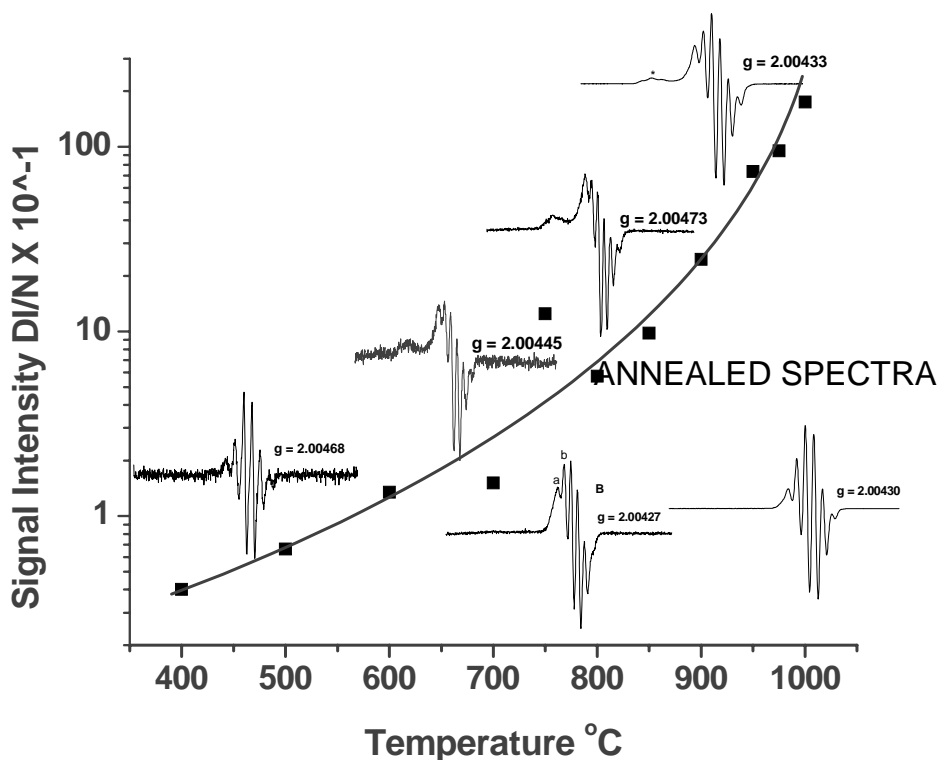


Figure 3.2 Temperature dependence of radicals Yield from the pyrolysis of Phenol. DI/N value is the double integrated (DI) intensity of the EPR spectrum that has been normalized (N) to account for the conversion time, receiver gain, number of data points and sweep width [<http://www.bruker-biospin.com/winepr.html?&L=0>]. A sharpe increase of radical intensity starting from 850 °C resulted from an abundant yield of radical from phenol pyrolysis beyond 850 °C

3.1.3 Persistent Free Radical Formation From Phenol

As it can be seen from the graph of **Figure 3.2**, the temperature dependence of radical formation from pyrolysis of phenol shows different shape of radical EPR spectra. At low temperature (< 450 °C) a clean 6 line spectrum was observed. As the temperature increases, the EPR spectra show increased shoulder, evidence that the EPR spectra at temperature higher than 400 °C are the convolution of several gas-phase formed radicals trapped onto the cold finger of the Dewar.

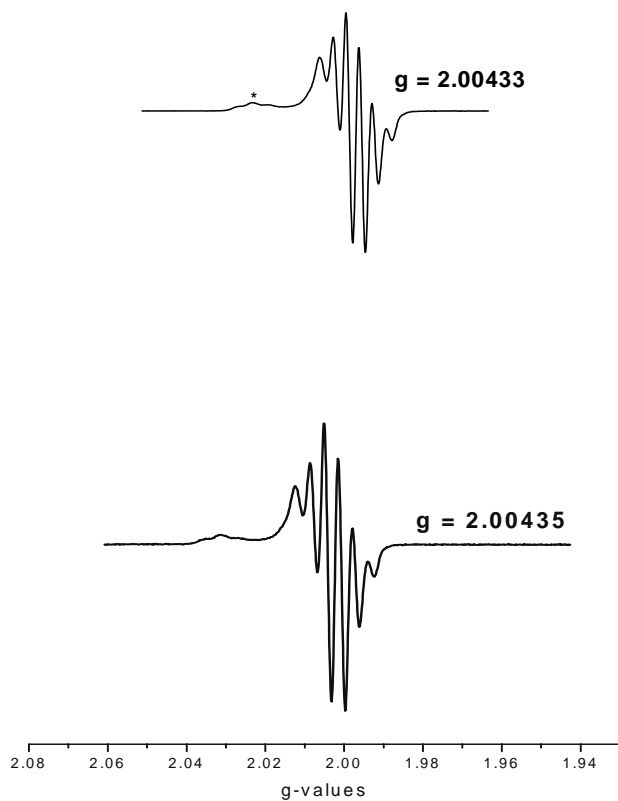


Figure 3.3 A representative EPR spectrum from the pyrolysis of phenol above 850°C (bottom spectrum) compare to its EPR spectrum at 750°C (top spectrum)

The 77 K EPR initial spectra from phenol pyrolysis at 950 °C, (**Figure.3.3**) are similar to the previously reported spectra from the gas-phase pyrolysis of of phenol at 750 °C ¹. At temperature below 750°C, The EPR spectra resemble the high-temperature pyrolysis spectra, but with somewhat altered spectral intensities

The LTIM EPR technique, in spite of its many advantages, is limited in identification of trapped radicals when the observed EPR spectra arise from two or more species ¹. One of the principal EPR spectral identification parameters, apparent g-value (as a maximum point of the integrated curve), does not convey conclusive structural information when the EPR spectrum is a convolution of two or more species. Constituent radicals in a mixture can only be distinguished by judicious variation of the experimental conditions (temperature, pressure, annealing

parameters etc) followed by computer analysis of digitally stored spectra. This procedure was used to simplify EPR spectra of gas-phase radicals trapped from phenol pyrolysis over the wide temperature region of 400 to 1000 ° C. As it will be clear from chapter 4, phenoxy and cyclopentadienyl (CPD) radicals EPR spectra were identified giving the evidence of phenoxy and CPD radicals being dominant potentially environmentally persistent free radicals in different temperature domain during the pyrolysis of phenol.

3.2 Low Pressure Pyrolysis of Hydroquinone

This paragraph shows results from low pressure pyrolysis of Hydroquinone over a temperature range of pyrolysis 350 to 1000°C at a total working pressure of ~ 0.1 Torr.

We employed the technique of the Low Temperature Matrix Isolation (LTMI) EPR ¹, in which hydroquinone vaporized at 75 ° C was pyrolyzed in a low pressure reactor (0.01- 0.1 torr) which was directly connected to a liquid nitrogen-cooled cold finger situated within the EPR cavity of a Bruker EPR spectrometer **Figure 2.3**

3.2.1 Total Radical Yield

Unlike the accumulation time dependence of phenol which followed a linear trend in all temperature domains, the time dependence of hydroquinone pyrolysis as well as of catechol reached saturation towards the 10-12 min radical accumulation. More importantly, in the pyrolysis of hydroquinone as of catechol, there was a decrease in radical intensity beyond 800° C

3.2.2 Temperature Dependence of Radical Yield

The 77 K EPR spectra from Hydroquinone pyrolysis over the temperature range of 350 to 975 °C as well as total radical yields vs. temperature is presented in **Figure 3.4**. As can be seen, the total radical yields increase from 350 to 850 ° C and decreases at higher temperature. Based on the identified types of radicals, three temperature region can be fairly divided: low

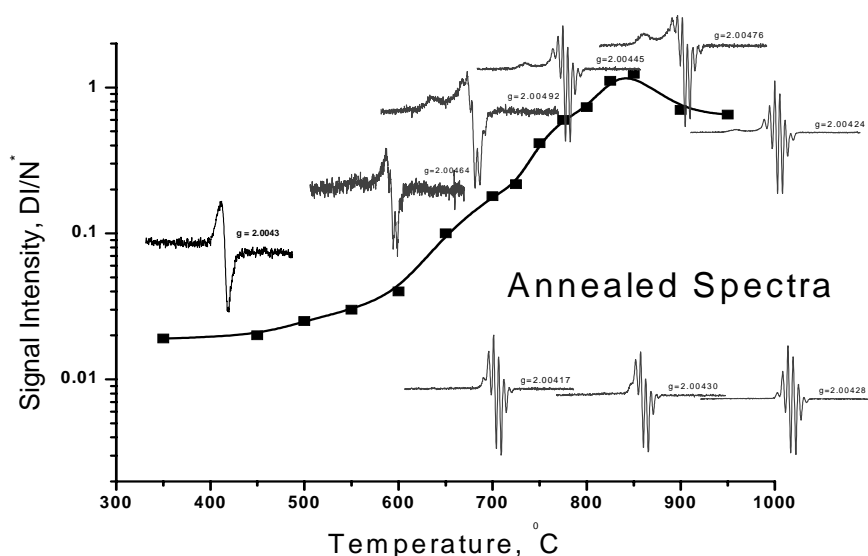


Figure 3.4 Temperature dependence of the total radical yields from the low pressure pyrolysis of hydroquinone in flow of CO₂ carrier gas (0.2 torr). DI/N value is the double integrated (DI) intensity of the EPR spectrum that has been normalized (N) to account for the conversion time, receiver gain, number of data points and sweep width [<http://www.bruker-biospin.com/winepr.html?&L=0>]. Right side; the representative EPR spectra of carbon dioxide matrix isolated radicals from the pyrolysis of hydroquinone are depicted above the black line (as un-annealed spectra at 77 K, 1 scan) and below the line (as annealed spectra). Left side; the representative EPR spectra of carbon dioxide matrix isolated radicals from the low temperature pyrolysis (black line, 5 scan). All spectra were registered at characteristic parameters; sweep width 200G, modulation amplitude 4G, time constant 5.12ms, microwave power 5mW.

above 850 °C DI/N value is the double integrated (DI) intensity of the EPR spectrum that has been normalized (N) to account for the conversion time, receiver gain, number of data points and sweep width [<http://www.bruker-biospin.com/winepr.html?&L=0>].

temperature region from 350 to 725 C where neutral p-semiquinone, p-SQ (p-hydroxyl phenoxy) radicals are dominant, high temperature region from 850 to 975 C where

Unlike the time dependence of phenol which followed a linear trend in all temperature domains, the time dependence of hydroquinone as well as of catechol reached saturation towards the 10-12min radical accumulation. More importantly, in the pyrolysis of hydroquinone as of catechol, there was a decrease in radicals intensity beyond 800 °C as depicted in **figure 3.4** cyclopentadienyl radicals (CPD radical) are dominant, and intermediate temperature region from 725 to 975 C where a mixture of p-SQ and CPD radicals exist

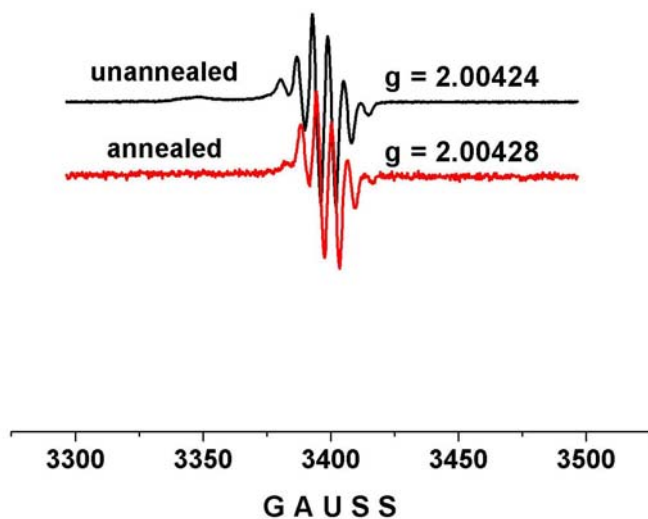


Figure.3.5 EPR spectra of frozen radicals from HQ pyrolysis at 950 C registered at sweep width 200 G, modulation 4 G, time constant 5.12 ms, and microwave power 5 mW. Black line is the un-annealed while the red line is the annealed EPR spectra of radicals.

3.2.3 Persistent Free Radical formation From Hydroquinone

If the nature of radicals from HQ pyrolysis generally is clear in low temperature (p-semiquinone) and high temperature regions (cyclopentadienyl radicals), their nature in the intermediate temperature region 725 to 850 °C is not straightforward. Based on proposed HQ

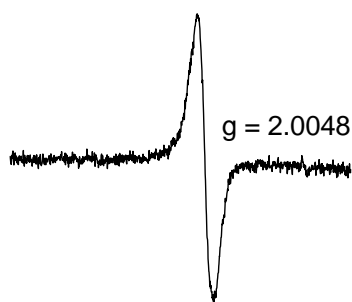


Figure 3.6 ERP featureless singlet line from the pyrolysis of HQ at temperature below 600°C

pyrolysis mechanisms^{1, 29, 30} CPD radicals, p-semiquinone, phenoxy, phenyl as well as

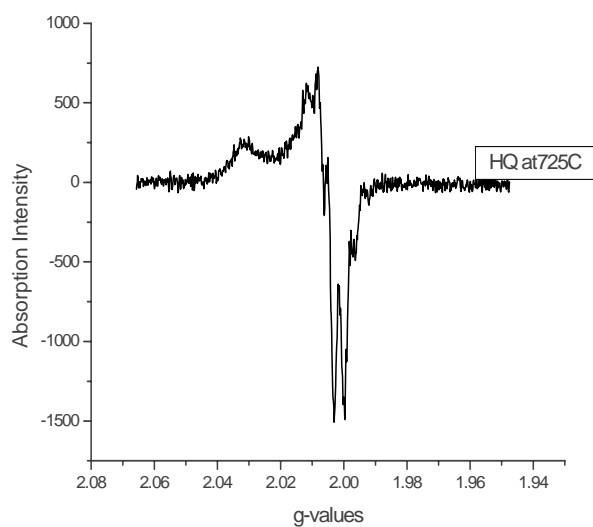


Figure 3.7 Representative EPR Spectra from the Pyrolysis of HQ at 700-800°C.

hydroxycyclopentadienyl (OHCPD) radicals all be formed. In the discussion (chapter 4), we will present some experimental evidences of coexistence of these mentioned radicals.

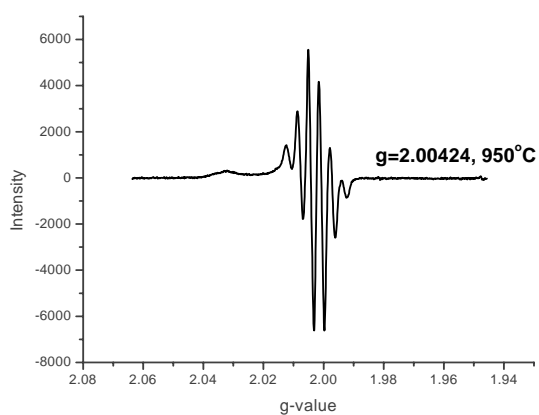


Figure 3.8 A Representative EPR spectrum from the pyrolysis of HQ at 800-1000°C

3.3 Low Pressure Catechol Pyrolysis

In the catechol pyrolysis experiments, catechol in solid state is vaporized at 75°C in an electrically heated vaporizer. The gas was pumped through a flow reactor which temperature is varied from 300 to 1000 °C. The feed rate of catechol is calculated by dividing the weight of catechol used by the time it elapses. The effluent pyrolysis products were condensed onto the finger of the Dewar cooled by liquid nitrogen. .Despite

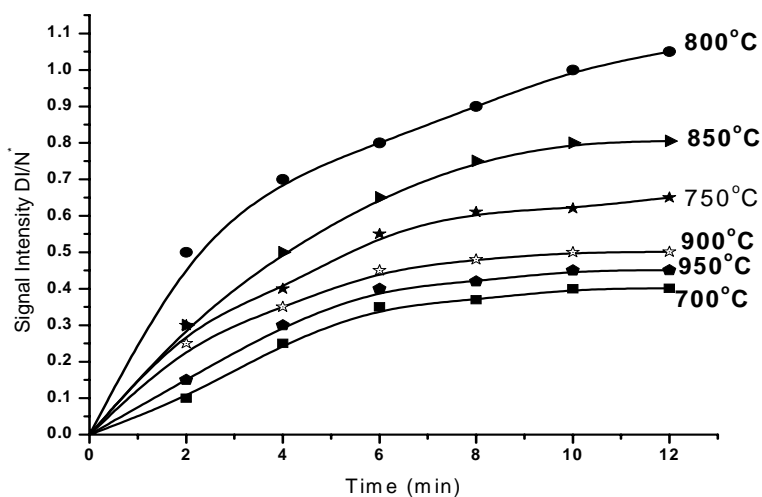


Figure 3.9 Time dependent accumulation of radicals from the pyrolysis of catechol. A non-linear trend was obtained at all temperatures where saturation is reached between 10 and 12 minutes of accumulation of radicals. The signal intensity DI/ N is the Double Integration (DI) of the surface area of the first derivative EPR spectrum normalized to N to account for the conversion time, receiver gain, number of data points, and sweep

the numerous advantages of LTMI-EPR technique, it is limited in identifying trapped radicals when the observed EPR spectra comprise more than one species ¹. Even the apparent g-value, one of the principal EPR spectral identification parameters does not convey conclusive structural information when the EPR spectrum is a convolution of two or more species²⁹. Therefore additional experiments were designed to appropriately distinguish radicals in a complex mixture arising from the gas-phase pyrolysis of

catechol. This comprises the photolysis at room temperature of catechol, the generation of pure CPD radical employing the tricarbonylcyclopentadienylmanganese, the computer analysis of digitally stored spectra acquired over a wide temperature range of 300-1000°C.

3.3.1 Total Radical Yield

The time dependence radical accumulation from the pyrolysis of CT shows trends that resemble those of HQ. A non-linear trend characterizes the accumulation of radicals from catechol pyrolysis where saturation is reached between 10 and 12 minutes of accumulation (Figure.3.9).

3.3.2 Temperature Dependence of Radical Yield

As the temperature dependence of radical yield of HQ pyrolysis, there is an increase of radical yield as the temperature increases. A maximum radical yield was observed around 850°C, followed by a decrease in yield as the temperature increases. Different shapes of radical EPR

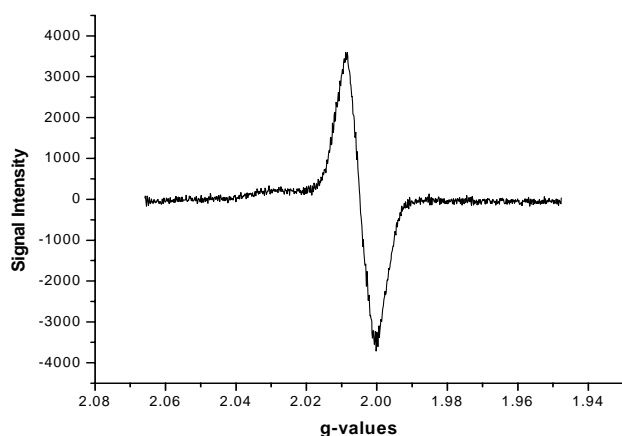


Figure 3.10 A representative EPR spectrum from the pyrolysis of CT at 400-600°C with $g = 2.00481-2.00610$, $\Delta_{p-p} = 14.480-15.780$ signal were observed.

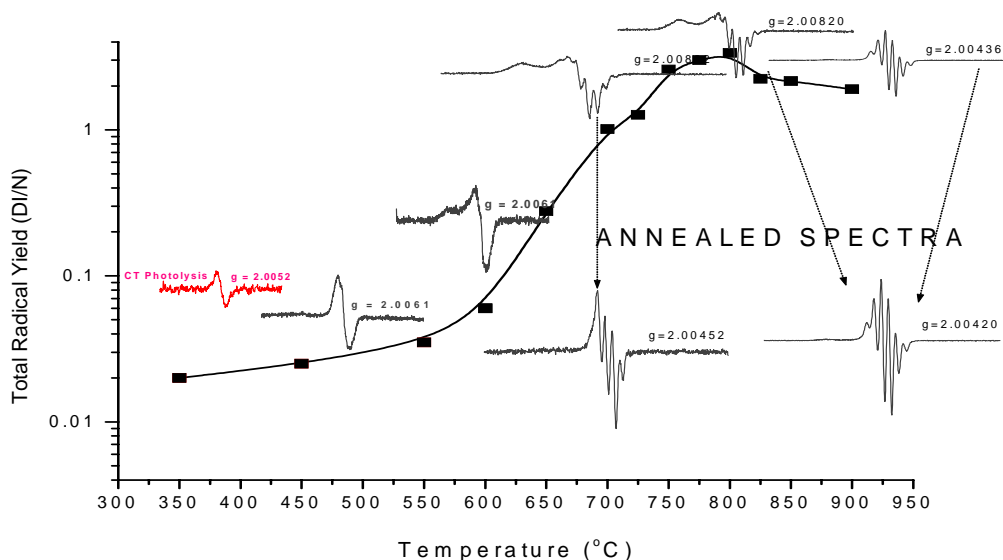


Figure 3.11: Temperature Dependence of Total Radicals Yield from the Gas-phase Pyrolysis of Catechol. An increase of signal intensity obtained by the Double Integration of the EPR first derivative signal normalized to N was observed that reached a maximum value at 750-800°C.

3.3.3 Persistent Free Radical From Catechol

As the pyrolysis temperature of CT increases, the shape of radical EPR spectrum varies from a singlet line at around 500°C to 6 line spectra with increase shoulder. This gives evidence that several radicals are formed during pyrolysis of CT and trapped onto the cold finger of the the liquid nitrogen cooled Dewar

3.4 Pyrolysis of Tobacco

After the detailed study of mainstream Tobacco smoke major components³⁶⁻³⁹ which are catechol, hydroquinone and phenols, allegedly causes of tobacco toxicity⁴⁰⁻⁴⁵, the next step was to determine radicals that are formed during the pyrolysis of tobacco. The goal of this important endeavor was to compare radicals formed from the pyrolysis of the standards and tobacco in order to establish the necessarily link if any at all.

The overall pyrolysis experiments of tobacco have followed the same experimental

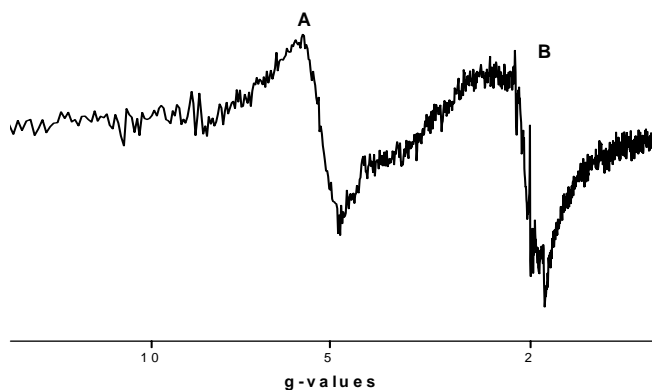


Figure 3.12 Overall width of raw BAT tobacco EPR spectrum.

procedures as for the precursors where the Low Temperature Matrix Isolation technique is coupled with EPR for the registration of the EPR signal of the frozen radicals arising from the gas-phase pyrolysis of tobacco at low and atmospheric pressure conditions. The carrier gas used in the pyrolysis study of tobacco was nitrogen. Four blends of tobacco obtained from Phillips Morris USA (Virginia, Burley, Oriental, and Mix) were employed in the low pressure study. For the atmospheric pressure study, we employed three blends (Bright, Burley, and Oriental) provided by British American Tobacco company. **Figure 3.12** The apparent singlet line marked A has a high g-value = 5.17122 while the six line splitting marked B with a g-value = 2.07221 represents a superposition of Manganese and organic radicals in tobacco.

3.4.1 Free Radical Yield

Figure 3.12 depicts the EPR spectrum of Tobacco in a wide magnetic field that shows the metallic contents of tobacco. The singlet line marked A represents iron EPR spectrum (literature) with high g-value = 5.17122 and total width $\Delta H_{total} = 210.934$ and the six lines spectrum

marked B depicts the superposition of manganese and organic radical in tobacco with a g-value = 2.07221 and $\Delta H_{\text{Total}} = 521.4\text{G}$.

A restriction of the magnetic field to measure only the organic radical in raw tobacco is

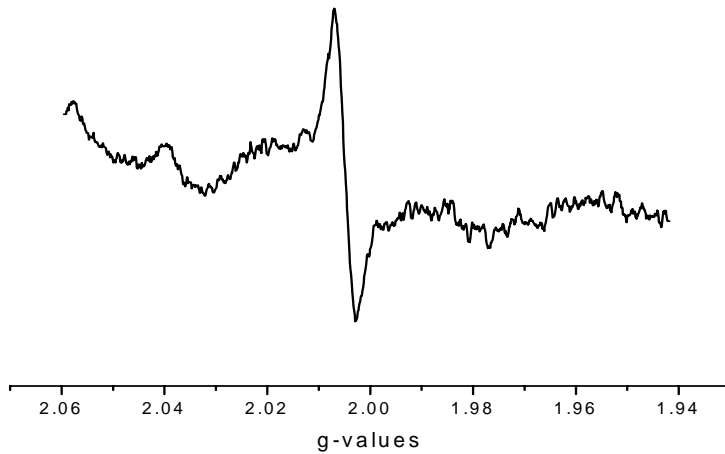


Figure 3.13 EPR spectrum of Organic radical in raw tobacco $g = 2.00474$ at the center with $\Delta H_{p-p} = 7.227\text{G}$

represented in **Figure 3.13** where the g-value = 2.00474 and $\Delta H_{p-p} = 7.227\text{G}$.

3.4.2 Persistent Free Radical From tobacco

The low and atmospheric pressure pyrolysis of all blends of tobacco yielded noisy,

Table 3.1 Concentration of Free Radical from four blends of Tobacco

| | Virginia | Burley | Mix | Oriental |
|--------|----------|--------|-------|----------|
| DI/N * | 0.0278 | 0.0727 | 0.138 | 0.0316 |

featureless singlet line EPR spectra. **Figure 3.15** presents the typical EPR spectrum from Virginia blend, a representative spectrum for all three blends.

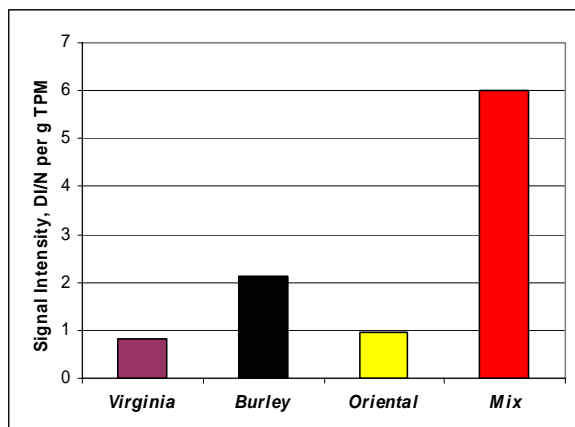


Figure 3.14. Radical yields observed in TPM condensed directly on the cold finger from gas phase pyrolysis of four tobacco blends. .

DI/N value is the double integrated (DI) intensity of the EPR spectrum that has been normalized (N) to account for the conversion time, receiver gain, number of data points and sweep width [<http://www.bruker-biospin.com/winepr.html?&L=0>]

Given the complexity of tobacco due to its numerous organics and inorganic components, collecting the Total Particulate Matter (TPM) on the filter gives insights of radicals production.

Figure 3.14 depicts the radical intensity yields collected on the cold finger of Dewar during the gas-phase pyrolysis of four blends of tobacco (Virginia, Burley, Oriental, and Mix).

3.5 Additional Experiments

The LTIM EPR technique, in spite of its many advantages, is limited in identification of trapped radicals when the observed EPR spectra arise from two or more species ¹. One of the principal EPR spectral identification parameters, the apparent g-value (as a maximum point of the integrated curve), does not convey conclusive structural information when the EPR spectrum is a convolution of two or more species. Constituent radicals in a mixture can only be distinguished by judicious variation of the experimental conditions (temperature, pressure, annealing parameters etc) followed by computer analysis of digitally stored spectra. Consequently, we performed additional experiments to clearly identify gas-phase radical EPR spectra of individual radical. The paragraphs will present the experiments along with the results they allow to achieve

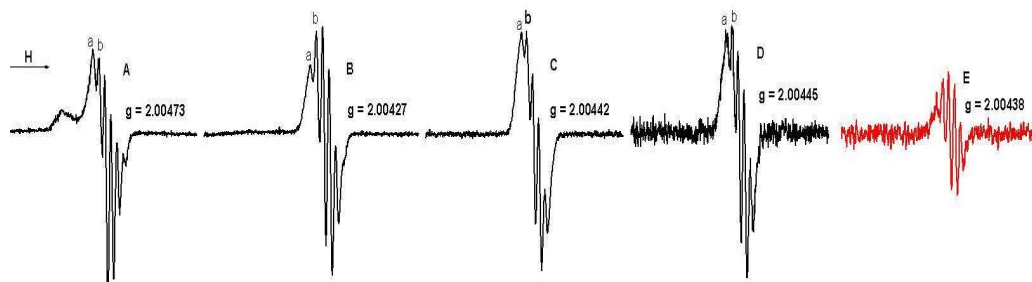


Figure 3.16 The step by step annealing of radicals from pyrolysis of phenol at 700 °C. All spectra were registered at the same conditions (Sweep width - 200G, modulation amplitude - 4G, microwave power - 20 mW, time constant - 5.12ms).

3.5.1 Annealing Experiments

During the pyrolysis experiments of CT, HQ, and phenol, radical EPR spectra were acquired during radical accumulation time. At the end of the accumulation period, the sample transfer line was close, thus the hot carrier gas which contact with the cold finger of Dewar that was

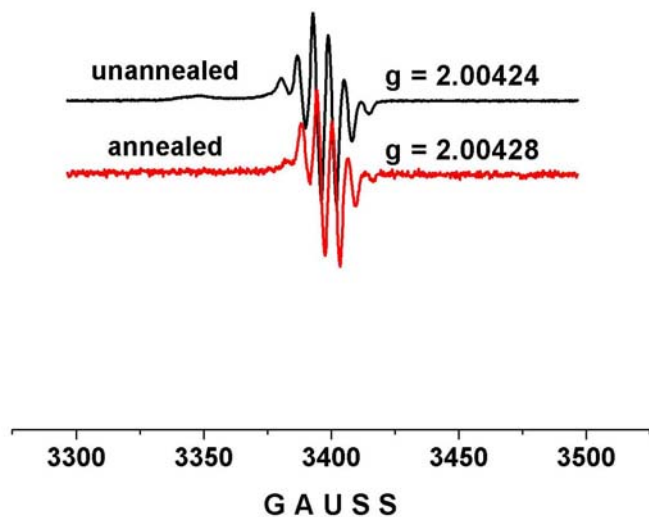


Figure.3.17 EPR spectra of frozen radicals from HQ pyrolysis at 950 C registered at sweep width 200 G, modulation 4 G, time constant 5.12 ms, and microwave power 5 mW. Black line is the un-annealed while the red line is the annealed EPR spectra of radicals.

/causing the boiling of liquid nitrogen is removed. This allowed acquisition of the last EPR

radical under less noisy conditions. We termed the last acquired EPR spectrum “initial radical EPR spectrum. In fact the initial radical EPR spectra are convolution of several radicals trapped onto the cold finger of the Dewar. The annealing experiments allow annealing the matrix, thus annihilating the more reactive radicals that diffuse and recombine as neutral molecules leaving in the spectrum the more persistent individual radicals. **Figure 3.16,3.17, 3.18.** show annealing results of initial EPR spectrum from the pyrolysis of phenol, hydroquinone and catechol respectively.

As it can be seen, in our annealing experiments, the more persistent free radical EPR spectra exhibit a sextet with intensity distribution of 1:5:10:10:5:1, a g-value of 2.00420-2.00504, hyperfine splitting constant of 6.02 G, and a peak-to-peak width of 3.01 G, characteristics of

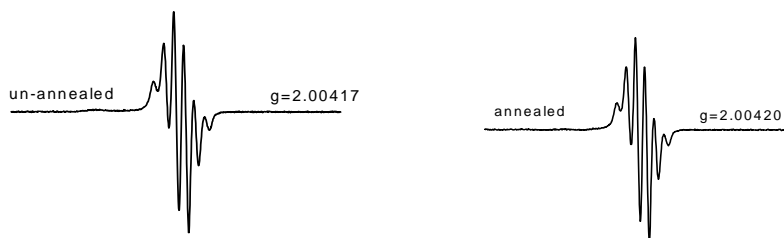


Figure 3.18. EPR spectra of carbon dioxide matrix isolated radicals from the pyrolysis of catechol at 850 °C before (un-annealed spectrum, $DI/N^a = 1.120$) and after annealing (middle spectrum, $DI/N^a = 1.114$). (^a DI/N value is the double integrated (DI) intensity of the EPR spectrum that has been normalized (N) to account for the conversion time, receiver gain, number of data points and sweep width [<http://www.bruker-biospin.com/winepr.html?&L=0>].

CPD radicals. The microwave power dependence experiments allow to observe some more radicals that annealing experiments could not allow.

3.5.2 Microwave Power Dependence Experiments

The power dependence of EPR spectra of radicals at 77 K from phenol pyrolysis at 700 °C, phenol photolysis at room temperature, and CPD radicals from $\eta^5\text{-C}_5\text{H}_5\text{Mn(CO)}_3$ pyrolysis at 250 °C are presented in **Figure 3.19**. CPD radical spectra were observable up to microwave

powers of 36 – 40 mW with insignificant saturation occurring at powers even greater than 40 mW. CPD radical spectra did not change in shape or intensity distribution over the entire region, which is consistent with reports in the literature¹⁹, while pure phenoxy radicals saturated easily at less than ~ 1.5 mW (triangles, dotted line in **Figure 3.19**). It is also evident from **Figure 3.19** that the magnetic susceptibility of phenoxy radicals at microwave powers less than 2 mW is significantly higher

than that of CPD radicals while at higher power, this is reversed. If we assume a mixture of these two radicals, we would expect an intermediate saturation behavior of this mixture as is the case of the EPR spectra from pyrolysis of phenol (cf. **Figure 3.19**), which begins to saturate at powers less than 10 mW.

The large magnetic susceptibility of CPD radicals at high power (20 mW)), causes the EPR spectra resulting from the pyrolysis of phenol (cf. **Spectrum A in Figure 3.20**) to be dominated

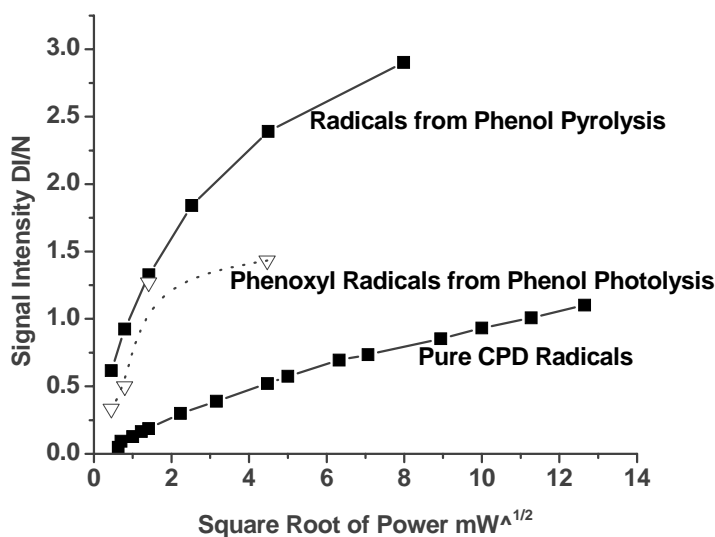


Figure 3.19 Microwave power dependence of CPD radicals at 77 K from pyrolysis of η^5 - $C_5H_5Mn(CO)_3$ at 250 °C (squares), radicals from phenol pyrolysis at 700 °C (circles) and phenol photolysis (triangles).

by the CPD spectrum. Decreasing the power, results in relative growth of two peaks marked “a” and “b” that resemble that of phenoxyl radicals (compared with overlaid spectra of pure phenoxyl radical, red line in spectrum D). Subtraction of the EPR spectrum of phenoxyl from spectrum D results in spectrum E that clearly resembles that of CPD. This is additional evidence of existence of phenoxyl as well as CPD radicals from phenol pyrolysis at 750 °C.

3.5.3 Photolysis of Phenol, Hydroquinone and Catechol

The goal of the photolysis experiments was to generate pure free radical EPR spectrum from the photo-dissociation of the hydrogen atom of the hydroxyl group of phenol, hydroquinone and catechol to compare to radical EPR spectra generated from the pyrolysis of the precursors.

- Photolysis of Phenol

The aim of the photolysis reaction of phenol is to generate pure phenoxy type radical to

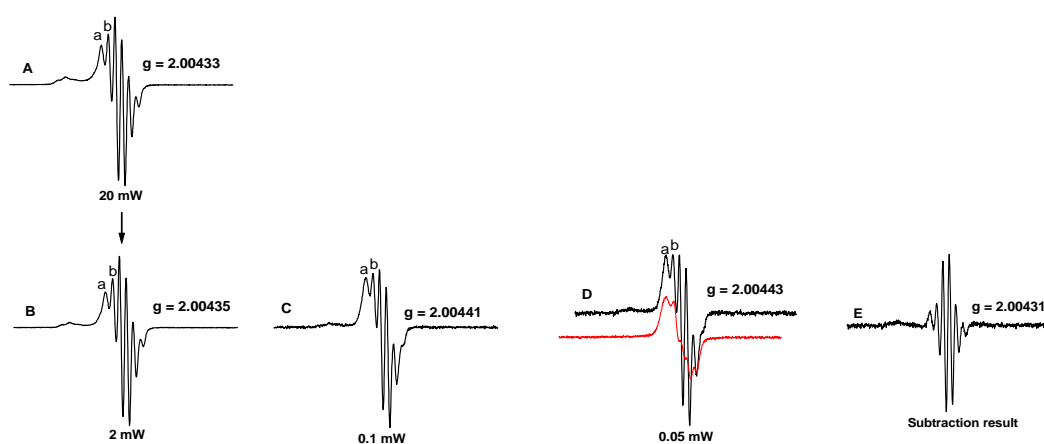


Figure 3.20. Effect of microwave power on the 77 K EPR spectra of radicals from the pyrolysis of phenol at 750 °C is depicted in spectra A-D. Overlaid in red in Spectrum D, is the EPR spectrum of pure phenoxyl radical. The peaks labeled a and b are the most dependent on microwave power. Subtraction of the spectrum of pure phenoxyl radical from spectrum D result in the residue spectrum E, which is characteristic of CPD radical.

compare with radicals observed during the gas-phase pyrolysis of phenol at low temperature domain. . It is known that 250 to 300 nm photoexcitation of phenol in solution results in its partial photo-dissociation to phenoxyl radical and a hydrogen atom ^{7, 9, 10}. The EPR spectrum from the room temperature, low pressure, photolysis of phenol vapor in CO₂ flow (total pressure ~ 0.2 torr) using the LTMI EPR technique is depicted in **Figure 3.21**. This broad spectrum consists of 5 nonresolved lines with apparent $g = 2.00600$ at 77 K in a carbon dioxide matrix and microwave power 0.202mW. A very complex spectrum, 15 or more lines, of phenoxyl radicals has been reported in liquid media ¹¹⁻¹³.

- Photolysis of Hydroquinone

In this study, the UV gas-phase photolysis of HQ was carried out using the same

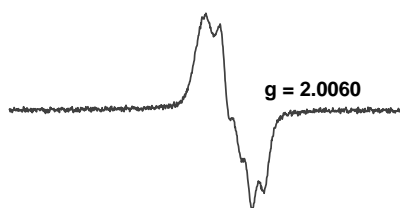


Fig 3.21: Photolysis of Phenol at room Temperature. A very broad 5 un-resolved lines spectrum with $g = 2.0060$

experimental equipment for pyrolysis. Instead of pyrolysis reactor as a photolytic cell a simple suprasil 1 quartz tube was used which was irradiated by UV light at 253.7nm from the side.

The aim of photochemical experiments of HQ was straightforward: generate oxygen-centered phenoxy type of radicals directly from the gas phase photolysis of suitable precursors at lower temperatures and freeze them at liquid nitrogen temperature. The huge advantage of photolysis is that it is possible to prevent thermal degradation of formed radicals and transfer them at low pressure to cold zone for EPR acquisition.

A singlet line EPR spectrum comparable to the HQ pyrolysis EPR spectrum at 350 ° C was observed. **Figure 3.22** depicts the photolysis of HQ.

- **Photolysis of Catechol**

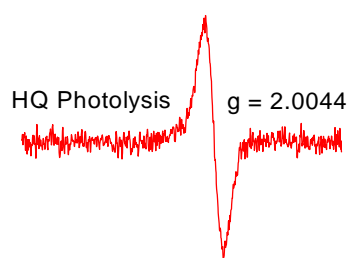


Figure 3.22. EPR spectrum of the products of the photolysis of HQ. A featureless singlet line characteristic of Para-Semiquinone Radical

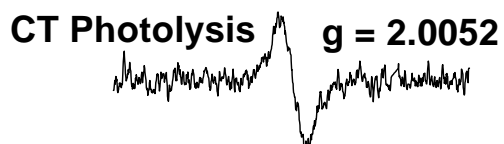


Figure. 3.23 CT) photolysis at room temperature yielded a very weak EPR signal with $g = 2.0052$, characteristic of oxygen-centered radical.

The photolysis of catechol at room temperature allows the oxygen-hydrogen homolytic bond dissociation, thus pertaining to the formation of the neutral O-semiquinone radical depicted in **Figure 3.23**. It may be argued the formation of radicals such as the neutral O-phenoxy di-radical from the elimination of both hydrogen atoms of the two OH groups of catechol, a biphotonic type radicals. Such a di-radical is highly unstable and will either decompose, transform, recombine or eliminate as neutral molecule³⁵.

3.5.4 Pyrolysis of Tricarbonyl-cyclopentadienylmanganese ($\eta^5\text{-C}_5\text{H}_5\text{Mn(CO)}_3$) at 250°C.

The mechanism of the gas-phase pyrolysis of $\eta^5\text{-C}_5\text{H}_5\text{Mn(CO)}_3$ has been thoroughly investigated⁸ using conventional and IR laser-powered homogeneous pyrolysis in combination with matrix isolation EPR spectroscopy. The decomposition was consistent with initial stepwise loss of CO, followed ultimately by release of CPD radical.

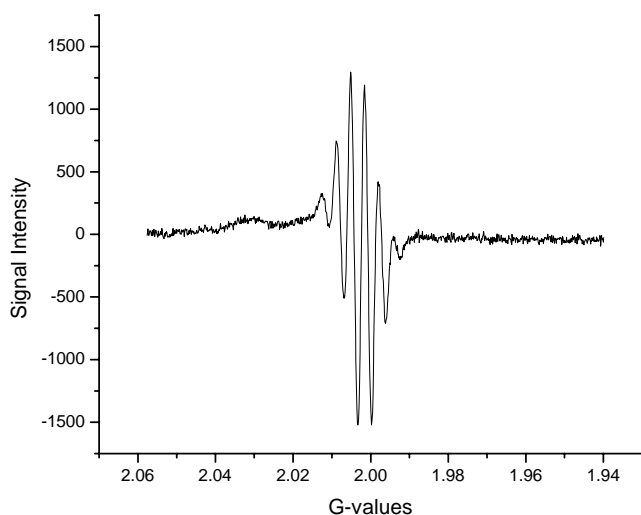


Figure 3.24 CPD EPR Spectrum of the Pyrolysis of Tricarbonylcyclopentadienylmanganese at 250°C. Pure CPD radical was generated with $g = 2.00438$, and $\Delta H_{p-p} = 3.32\text{G}$

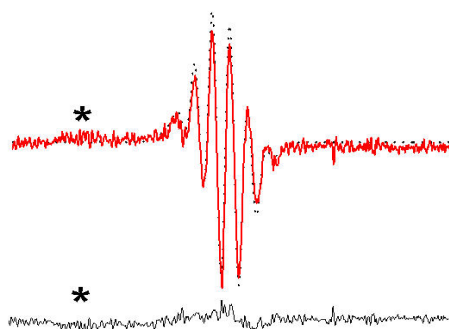


Figure 3.25. Comparison and subtraction of EPR spectra of carbon dioxide matrix isolated CPD radicals from the pyrolysis of ($\eta^5\text{-C}_5\text{H}_5\text{Mn}(\text{CO})_3$) at 250 °C (red line, $g = 2.00431$) with the annealed-residue spectrum of precursor pyrolysis at 950 °C (dotted line, $g = 2.00430$). The lower trace is the difference spectrum. The spectra were registered at a sweep width of 150 G, modulation amplitude of 4 G, time constant of 5.12 ms, microwave power of 5m W.

We generated CPD radicals from pyrolysis of $\eta^5\text{-C}_5\text{H}_5\text{Mn}(\text{CO})_3$ in a CO_2 gas flow at less than 0.2 Torr total pressure. The spectrum exhibits an isotropic 1:5:10:10:5:1 sextet. The EPR spectrum of these radicals was compared and subtracted from the annealed EPR spectrum of phenol, HQ and CT pyrolysis products at 950 °C (cf. **Figure 3.25, dotted black line**). Clearly the spectra are in excellent agreement, and the difference spectrum presented in the lower trace indicates that very few other radicals were present after annealing.

This mathematical subtraction of spectra clearly shows that at temperature above 800°C, phenol, HQ and CT pyrolysis yields CPD as dominant radical.

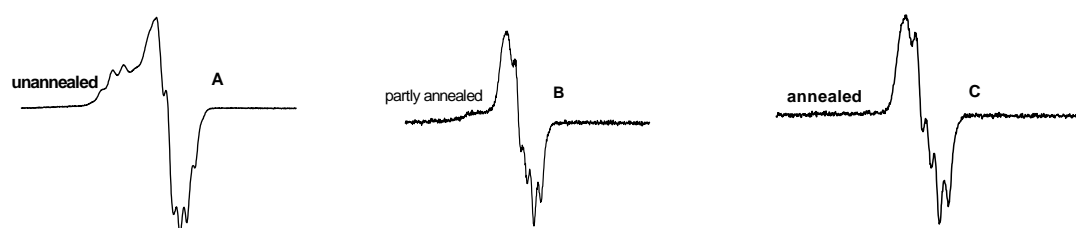


Figure 3.26. Step by step annihilation of initial spectrum A ($g = 2.00745$) to the final phenoxyl radical spectrum C ($g = 2.00582$). EPR spectra registration conditions: sweep width - 200G, modulation amplitude - 4G, time constant - 5.12ms, microwave power - 5mW. The control reaction of 450 ppm of DTBP in a carbon dioxide flow produced a very weak anisotropic signal.

3.5.5 Pyrolysis of Di-tert-butylperoxide

Di-tert-butylperoxide (DTBP), when pyrolyzed at 250°C yields the tert-butoxy radical. The pyrolysis of DTBP was used to generate phenoxy radicals through reacting the radicals produced by its decomposition with phenol¹⁴⁻¹⁶:

1. $t\text{-BuO-OBu-t} \rightarrow 2 t\text{-BuO}\cdot$
2. $t\text{-BuO}\cdot \rightarrow \text{Me}\cdot + \text{Me}_2\text{CO}$
3. $t\text{-BuO}\cdot + \text{RH(PhOH)} \rightarrow t\text{-BuOH} + \text{R}\cdot(\text{PhO}\cdot)$.

Accordingly, we pyrolyzed a mixture of 450 ppm of DTBP and 250 ppm phenol at 250 C in a flow of carbon dioxide (~0.2 torr). The EPR spectra at 77 K of the pyrolysis products are depicted in **Figure 3.26**. Step by step annealing of the matrix converted the un-annealed spectrum A ($g = 2.00745$) to intermediate spectrum B ($g = 2.00607$) and the fully annealed spectrum C ($g = 2.00582$) which matches exactly the spectrum of the photochemically generated phenol

3.5.6 Atmospheric Pressure Pyrolysis of Phenol, Hydroquinone, and Catechol

Atmospheric pressure pyrolysis of the precursors at 750°C was performed to see the influence of high gas-phase radical concentration on their EPR spectra. It should be expected that the more radicals are formed due to the higher sample concentration, the easier will be their radical-radical recombination to form neutral molecules

- **Atmospheric Pressure Pyrolysis of Phenol at 750°C**

atmospheric pyrolysis was undertaken from 400 to 750 ° C. The noticeable point about the atmospheric pressure pyrolysis of phenol is that the initial spectra are so noisy that any

reasonable assignment is possible. Most of the time, the short time accumulation of radicals, and the difficulty turning EPR cavity did not permit a time dependence of radical accumulation. Interestingly, after annealing of the matrix, very persistent radicals were observed that lasted more than one hour. Additionally, clear CPD radical was observed superposed to a very broad radical with total width of 156G. **Figure 3.27A**. Further annihilation permits to get spectrum in **Figure 3.27B**. At lower temperature, different shapes of radicals EPR spectra were observed. For instance, from 400 to 600 ° C, the spectra depicted in **Figure 3.27B** has characteristics close the those of Hydroxycyclohexadienyl (OHCHD) reported in the literature ^{23, 24}. The OHCHD type radicals have g value of 2.0028 ²⁴ and a total width of ~ 130 -135G. A g-value of 2.0028 is a pure carbon-centered radical. However, it can also characterize a carbon-centered

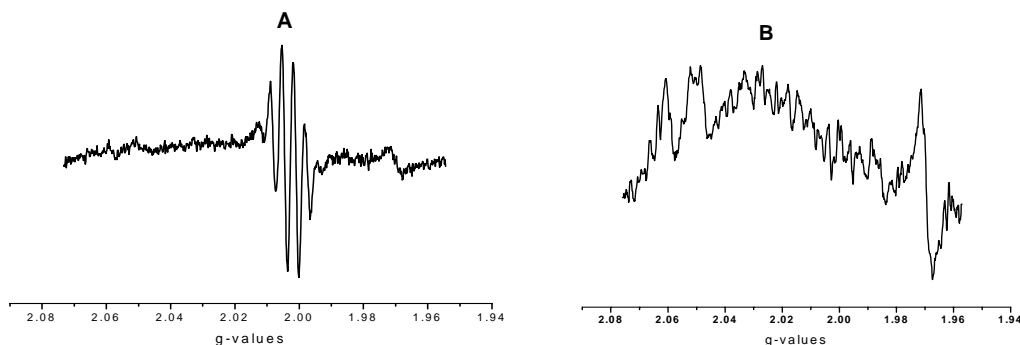


Figure 3.27 Atmospheric pressure pyrolysis of Phenol at 750 ° C. Very persistent superposition of radicals was observed. A: after annihilation with a total width of $\Delta H_{Tot}=156G$, clearly shows the sextet characteristic of CPD which is superposed with other unidentified radicals, and $g= 2.00455$. B: after further annihilation $\Delta H_{Tot}=136G$ close to that of hydroxycyclohexanedieryl radical.

radical which carbon atom is vicinal to an oxygen atom²⁵. The radical EPR spectrum in **Figure 3.27B** has a g-value 2.00334, and a total width of 136G vs. 2.0028 and 130-135G

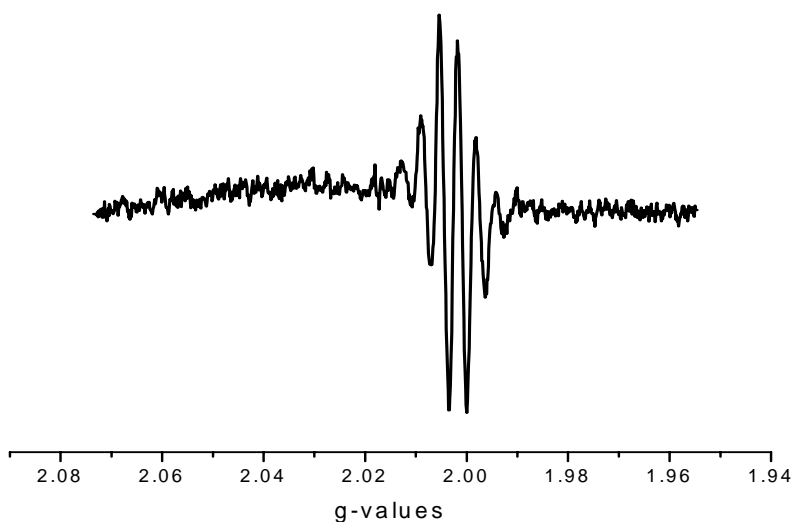


Figure 3.28 Apparent superposition of several radicals: CPD arises from the known sextet; phenoxy radical as shown by the broadening of the first line of the spectrum; an additional seventh line on the right side of the spectrum, evidence of the presence of an un-identified radicals.

reported respectively for OHCHD radical in the literature^{23, 24} Also the broadening of the first line in the spectrum presented in **figure. 3.28** shows presence of phenoxy radical that has already been identified²⁶. A seventh line could be observed in addition to the regular CPD radical sextet and intensity distribution, giving the evidence of the presence of an un-identified radical. CPD radicals, unlike the low pressure pyrolysis were dominant even at low temperature. This may be due to the fact that phenoxy radicals, due to it high pressure react to form PCDD/F or Hydroxy naphthalene, therefore disappear from the system as will be seen in the discussion part of this work.

- **Atmospheric Pressure Pyrolysis of Hydroquinone**

As in the case of phenol, the goal of the atmospheric pressure pyrolysis of Hydroquinone is two fold: First it consists in having a close look to the change in radical formation induced by the high gas pressure. Second, the simultaneous accumulation of gas-phase formed radicals and pyrolysis products collection in a trap allows GC-MS analysis to determine the very unstable radicals that condense to form molecular products. The atmospheric pyrolysis of hydroquinone was performed at 750 °C.

Unlike the low pressure pyrolysis at the same temperature where very weak and non-well resolved EPR spectra were registered at the beginning of the accumulation process, the atmospheric pressure pyrolysis yields well resolved and strong EPR signal at the beginning of the accumulation. It is clear that CPD is dominant radicals at this temperature while in the low pressure pyrolysis, a complex mixture of radicals was detected. **Figure 3.29** shows the EPR spectrum of radical at 6min accumulation time. It is clear this is a superposition of several radicals. However, the CPD sextet can be very well seen. Annealed and further annealed spectra show a clear dominance of CPD radicals.

- **Atmospheric Pressure Pyrolysis of Catechol**

As in the cases of phenol and hydroquinone, the low pressure pyrolysis of CT has been performed. **Figure.3.30** represents typical radical EPR spectrum from the pyrolysis of CT. The first line of the EPR spectrum is broadened. This is the evidence of the superposition of at least two radicals from which the sextet clearly indicates CPD radicals. The same broadening seen in the case of the pyrolysis of HQ is also seen here, giving evidence of the formation of phenoxy r.

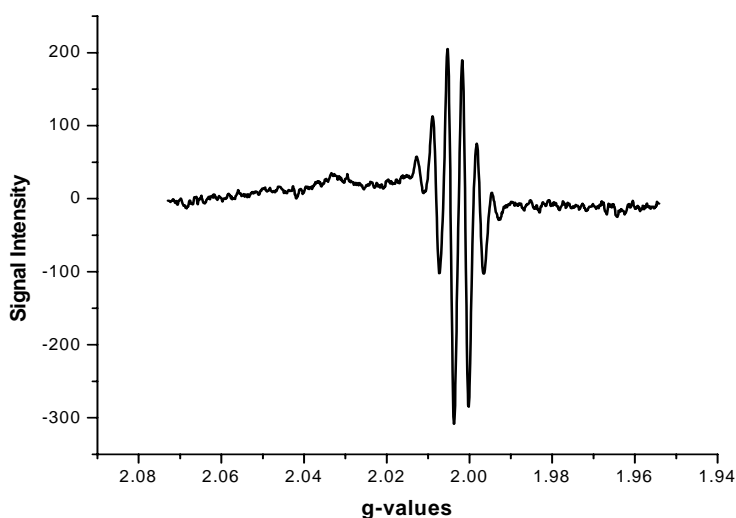


Fig.3.29 Atmospheric Pyrolysis of HQ. Strong and well resolved EPR spectra with shoulder at the beginning of accumulation of radicals. CPD radical is superposed to unknown radicals.

3.5.7 Effects of Trace of Oxygen on Radical: Case Study of Hydroquinone

Tobacco smoking is a process that involves oxygen. Thus it is important to have a close look at the effects of oxygen on the standards, major components of mainstream tobacco smoke

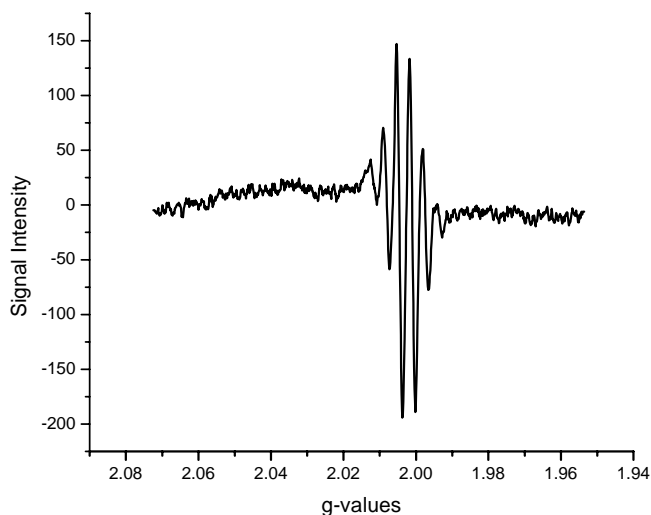


Figure 3.30 EPR spectrum of radicals from the atmospheric pressure pyrolysis of CT. The broadening of the first spectrum line is indicative of superposition of at least two radicals. The sextet represents the CPD. The more likely cause of the broadening of the line is phenoxy radical.

which are catechol, hydroquinone and phenols³⁶⁻³⁹. In this endeavor, we use hydroquinone as

case study, varying oxygen concentration from 15 to 700ppm. The following paragraphs report on the interesting findings.

- **The Oxygen EPR signal Associated with the EPR signal of pyrolyzed HQ**

The LTMI EPR technique is a great tool to identifying the trace amounts of oxygen in a sample frozen on cold finger ⁴⁶. The presence of oxygen in the pyrolysis system can be directly viewed from the two sides of EPR spectra (**Figure. 3.31, black line**), which represents the most important oxygen line known as E line ($K=1, J=2, M=1 \rightarrow 2$ ⁴⁶.) Note that the oxygen peaks in both sides of initial spectrum can be removed easily by annealing procedure (**Figure.3.31, red line**). The black line is a convolution of two radicals: the p-SQ radical that we had already identified from both the pyrolysis below 600 ° C and the room temperature photolysis of HQ

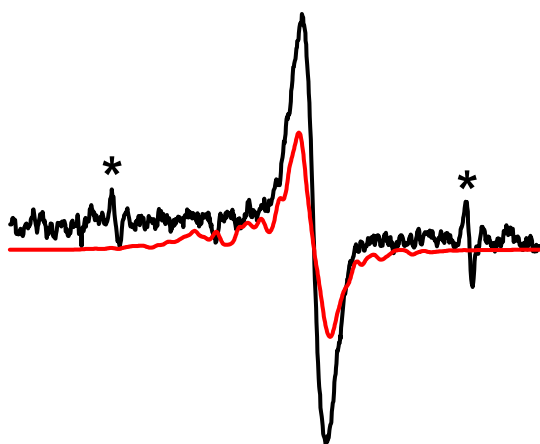


Figure.3.31 Frozen p-SQ radicals EPR spectra from pyrolysis of HQ at 550 ° C: the black line is un-annealed spectrum (peaks with asterisk represent adsorbed molecular oxygen), the red line after annealing. (Fig. 4, red line); and the Oxygen radicalspectrum marked by * in the black line of **Figure3.31**

- **Effects of Oxygen Concentration on the Nature of Radicals**

We have pyrolyzed HQ in varying Oxygen concentrations from 15 to 700 ppm. The lowest concentration of O₂ was ~ 15 ppm. This value corresponds to the background vacuum value of

10^{-4} torr of air. The spectrum of radicals from HQ pyrolysis was assigned as **A** in **Figure.3.32**.

Increasing oxygen concentration in the carrier gas up to 700 ppm and higher leads to the formation of broader spectra **B** (~ 350 ppm O_2) and **C** (at 700 ppm O_2 and higher). The mathematical difference **C-A** gives EPR spectrum which is typical for the RO_2 and, particularly CH_3O_2 radicals well documented in the literature by the shape and overall spread (~ 75 -80 gauss), hyperfine splitting in the bottom of spectra ~ 5.42 G and high g value 2.010 at crossing of the base line^{3, 46}. The rationale of the formation of CH_3O_2 radical during pyrolysis of HQ in trace of oxygen will be discussed in chapter 4.

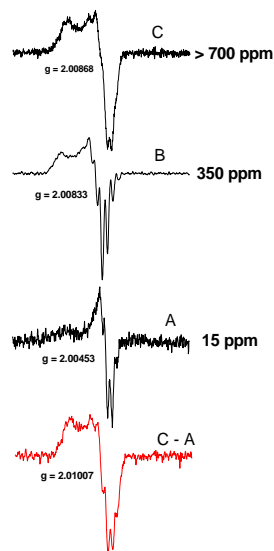


Figure 3.32 The effect of oxygen on the shape of the EPR spectra of frozen radical from the pyrolysis of HQ at $750^\circ C$. The spectrum **C-A** subtraction represents CH_3O_2 radicals EPR spectrum

3.5.8 GC-MS Analysis of Products of Atmospheric Pressure Pyrolysis of Phenol Hydroquinone and Catechol

The GC-MS experiment is additional experiment to analyze the pyrolysis products distribution during the gas phase atmospheric pressure pyrolysis of the precursors. A liquid nitrogen cooled trap was set on the atmospheric line of **figure 2.4**. Simultaneous radical accumulation on the cold finger of the Dewar and pyrolysis products accumulation in the trap were performed. The chromatogram showed in addition to several other compounds the formation of naphthalene. This result is consistent with the literature²⁷. Naphthalene is known to form from the condensation of two CPD radicals as shown in **Scheme 1.6**²⁸.

The GC-MS analysis of the products of the pyrolysis of hydroquinone reveals beside the formation of naphthalene as the result of the condensation of two CPD radical, interesting two ring compounds such as indene and hydroxyl-indene. As we will discuss in chapter 4, the GC-MS detection of indene and hydroxyl-indene is the evidence that hydroxycyclopentadienyl (HO-CPD) radical is formed, but recombines either with CPD or another HO-CPD to form either indene or hydroxyl-indene through CO elimination

The GC-MS analysis of the products of Catechol pyrolysis reveals formation of fluorene ($m/z = 166$), and 1H-Indenol ($m/z = 132$) and its isomer 1H-Inden-1-one_2,3_ dihydro, acenaphthylene ($m/z = 152$), Benzofuran-7-methyl, Benzofuran-2-methyl ($m/z = 132$). As will be shown in chapter 4, the products of Catechol pyrolysis give additional evidence of both labile and persistent radical formation

3.6 References

1. L. Khachatryan, Adoukpe, J., Maskos, M., and Dellinger, B., "Formation of Cyclopentadienyl Radicals from the Gas-Phase Pyrolysis of Hydroquinone, Catechol, and Phenol," *Environ. Sci. Technol.*, *40*, 5071-5076 (2006).
2. A.A. Mantashyan, Khachatryan, L.A., Niazyan, O.M., Arsentiev, S.D., "On the reactions of peroxy radicals in the process of slow combustion of methane and ethylene," *Combustion and Flame*, *43* (1981), 221.
3. L. Khachatryan, Niazyan, O., Mantashyan, A.H., Vedeneev, V.I., Teitel'boim, M.A., "Experimental determination of the equilibrium constant of the reaction $\text{CH}_3 + \text{O}_2 \rightleftharpoons \text{CH}_3\text{O}_2$ during the gas-phase oxidation of methane.," *Int.J.Chem.Kin.*, *14* (1982), 1231-41.
4. A.Z. Aruthunyan, Grigoryan, G.L., Nalbandyan, A.B., *Kin. i Kat.*, *27* (1986), 1352.
5. S.-I. Ohnishi, and Nitta, I, "EPR Study of Free Radicals Produced in Irradiated Cyclopentadiene and Cyclohexene: The Cyclopentadienyl and Cyclohexenyl Radicals," *J.Chem.Phys*, *39* (1963), 2848-49.
6. G.R. Liebling, and McConnell, H.M., "Study of molecular orbital degeneracy in C_5H_5 ," *J.Chem.Phys*, *42* (1965), 3931-34.
7. A. Bussandri, and Willigen, H. van, "FT-EPR study of the wavelength dependence of the photochemistry of phenols," *J.Chem.Phys*, *106* (2002), 1524-32.

8. D.K. Russell, Davidson, I.M.T., Ellis, A.M., Mills, G.P., Pennington, M., Povey, I.M., Raynor, J.B., Saydam, S., Workman, A.D., "Mechanism of pyrolysis of tricarbonyl(cyclopentadienyl)manganese and tricarbonyl(methylcyclopentadienyl)manganese," *Organometallics*, *14* (1995), 3717-23.
9. A.S. Jeevarajan, and Fessenden, R.W., "Unusual chemically induced dynamic electron polarization of electrons by photoionization," *J.Chem.Phys*, *96* (1992), 1520-23.
10. A. Bussandri, and Willigen, H. van, "Photoionization of phenolates and scavenging of hydrated electrons by NO₃⁻: A study of the reaction mechanism by FT-EPR " *J.Phys. Chem.*, *105* (2001), 4669-75.
11. T.J. Stone, Waters, W.A., "ESR spectra of transient aryloxy and arylamino free radicals," *Proc.Chem.Soc., London*, (1962), 253-54.
12. P. Neta, and Fessenden, R.W., "Hydroxyl radical reactions with phenols and anilines as studied by ESR.," *J.Phys. Chem.*, *78* (1974), 523-29.
13. F. Graf, Loth, K., and Gunthard, H-H., "Chlorine hyperfine splittings and spin density distribution of peroxy radicals. An ESR and Quantum chemical study.," *Helvetica Chimica Acta.*, *60* (1977), 710-21.
14. L. Batt, Benson, S.W., "Pyrolysis of Di-tertiary butyl peroxide: Temperature gradients and chain contribution to the rate," *J.Chem.Phys*, *36* (1962), 895-901.
15. M.F.R. Mulcahy, Williams, D.J., and Wilmshurst, J.R., "Reactions of free radicals with aromatic compounds in the gaseous phase " *Aust.J.Chem.*, *17* (1964), 1329-41.
16. a.P. Yip. C.K., H.O., "Thermal decomposition of di-tert-butyl peroxide in binary mixtures near the critical point," *Can.J.Chem.*, *49* (1971), 2290-96.
17. L. Khachatryan, Adoukpe, J., Maskos, Z., Dellinger, B., "Formation of cyclopentadienyl radical from the gas-phase pyrolysis of hydroquinone, catechol and phenol," *Environ. Sci. Technol.*, *40* (2006), 5071-76.
18. P.J. Barker, Davies, A.G., and Tse, M-W. , "The photolysis of cyclopentadienyl compounds of tin and mercury. Electron spin resonance spectra and electronic configuration of the cyclopentadienyl, deuteriocyclopentadienyl, and alkylcyclopentadienyl radicals. ," *J. Chem. Soc., Perkin Transaction 2*, (1980), 941-48.
19. P.J. Barker, Davies, A.G., and Tse, M-W., "The photolysis of cyclopentadienyl compounds of Tin and mercury. ESR spectra and electronic configuration of the cyclopentadienyl, deuteriocyclopentadienyl, and alkylcyclopentadienyl radicals," *J.Chem.Soc., Perkin Transaction 2*, (1980), 941-48.
20. G. NIST Chemical Kinetics Database 17, MD, . (1998).

21. A.J. Collussi, Zabel, F., and Benson, S.W., "The very low-pressure pyrolysis of phenyl ethyl ether, phenyl allyl ether, and benzyl methyl ether and the enthalpy of formation of the phenoxy radical.," *Inern. J. Chem. Kin.*, 9 (1977), 161-78.
22. R. Liu, Morokuma, K., Mebel, A.M., Lin, M.C., "Ab initio study of the mechanism for the thermal decomposition of the phenoxy radical," *J.Phys. Chem.*, 100 (1996), 9314-22.
23. D. Campbell, and Turner, D.T., "ESR study of cyclohexadienyl radicals formed by gamma-irradiation of solid substituted benzenes," *Can.J.Chem.*, 45 (1967), 881.
24. M.B. Yim, and Wood, D.E., "Free radicals in adamantane matrix. X. EPR and INDO study of fluorinated cyclohexadienyl radicals," *J.Am.Chem.Soc.*, 97 (1975), 1004-10.
25. Z.D. Maskos, B., "Formation of the Secondary Radicals from the Aging of Tobacco Smoke," *Energy & Fuel*, 22 (2008), 382-88.
26. L. Khachatryan, Adoukpe, J., and Dellinger, B., "Phenoxy and cyclopentadienyl radicals from the gas-phase pyrolysis of phenol," *J.Phys.Chem., A*, 112, pp 481-487 (2008).
27. K. Brezinsky, Pecullan, M., Glassman, I., "Pyrolysis and oxidation of phenol," *Journal of Physical Chemistry A*, 102 (1998), 8614-19.
28. C.F. Melius, Colvin, M.E., Marinov, N.M., Pitz, W.J., Senkan, S.M., "Reaction mechanisms in aromatic hydrocarbon formation involving the C₅H₅ cyclopentadienyl moiety," *Proc. Combust. Inst.*, 26 (1996), 685-92.
29. B. Dellinger, S. Lomnicki, L. Khachatryan, Z. Maskos, R. Hall, J. Adoukpe, McFerrin. C. and H. Truong, "Formation and stabilization of persistent free radicals" *ScienceDirect, Proceedings of the Combustion Institute*, 31 (2007), 521-28.
30. H. Truong, Copper II Oxide Mediated Formation and Stabilization of Combustion Generated Persistent Free Radical In *Chemistry Department*, (Baton Rouge: Louisiana State University, 2007), 157.
31. E.B. Ledesma, Marsh, N.D., Sandrowitz, A.K., and Wornat, M.J, "An Experimental Study on the Thermal Decomposition of Catechol," *Proc. Combust. Inst.*, 29 (2002), 2299-306.
32. T. Sakai, and Hattori, M., "Thermal Decomposition of Catechol, Hydroquinone and Resorsinol.," *Chemistry Letters*, (1976), 1153-56.
33. S.D.E. E-J., Miser, W.G., Chan, and M.R., Hajaligol, "Catalytic Cracking of Catechols and Hydroquinons in the Presence of Nano-Particle Iron Oxide," *Appl.Catal., B, Submitted* (2004).
34. E.B.L. M. J. Wornat, N. D. Marsh., "Polycyclic aromatic hydrocarbons from the pyrolysis of catechol (ortho-dihydroxybenzene), a model fuel representative of entities in tobacco, coal, and lignin.," *Fuel*, 80 (2001), 1711-26.

35. G. Porter, "Flash Photolysis and some of its applications," *Nobel Lecture*, (1967).
36. E. Roemer, Stabbert, R., Rustemeier, K., Veltel, D. J., Meisgen, T. J., Reininghaus, W., Carchman, R. A., Gaworski, C. L., Podraza, K. F., "Chemical composition, cytotoxicity and mutagenicity of smoke from US commercial and reference cigarettes smoked under sets of machine.," *Toxicology*, *195* (2004), 31-52.
37. W.S.M. Schlotzhauer, R. M.; Snook, M. E.; Williamson, R. E. , "Pyrolytic Studies on the Contribution of Tobacco Leaf Constituents to the Formation of Smoke Catechols," *Journal of Agricultural and Food Chemistry* *30* (1982), 372-74.
38. S.G. Carmella, Hecht, S.S., Tso, T.C., Hoffman, D., "Roles of tobacco cellulose, sugars, and chlorogenic acid as precursors to catechol in cigarette smoke," *Journal of Agricultural and Food Chemistry*, *32* (1984), 267-73.
39. M.E. Counts, Morton, M.J., Laffoon, S.W., Cox, R.H., Lipowicz, P.J., "Smoke composition and predicting relationships for international commercial cigarettes smoked with three machine-smoking conditions," *Regulatory Toxicology and Pharmacology*, *41* (2005), 185–227.
40. S.S.C. Hecht, S.; Mori, H.; Hoffmann, D., , "A Study of Tobacco Carcinogenesis .Role of Catechol as a Major Cocarcinogen in the Weakly Acidic Fraction of Smoke Condensate. ," *Journal of the National Cancer Institute* *66* (1981), 163-69.
41. J.M.M. Daisey, K. R. R.; Hodgson, A. T., "Toxic volatile organic compounds in simulated environmental tobacco smoke: Emission factors for exposure assessment. ," *Journal of Exposure Analysis and Environmental Epidemiology* *8*(1998), 313-34.
42. R.M.S. Bruce, J.; Neal, M. W., "Summary Review of the Health-Effects Associated with Phenol. ," *Toxicology and Industrial Health* *3*(1987), 535-68.
43. C.W. Flickinger, "Benzenediols - Catechol, Resorcinol and Hydroquinone - Review of Industrial Toxicology and Current Industrial Exposure Limits. ," *American Industrial Hygiene Association Journal* *37* (1976), 596-606.
44. P.T. Leanderson, C., , "Cigarette Smoke-Induced DNA-Damage - Role of Hydroquinone and Catechol in the Formation of the Oxidative DNA-Adduct, 8-Hydroxydeoxyguanosine. ." *Chemico-Biological Interactions* *1990*, *75* (1990), 71-81.
45. M.H. Bilimoria, "Detection of Mutagenic Activity of Chemicals and Tobacco-Smoke in a Bacterial System," *Mutation Research*, *31* (1975), 328-38.
46. M. Carlier, Pauwels, J.P., and Sochet, L-R., "Application of ESR techniques to the study of gas-phase oxidation and combustion phenomena," *Oxidation Communication*, *6* (1984), 141-56.

CHAPTER 4: DISCUSSION *

4.1 Radicals from Phenol

The room temperature photolysis of Phenol yielded a five line non-well resolved EPR spectrum that we positively identified as phenoxy radical. The pyrolysis of phenol at both low and atmospheric pressures yielded superposition of radicals difficult to identify without additional mathematical and experimental tools. Even the LTMI technique, in spite of its numerous advantages, is limited in the identification of trapped radicals when the observed EPR spectra are the convolution of more than two radicals.¹ However, CPD radical was clearly identified at high temperature as dominant radicals. Intermediate temperature phenol pyrolysis is very complicated to interpret as far as the type of gas-phase formed free radicals. It is believed that CPD formed from either catechol or hydroquinone pyrolysis derived from phenol known to be intermediate product of the pyrolysis of both precursors. In the following paragraphs, the discussion during which generated free radical spectra will be compared and contrast to gas-phase radical spectra from the pyrolysis of phenol will be presented along with detailed free radical identification methods.

The positive identification of radicals formed during the pyrolysis of phenol between 800 and 1000°C was achieved by combining several experimental and mathematical tools. The annealing of the initial spectra showed that approximately half of the initial radicals were made of phenoxy radicals and some other un-identified radicals such as phenyl, and alkyl radicals. The second half is basically made of well resolved, symmetrical, annealed spectrum that was identified to CPD.

The CPD radical from the pyrolysis of phenol has been compared to the pure one generated by pyrolysing the tricarbonylcyclopentadienylmanganese at 250°C in a CO₂ gas flow at less than 0.2 Torr total pressure. The spectrum exhibits an isotropic 1:5:10:10:5:1 sextet² that matched

the CPD from the pyrolysis of phenol. The positive identification of phenoxy radical was done by comparing the pure phenoxy radical generated from both the photolysis of phenol³⁻⁵ and its low pressure, gas-phase reaction with the di-ter-butylperoxide⁶⁻⁸ to the 5 line spectrum observed in the stepwise annealing experiments

Due to the small difference of the components of the g-tensors for phenoxy radicals, an anisotropic spectral analysis is impossible on the X-band because many anisotropic peaks overlap⁹. The single characteristic parameter in our case is the high g-value (2.00482-2.00500 at high microwave power, >2 mW) which is in the range of g-value for phenoxy radicals in liquid solution (~2.00461) and substituted phenoxy radicals (non-halogenated) in various media of ~2.00530 (**Table 1.1**). This shift of the g-value depends significantly on the spin density of the phenolic oxygen, ρ_o^π . Theoretical and experimental studies of model compounds suggest that there is a positive, direct proportionality between ρ_o^π and the g-value^{10, 11}. The presence of a hydrogen bond to the oxygen reduces ρ_o^π and, consequently, the g-factor^{12, 13}. As a result, hydrogen bonding in aqueous solution results in the somewhat lower g-factor of 2.00461¹⁴ while higher g-values of ~ 2.00530 are observed in more non polar solvents such as CCl₄^{15, 16}(**Cf. Table 1.1**).

We performed additional experiments to determine if phenoxy radical was generated by pyrolysing phenol without carrier gas. The reason for this is that if CPD/Phenoxy radicals are not diluted by CO₂ then, based on their differing stability/reactivity behaviour, they may partially dimerize and result in simpler, more interpretable EPR spectra. In the absence of CO₂, the spectrum (**cf. Figure 4.1, line A**) resembles the residue (difference) spectrum. Annealing converted spectrum A (DI/N= 24.18) to much better resolved spectrum B (DI/N=11.07), and finally spectrum C (DI/N=8.00). Decreasing the microwave power to 0.2 mW resulted in spectrum D (red line, DI/N = 3.7, g = 2.00468). This residue spectrum matches very well the

EPR spectrum of pure phenoxyl radical (overlaid at the same g value scale, red line in spectrum D). Thus, the combination of performing the experiments without a matrix and with annealing promotes CPD/Phenoxyl radicals destruction at different rates, that, along with reducing the microwave power (masking of CPD radicals), enhances the spectrum of phenoxyl over that of CPD such that it can be clearly resolved (*vide infra*, **Figure 4.1**). All these procedures result in a residue spectrum (**Figure 4.1D**) nearly identical to that of phenoxyl and confirming its formation from pyrolysis of phenol from 800 to 1000°C.

The EPR spectra in the temperature region of 700 to 800 ° C is similar to the high temperature phenol pyrolysis spectra, but with somewhat altered intensities. Using the observation that

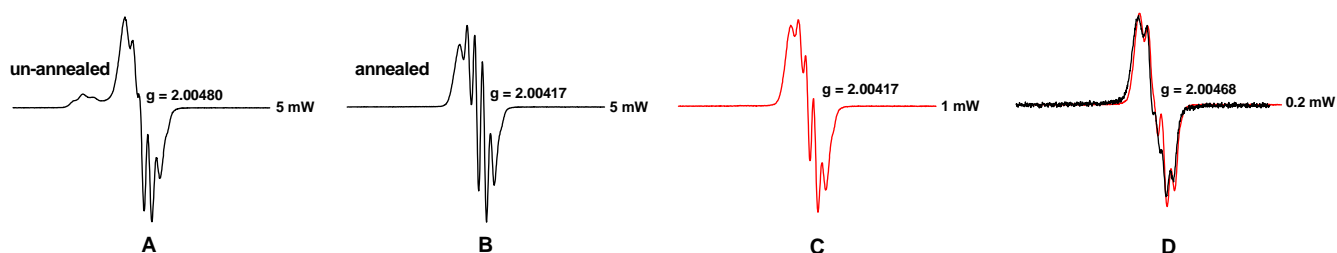


Figure 4.1 EPR spectra of frozen radicals (at 77 K) from phenol pyrolysis at 950 °C. A - Initial spectrum at 5 mW power. B - After annealing at 5 mW power. C - Annealed spectrum at 1 mW. D -annealed spectrum at 0.2mW (red line) overlaid with the spectrum of pure phenoxyl (black line) recorded under the same conditions (from phenol photolysis at 0.2 mW power).

increasing the microwave power readily saturates the EPR spectrum of phenoxy radicals but not CPD radicals^{1, 17}, we performed a series of phenol pyrolysis experiments from 700 to 800°C to further investigate the nature of radicals in the mixture.

CPD radical spectra were not readily saturated at microwave power below 40mW. Also the spectra shape and intensity distribution were not change with microwave power variation, which is consistent with reports in the literature¹⁷. However, phenoxy radicals saturated easily at microwave power less than 2 mW. That fundamental difference behavior of CPD and phenoxy

radical to microwave power variation gives the evidence that the pyrolysis of phenol between 700-800°C yielded a mixture approximately made of 50% CPD and 50% phenoxy radical as supported by the calculations in chapter 3.

At 400° C, the pyrolysis of phenol yielded a weak EPR signal that was clearly identifiable as CPD radical (cf **Figure. 4.2A**). The high activation energy barrier of CPD for the elimination of

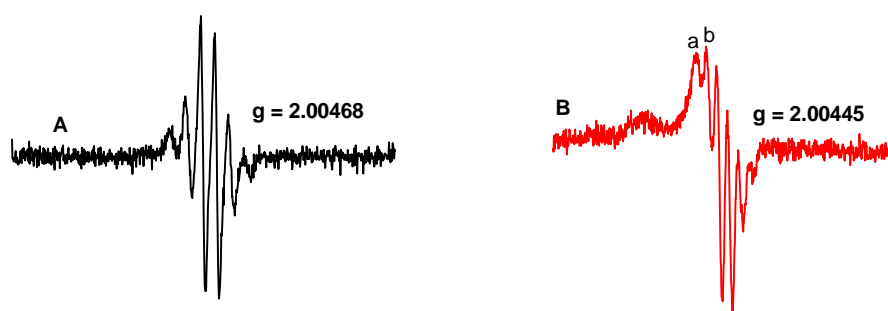


Figure 4.2. 77K EPR spectra of radicals from pyrolysis of phenol in CO₂ flow at 400 °C (spectrum A) and at 600 °C (spectrum B). Registration parameters: Spectrum A- sweep width -200G; modulation amplitude -2G, time constant -20.48ms, power 2 mW, 5 scans. Spectrum B - sweep width- 200G, modulation amplitude- 4G, time constant- 5.12ms, power- 2 mW, 1 scan.

CO from phenoxy radical (44-52 Kcal/mol) would seem to preclude CPD formation at 400°C via gas-phase reaction¹⁸⁻²⁰. Consequently, the formation of CPD is attributed to a wall reaction. At a contact time of ~ 4ms and a pressure of 0.2 Torr (reactor diameter ~ 12mm), the calculated diffusion time of a gas-phase phenol molecule to the quartz wall is only ~ 70 μs, which means that the phenol molecules can collide with with the wall almost 60 times prior to exiting the reaction zone.

The fact that we did not observe characteristic peaks for phenoxy radical at 400 °C suggests that the wall reaction of phenol proceeds directly to CPD without forming phenoxy radical as a stable intermediate. Surface-induced decomposition of phenol has been reported as low as 125 K through rupture of C₆H₅O-H bonds²¹. In this work, a surface reaction mechanism on Pt(III) was developed in which surface-adsorbed C₅H₃ and H₂ (or C₅H₅, the authors could not

distinguish these products) were formed. Increasing the temperature to 600 °C accelerates the homogeneous gas-phase formation of phenoxy radicals, resulting in the characteristic peaks of phenoxy radical labeled a) and b) depicted in **Figure 4.2 B**.

The high CPD radical to phenoxy radical ratio was a bit surprising in the light of the stability of phenoxy radical proposed in the literature^{22, 23}. To address this question using our experimental results, we have modeled our experimental data with a core phenol pyrolysis model from the literature²⁴ using CHEMKIN kinetic package²⁵ and a perfectly-stirred, plug-flow reactor application (150 ppm phenol in flow of CO₂, total flow pressure 0.2 torr, contact time 4 ms). The reaction kinetic input file was that proposed by Horn²⁴ without any changes in the kinetic parameters (**cf. Table 4.1**).

Table 4.1 Reaction Kinetic Model for the Pyrolysis of Phenol adapted from reference²⁴

| | Reactions Considered | A | B | E |
|----|---------------------------------|----------|----------|----------|
| 1 | $C_6H_5OH = C_5H_6 + CO$ | 1.00E+12 | 0.0 | 60740.0 |
| 2 | $C_6H_5OH = C_6H_5O + H$ | 3.20E+15 | 0.0 | 81500.0 |
| 3 | $C_6H_5OH + H = C_6H_6 + OH$ | 2.20E+13 | 0.0 | 8000.0 |
| 4 | $C_6H_5OH + H = C_6H_5O + H_2$ | 1.15E+14 | 0.0 | 12400.0 |
| 5 | $C_6H_5OH + H = C_6H_5O + H_2O$ | 6.00E+14 | 0.0 | 0.00 |
| 6 | $C_6H_5O = C_5H_5 + CO$ | 7.40E+11 | 0.0 | 43800.0 |
| 7 | $C_5H_6 = C_5H_5 + H$ | 4.00E+14 | 0.0 | 77000.0 |
| 8 | $C_5H_6 + H = C_5H_5 + H_2$ | 2.80E+13 | 0.0 | 2260.0 |
| 9 | $C_5H_6 + H = C_3H_5 + C_2H_2$ | 6.60E+14 | 0.0 | 12310.0 |
| 10 | $C_5H_5 = C_5H_5(L)$ | 7.50E+11 | 1.0 | 77000.0 |
| 11 | $C_5H_5(L) = C_3H_3 + C_2H_2$ | 3.70E+11 | 0.0 | 30000.0 |

(Table cont'd)

| | | | | |
|----|--|----------|-------|---------|
| 12 | $2 \text{ C}_5\text{H}_5 = \text{C}_{10}\text{H}_8 + 2\text{H}$ | 2.00E+13 | 0.0 | 4000.0 |
| 13 | $2 \text{ C}_3\text{H}_3 = \text{C}_6\text{H}_5 + \text{H}$ | 1.00E+13 | 0.0 | 0.0 |
| 14 | $\text{C}_3\text{H}_3 + \text{H} = \text{C}_3\text{H}_4$ | 5.00E+13 | 0.0 | 0.0 |
| 15 | $\text{C}_3\text{H}_4 + \text{H} = \text{C}_3\text{H}_3 + \text{H}_2$ | 5.00E+07 | 2.0 | 5000.0 |
| 16 | $\text{C}_3\text{H}_4 + \text{H} = \text{CH}_3 + \text{C}_2\text{H}_2$ | 1.00E+14 | 0.0 | 4000.0 |
| 17 | $\text{C}_6\text{H}_5 = \text{C}_6\text{H}_5(\text{L})$ | 2.50E+13 | 0.0 | 70500.0 |
| 18 | $\text{C}_6\text{H}_5(\text{L}) = \text{C}_4\text{H}_3 + \text{C}_2\text{H}_2$ | 7.90E+62 | -14.7 | 57000.0 |
| 19 | $\text{C}_4\text{H}_3 = \text{C}_4\text{H}_2 + \text{H}$ | 1.60E+43 | -9.3 | 43100.0 |

A is in units of mole-cm-sec-K. E is in units of cal/mole, ($k = A T^b \exp(-E/RT)$)

Examination of the results in **Table 4.2** indicates that the C_5H_5 to $\text{C}_6\text{H}_5\text{O}$ ratio is >1 above 1073 K and CPD increasingly dominates as the temperature increases.

Table 4.2 CPD and Phenoxy concentrations from the Phenol Reaction Kinetic Model

| | 873 K | 973 K | 1073 K | 1173 K | 1273 K |
|--|----------|----------|----------|----------|----------|
| C_5H_5 | 0.64E-10 | 0.80E-07 | 0.12E-04 | 0.36E-03 | 0.38E-02 |
| $\text{C}_6\text{H}_5\text{O}$ | 0.28E-08 | 0.28E-06 | 0.48E-05 | 0.18E-04 | 0.43E-04 |
| $\text{C}_5\text{H}_5/\text{C}_6\text{H}_5\text{O}$ | 0.023 | 0.3 | 2.5 | 19.7 | 88.4 |
| Percent consumption of $\text{C}_6\text{H}_5\text{OH}$ | 0.0 | 2.0 | 2.4 | 4.0 | 26.0 |

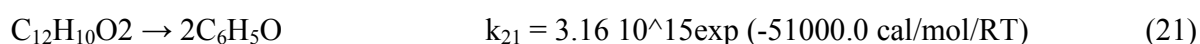
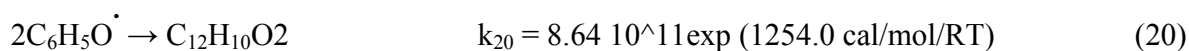
Based on this model, phenoxy radical concentrations are most sensitive to the rates of reactions 2 and reaction 6. Reactions 4, 3, and 5 affect its concentration to a lesser degree in the order given. The CPD radical concentration is most sensitive to reaction 2 with lesser sensitivity to reactions 6, 4, 3, 1, in that order.

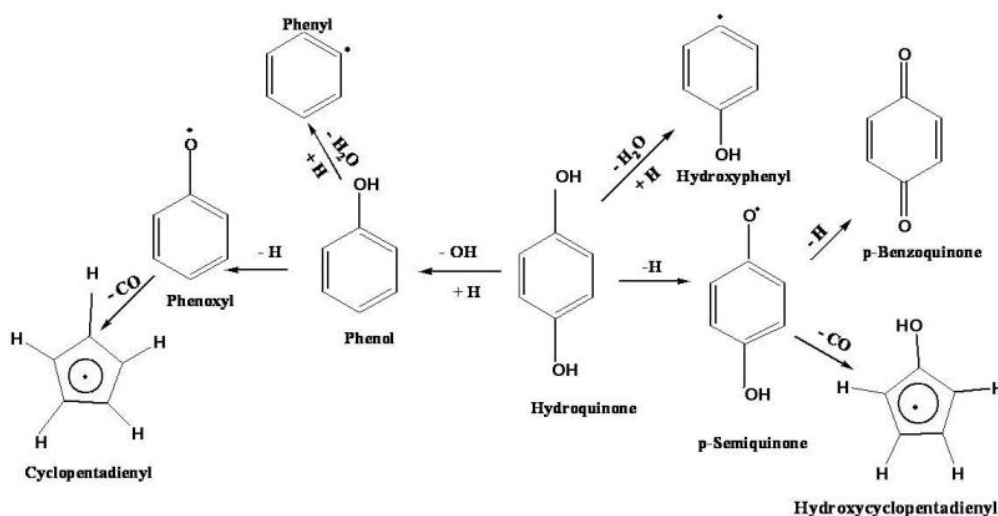
The high CPD to phenoxy ratio can be understood if we analyze closely the results of the scheme in **Table 4.1**

1. The relation, $k_2 = 0.15k_1$, was necessary to explain the experimental yields of hydrogen atoms at very short times ($\sim 200\mu\text{s}$) for the pyrolysis of phenol in shock-tube experiments according to reference ²⁴. This results in a significant contribution to CPD formation through reactions 1 and 8.
2. Phenoxy radicals are actively decomposed to CPD at a higher rate (reaction 6) than CPD is decomposed to olefinic products (reactions 10 and 11).
3. The generation of radicals in chain propagation reactions also favors CPD radical (reaction 8) over phenoxy (reaction 4) because $[\text{H}] \gg [\text{OH}]$ ²⁴ and formation of phenoxy through well known reaction $\text{C}_6\text{H}_5\text{OH} + \text{OH} \rightarrow \text{C}_6\text{H}_5\text{O} + \text{H}_2\text{O}$ is depressed.

These factors result in CPD being the dominant Environmentally Persistent Free Radical at temperatures > 973 K. Below 973 K, the modeling calculation does not result in any conversion of phenol to CPD radical. However, because we have experimentally demonstrated the existence of CPD radicals at temperatures < 973 that is not predicted by the model, formation of CPD by wall reactions is therefore implicated.

Insertion of a pathway for dimerization of phenoxy radicals (reactions 20 and 21) ²⁶ did not change significantly the C_5H_5 to $\text{C}_6\text{H}_5\text{O}$ ratio, probably due to the low steady-state concentration of phenoxy radicals at 1173 K.





Scheme 4.1 Thermal degradation of the model compound HQ. Mechanism of the formation of various radicals (reference 32)

The rate of dimerization reaction of CPD, $k_{12} = 2.00 \cdot 10^{13} \exp(-4000 \text{ cal/mol/RT})$ cm³/mole.sec is comparable with the dimerization reaction of phenoxy radicals, $k_{20} = 8.6 \cdot 10^{11} \exp(1254 \text{ cal/mol/RT})$ ²⁷, (e.g. $k_{12}/k_{20} \sim 1.3$ at 700 K and 3 at 1000 K)

All of these factors lead to CPD radicals being the dominant Persistent Free Radical over phenoxy radicals under low pressure conditions.

The atmospheric pressure pyrolysis of phenol at 750 ° C gave additional information leading to the confirmation of the formation of CPD and phenoxy radicals during pyrolysis of Phenol. The GC-MS analysis reveals the formation of naphthalene known in the literature to proceed from condensation of two CPD²⁸. We did not observe any dioxin or furan type molecules that would suggest formation of phenoxy radical. However, the low phenoxy radical to CPD radical ratio could explain that phenoxy radicals are formed and rapidly decompose to CPD to the extent where their steady state concentrations did not allow formation of detectable level of PCDD/Fs. We can now confirm, given those results that the decomposition pathway of phenol above 750 ° C is: $\text{PhOH} \rightarrow \text{PhO}^{\bullet} \rightarrow \text{CPD}$

4.2 Radicals from Hydroquinone

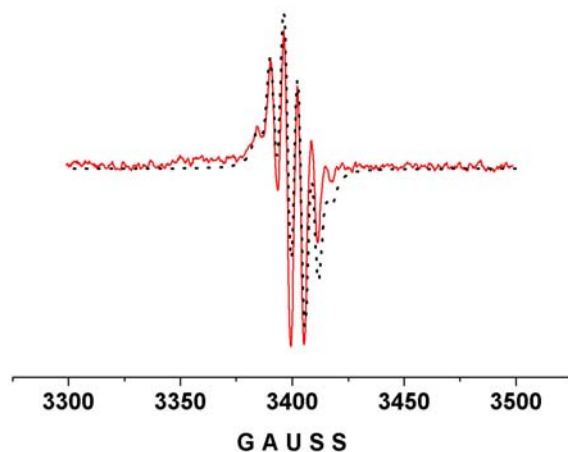


Figure 4.3 Comparison of experimental EPR spectrum from HQ pyrolysis (red solid line) with the calculated EPR spectrum of CPD (black dotted line). The following experimental inputs were used for theoretical calculations of the CPD radical EPR: 5 equivalent protons, $g = 2.0051$, coupling constant of 6.0G, peak to peak distance 3G. (Very similar spectra were obtained from the pyrolysis of CT)

In the light of **Scheme 4.1**²⁹, the major radicals expected to be formed from the thermal decomposition of Hydroquinone going to the left-hand side of the scheme are respectively phenoxy and CPD radicals, and to the right-hand side, p-semiquinone and hydroxycyclopentadienyl radicals. The following paragraphs report on the efforts of positive identification of those radicals.

The gas-phase pyrolysis of HQ at temperatures above 850°C, critical temperature at which the maximum yield of Persistent Free Radicals was achieved, yielded EPR spectra basically dominated by the apparent sextet that we have identified to CPD radical. The initial spectra with resolved shape and g -value of 2.0042 closely resemble the literature CPD radical EPR spectrum³⁰ **Figure 4.3** exhibits the superposition of the computer-generated CPD radical (black dotted line) with the experimental annealed spectra (solid redline) of HQ pyrolysis above 850°C. It should be noted that during annihilation, the initial relative concentration of frozen radicals

(DI/N = 1.47) decreased by nearly a factor of 10, and we still observed a very strong EPR signal that, compared to the pure CPD radical spectrum generated from the pyrolysis of $\eta^5\text{-C}_5\text{H}_5\text{Mn(CO)}_3$, exhibits same EPR characteristics (six well resolved lines, g-value, $\Delta\text{Hp-p}$) as this later.

In this temperature region of 725-850°C, a complex mixture of radicals was observed that only a combination of experimental and mathematical tools could help to dissociate. In the following paragraphs the methods used in discerning p-Semiquinone, phenoxy, CPD, and Hydroxycyclopentadienyl (OHCPD) were reported

The pyrolysis of HQ in CO₂ produced broad, but to some extent resolved spectra (**Figure.4.4**, spectrum A). Annealing converted spectrum A to isotropic spectrum B, which through lowering the microwave power from 5mW to 1mW, converted to an almost singlet line, spectrum C.

The disappearance of resolved lines by lowering the microwave power has previously been observed during pyrolysis of phenol³¹. At low microwave power (≤ 1 mW), the higher magnetic susceptibility of phenoxy radicals (as well as for substituted phenoxy radicals, *vide infra*) results in the EPR signal of phenoxy radicals being stronger than CPD radicals. At higher microwave power (> 10 mW), the phenoxy spectrum is saturated (structure is lost) and the CPD spectrum is more apparent³¹.

We employed a combination of methods to clearly distinguish radicals formed and trapped on to the cold finger of the Dewar. In addition to the microwave power variation that masques some radicals magnetically susceptible to low or high microwave power, we used the mathematical tools such as WINEPR and SimFonia software to calculate the g-values, the widths of the spectra and most importantly to substrate EPR spectra of pure generated radical from a complex mixture of radicals.

The difference spectrum, D in **Figure 4.4** (spectrum B minus spectrum C) matches our CPD spectrum generated from the pyrolysis of HQ, which perfectly matches the spectrum of pure CPD (spectrum E in **Figure 4.4**) generated from the pyrolysis of $\eta^5\text{-C}_5\text{H}_5\text{Mn}(\text{CO})_3$ at 250 °C³¹.

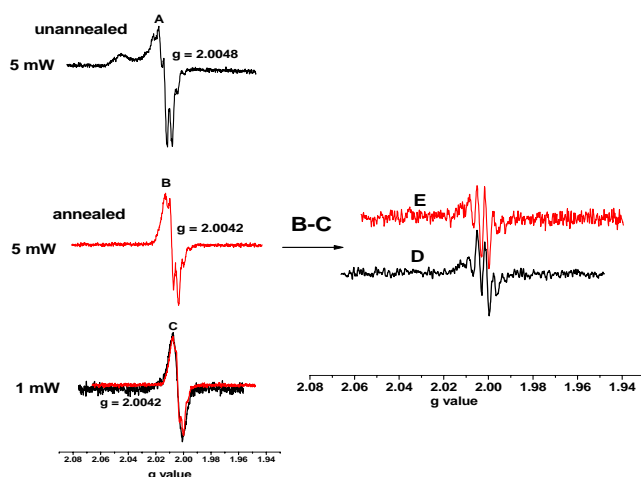


Fig.4.4. EPR spectra of radicals trapped on the cold finger from the pyrolysis of HQ at 825 °C in CO₂ flow: Conversion of spectrum A to B by annihilation, B to C (black line) by decreasing of power from 5 to 1mW; B-C=D is simple subtraction result, spectrum E is CPD radical EPR spectrum. On spectrum C (black line) the EPR spectrum of p-semiquinone radicals (red line) from HQ photolysis is overlaid. All spectra were registered at sweep width 200 G, modulation 4 G, time constant 5.12 ms.

Thus the annealed Spectrum B (DI/N = 0.4) is a mixture of a trace of CPD radical (DI/N = 0.08) (Spectrum D in **Figure 4.4**) and a dominant p-SQ radical (DI/N = 0.32) (Spectrum C in **Figure 4.4**).

Based on the possible mechanism for thermal decomposition of HQ depicted in **Scheme 4.1**, hydroxycyclopentadienyl (OHCPD) radical might be formed³². The unimolecular decomposition of HQ results in the formation of p-SQ radical, which in analogy to phenoxyl radical should form OHCPD upon decomposition via expulsion of CO³³. OHCPD is also more stable thermodynamically with a $\Delta_f H = 45.0$ kcal/mol vs. $\Delta_f H = 63.7$ kcal/mol for CPD^{34, 35}.

The *ab-initio* calculated activation energies for formation of OHCPD and CPD via expulsion of CO from p-SQ and phenoxy radical are similar, being 59.3-65.1 kcal/mol and 56.4-62.9 kcal/mol for p-SQ and phenoxy radical, respectively²³.

However, we did not observe OHCPD in significant concentrations. Because the addition of an OH group to CPD radical should have a minimal effect on the hyperfine splitting interaction on ring protons³⁶, the EPR spectrum of OHCPD radical can be calculated using available EPR data for CPD radicals ($g = 2.0044$, $hsc = 6$ G, line width ~ 3 G) for 4 equivalent protons using Bruker Simphonia simulation package (<http://wwwbruker-biospin.com/winepr.html?&L=0>). To the best of our knowledge, literature EPR spectrum data of OHCPD radicals does not exist. The calculated EPR spectrum for OHCPD is a simple 5-line spectrum with an intensity distribution 1:4:6:4:1, whereas, all CPD radicals that we have identified possessed 6 lines with an intensity distribution 1:5:10:10:5:1 that matches the literature³¹. We were not able to detect any 5-line similar to the calculated spectrum of OHCPD radical.

The absence of OHCPD suggests that the formation of p-BQ in **Scheme 4.1** through reaction 2 dominates over the formation of OHCPD via reaction 1. Indeed, a simple calculation of the ratio of k_2 to k_1 indicates that at > 900 K the main channel of p-SQ radical decomposition is formation of p-BQ which dominates by an order of magnitude.

Table 4.3 Calculated Ratios of k_2 to k_1 for Pathways Depicted in Figure 4.4

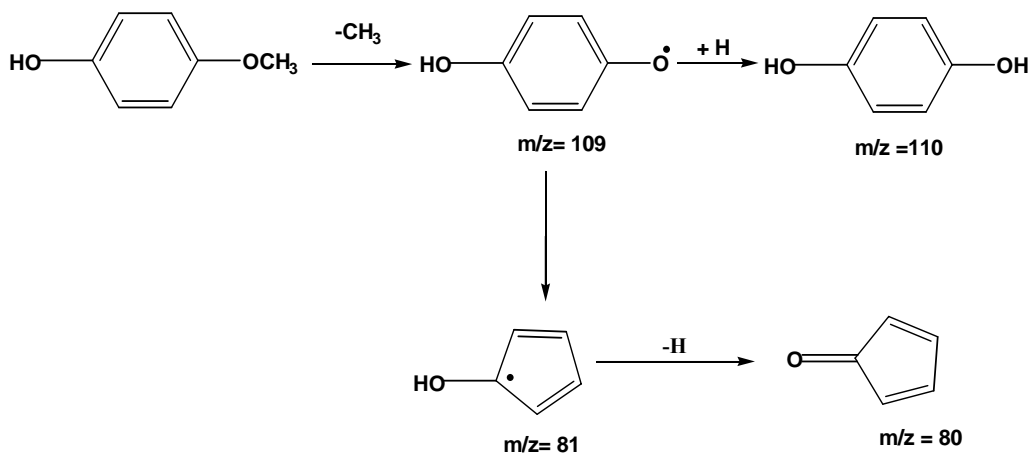
| Temperature(K), | 700 | 900 | 1000 | 1100 | 1200 |
|-----------------|------|------|------|------|------|
| k_2/k_1^a | 2.96 | 11.4 | 18.3 | 27 | 37 |

^a An average value of $E_1 = 62.4$ kcal/mol and $E_2 = 70.84$ kcal/mol was calculated using 5 different *ab-initio* basis sets. Pre-exponential factors were taken as $A_1 = 2.5E+12$ s⁻¹ and $A_2 = 3.2E+15$ s⁻¹

The formation of the very stable p-BQ by loss of a second hydroxyl hydrogen versus OHCPD formation by expulsion of CO from the p-SQ radicals has been previously proposed at temperatures $> 1200\text{ K}$ ³⁷.

Although p-BQ was the major product formed as p-SQ decomposed, cyclopentadienone was observed as the p-SQ concentration decreased, implicating that the decomposition of p-BQ proceeded partially through the proposed OHCPD intermediate. Since it supposedly polymerizes very rapidly³⁷, it was not possible to detect cyclopentadienone.

The next step in this work was to identify some products from HQ pyrolysis at $750\text{ }^{\circ}\text{C}$ which can be additional evidence to the formation of OHCPD or CPD radicals. It is known that recombination of two cyclopentadienyl radicals, followed by rearrangement and 2 H elimination can result in formation of naphthalene³⁸. Similarly, the recombination of two OHCPD radicals may form dihydroxynaphthalene. By freezing all pyrolysis products on cold trap for further GC-MS analysis, in addition to p-BQ product we have identified naphthalene (recombination of 2



Scheme 4.2 Mechanism of the formation of OHCHD radical followed by generation of cyclopentadienone molecule (adapted from reference 40)

CPD radicals), hydroxyl-indene, and indene. The indene formation results from the cross reaction between CPD and OHCPD radicals:

$\text{OHCPD} + \text{CPD} \rightarrow (\text{OH})\text{C}_{10}\text{H}_7$ (hydroxynaphtalene, $M=144$) $\rightarrow \text{CO} + \text{C}_9\text{H}_8$ (Indene, $M/Z = 116$)

While the hydroxyindene ($\text{C}_9\text{H}_8(\text{OH})$, $M/Z = 132$) is a result of cross reaction between two OHCPD radicals:

$\text{OHCPD} + \text{OHCPD} \rightarrow 2\text{H} + \text{C}_{10}\text{H}_6(\text{OH})_2$ (dihydroxynaphtalene, $M/Z = 160$)

$\text{C}_{10}\text{H}_6(\text{OH})_2 \rightarrow \text{CO} + \text{C}_9\text{H}_7(\text{OH})$.

In fact the products of direct recombination of OHCPD and CPD radicals, $(\text{OH})\text{C}_{10}\text{H}_7$ (hydroxynaphtalene) and two OHCPD radicals, $\text{C}_{10}\text{H}_6(\text{OH})_2$ have not been found in our GC-MS analysis of HQ pyrolysis. However products of their decomposition, indene and hydroxyindene have been identified. These facts indicate that hydroxynaphtalene, as well as dihydroxynaphtalene are instable at high temperatures and by repulsion of CO converted to stable products which are indene and hydroxynaphtene.

In a previous report, effort in identifying phenoxy radicals by LTMI EPR technique was reported³¹. It was shown that phenoxy radicals are very reactive species and that their steady state concentration is too low. Several approaches were integrated to show the presence of

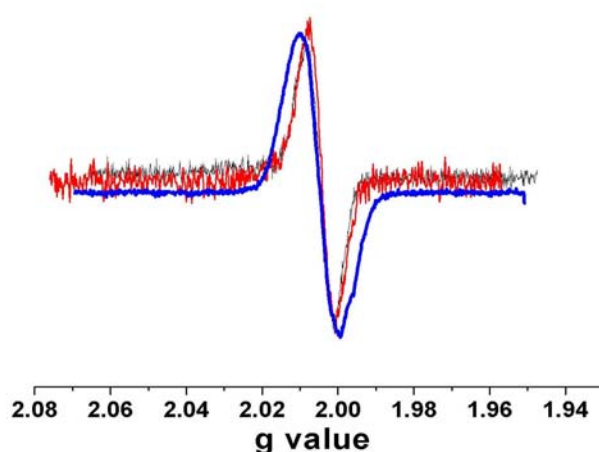


Figure 4.5. Comparison of EPR spectra of frozen radicals at liquid N_2 temperature from pyrolysis of HQ at 550°C (black), photolysis of HQ (red), and photolysis of phenol (blue) at room temperature. All spectra were registered at 77 K at sweep widths 200 G, amplitude of modulation 4 G, microwave power of 5 mw.

phenoxy radical in the pyrolysis radical products of phenol³¹ and to conclude that phenoxy radical was not dominant radical observed during the pyrolysis of phenol.

Even though phenol is a major molecular product from the pyrolysis of HQ at temperature higher than 700 °C³⁹, phenoxy radical was not detected in our study. It is understandable when we compare the low yield (less than 5 %) of phenol concentration³⁹. As simply can be seen, phenol is accumulated during HQ pyrolysis 200 times less than what it is as initial pure reagent²⁹. Consequently, the phenoxy radical concentration should be much lower in the process of pyrolysis of HQ and can not be detected by LTMI EPR method employed in this work. To confirm the assignment of the featureless spectrum at low temperature pyrolysis of HQ that we identified to p-SQ radical, we attempted to generate pure p-SQ radical via photolysis of a suitable molecular precursor.

Figure 4.5 presents representative spectra from the pyrolysis of HQ (black line), photolysis of HQ (red line), as well as from phenol (as a reference spectrum, blue line). It's known from the literature that UV irradiation at < 300 nm will generate various aromatic oxy-radicals from the phenol¹⁵, Catechol⁴⁰ and hydroquinone⁴¹. In the case of HQ photolysis, we generated a featureless singlet line at 77 K which, based on its high g-value (2.0044), can be attributed to p-SQ. As depicted in **Figure 4. 5**, this spectrum (red line, ΔH (p-p) = 12G, $g = 2.0044$) exactly matched the spectrum from the pyrolysis of HQ (black line, ΔH (p-p) = 12G, $g = 2.0049$). A reference spectrum generated from the photolysis of phenol is also presented in **Figure4. 5** (blue line). The g value = 2.0047 is typical of oxygen-centered radicals and is in the range of g-values for phenoxy-type radicals generated at various conditions, e.g., $g = 2.0045 - 2.0049$ ⁴² and 2.0053⁴⁰.

Although the spectrum obtained from the photolysis of HQ was an exact match to the spectrum obtained from its pyrolysis, the g-value of 2.0047 of radicals from low pressure (0.1 -

0.08 torr) photolysis of phenol is very close to the g-value from the very low pressure (~ 0.01 - 0.1 torr) pyrolysis of HQ ($g = 2.0049$) or photolysis of HQ ($g = 2.0044$). The single difference is the broadening (ΔH (p-p) = 18 G) produced from phenol compared to that produced from HQ (ΔH (p-p) = 18 G). The reason for the differences in peak widths can be explained using Bader valence electron density data analysis for the various radicals of interest (cf. **Table 4.4**)²³.

Table 4.4 Bader Valence Electron Charge Densities

| Radical | % | | |
|---------------|--------|----------|--------|
| | Carbon | Hydrogen | Oxygen |
| o-Semiquinone | 52.2 | 10.6 | 37.2 |
| p-Semiquinone | 49.8 | 13.4 | 36.8 |
| Phenoxy | 63.6 | 14.8 | 21.6 |
| Phenyl | 82.2 | 17.8 | na |

The delocalization over the aromatic ring in phenoxy radical is significantly higher (63.6%) than in p-semiquinone radical (49.8%). According to the McConnell relation^{43, 44} for protons directly bonded to the carbon atoms of the benzene nucleus, $a_i^H = Q \rho_i^\pi$, where: the proton coupling constant, a_i^H , (in gauss, for the proton at position i) is directly proportional to the spin density, ρ_i^π , of a carbon atom i in the aromatic ring, and Q is a proportionality constant expressed in magnetic-field units. It follows from the equation that the higher the spin density on particular carbon atom, the higher is the a_i^H (and hence the total spread of spectrum⁴⁵). Consequently, a high spin density over the aromatic ring in phenoxy radical leads to a wider overall spectrum than in case of o- or p-semiquinone radicals that have greater spin density on the oxygen. Exactly the same featureless spectrum with a relatively narrow ΔH (p-p) of 12 G was obtained

for pyrolysis of CT under the same conditions (not shown). This is again consistent with the low percentage of charge distribution on carbon for the expected o-SQ.

The expected ratio of spin densities for phenoxy and p-semiquinone radicals is $63.6\% / 49.8\% = 1.3$, which is quite close to the ratio of peak-to-peak widths for suspected radicals, $18\text{ G} / 12\text{ G} = 1.5$. The slightly higher predicted spectral width may be due to the concentration broadening of EPR spectra in the case of phenol (vapor pressure ~ 0.1 torr) while for HQ the vapor pressure is estimated ~ 0.01 torr at $70\text{ }^\circ\text{C}$.

Based on this analysis, we feel confident in assigning the spectrum for pyrolysis of HQ from 350 to $725\text{ }^\circ\text{C}$ as p-SQ.

4.3 Radicals from Catechol

The almost perfect match of the un-annealed and the annealed spectra observable

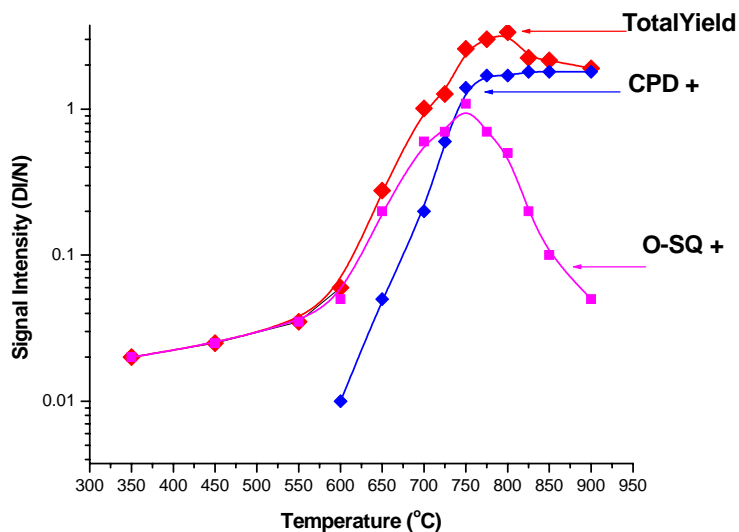


Fig 4.6 Total radical yield from the gas phase pyrolysis of catechol. The CPD+ shows an increase with temperature and reaches a saturation with total conversion of Catechol to CPD plus other unidentified radicals. Simultaneously, it was observed a faster increase of O-semiquinone radicals up to $650\text{ }^\circ\text{C}$ where the O-semiquinone radical dominates, reaches a maximum yield around $750\text{ }^\circ\text{C}$ followed by a sharp decrease where the CPD type radicals dominate.

from **Figure 3.21** demonstrates that at temperature above 850 ° C, it is reasonable to conclude that only CPD radicals dominate. The other radicals observed at lower temperature either decompose or recombine. This experimental fact makes CPD the most persistent radical above 800 ° C. All spectra were registered at sweep width 200G, modulation amplitude 4G, time constant 5.12ms, microwave power 5mW.

The calculated DI/N using the Simphonia Software for both the un-annealed and the annealed spectra shows values which are consistent with the total conversion of Catechol to a sole radical at temperature above 800 ° C (**Figure 4.6**). We have compared the annealed spectra for the pyrolysis temperatures of Catechol above 800°C to that of cyclopentadienyl radical generated from the low temperature pyrolysis of tricarbonyl cyclopentadienyl manganese²⁹. All the annealed spectra exhibit an isotropic 1:5:10:10:5:1 sextet which were consistent with the cyclopentadienyl radical from the suitable precursor. It is then reasonable to suggest that at temperatures higher than 800°C, only CPD can be observed as radical from the pyrolysis of catechol, the other short life radicals at those temperatures either recombine to neutral molecules or completely decompose. It has been reported that catechol starts decomposing around 500°C, leading to a maximum phenol yield at 800°C⁴⁶. Consequently, phenoxy radical should be expected from the pyrolysis of catechol between 700°C and 800°C. Unfortunately, this was not the case, thus confirming what we have observed as phenol behavior above 700 ° C²⁹. However, cyclopentadiene reaches its maximum yield at 800°C⁴⁶. Given that assumption on radical species such as cyclopentadienyl, vinyl, propargyl and phenoxy radical formation was made solely based on the observation of their stable forms, our experiment proves that phenoxy type radical observed from the thermal cracking of phenol at temperature above 700°C is not dominant in that temperature range, rather, the CPD type radical dominates the spectra²⁹. This finding is consistent with catechol thermal decomposition where phenoxy type radical was not

observed at temperature above 800 °C. A plausible route of catechol pyrolysis above 800 °C is a simultaneous scission of C-OH bond and the O-H bond to form water and phenoxy radical that immediately undergoes CO elimination to form CPD.

A spectrum acquired from the pyrolysis of catechol at 750 °C was subjected to the microwave power variation. As it can be observed, the shape of the spectra changes as the microwave power varies. The initial spectrum, registered at 5mW, obviously depicts a mixture of radicals where the dominant one is the CPD as it shows the characteristic splittings ¹. At microwave power above 5mW, the CPD radical shape was observable from the spectrum. The saturation was reached at 20mW. When the matrix was annealed, the 6lines spectrum is converted to a singlet line with a slight splitting at the center. As it can be seen, the annealed matrix spectrum at higher power is identical to the initial spectrum registered at power below 2mW. Since the matrix annealed spectrum depicts only one radical, the most persistent at the pyrolysis temperature, we have identified the matrix annealed spectrum to that of O-semiquinone. The evidence of this identification will be shown in next paragraph. Our understanding of spectral shape dependence on microwave power is that some radicals are very sensitive to low microwave power while others are to the high microwave power. In our experiment, the radicals in the pyrolysis mainstream mixture, basically the CPD and the O-semiquinone obey that observation. At low microwave power, we believe that CPD is not sensitive. The singlet line with slight splitting in the center is the O-semiquinone radical that is very sensitive to low power. However, at high power, the CPD radicals are more sensitive, thus masking the O-semiquinone radicals in the mixture. After annealing the matrix, the 6 line spectrum converts to a singlet line with slight splitting at the center even at high power, showing that the CPD and o-SQ radicals were dominant radicals in this temperature region.

Surprisingly, the anticipated phenoxy and hydroxy-CPD radicals were not isolated as products of the pyrolysis of catechol at any temperature range. In the scheme of catechol decomposition pathway that we published¹ using hydroquinone as model compound, we initially envisioned the formation of phenoxy radical from Catechol thermal decomposition via phenol formation followed by hydrogen atom elimination. The phenoxy radical would further decompose eliminating CO molecule to form the cyclopentadienyl radical. Also, we suggested that Hydroxy-CPD radical should be formed from the CO molecule elimination from the O-semiquinone radical. The suggested decomposition pathways were based on studies that reported phenol as major primary product of catechol decomposition with a maximum yield at 800°C⁴⁶, of 2-MonoChlorophenol thermal decomposition at even lower temperature⁴⁷, of thermal decarbonylation of catechol, hydroquinone and resorlsinol⁴⁸ and anisole pyrolysis, all yielding phenoxy radical⁴⁹.

In our catechol pyrolysis experiments, phenoxy radical may be formed as reported in the literature^{46, 47, 49}. The reasons why the EPR spectra don't show phenoxy radical are several folds. It may be said that our handling of the radical acquisition is not allowing us to detect phenoxy radical. This is not possible since in a parallel experiment of pure phenol pyrolysis, we were able to acquire and identify phenoxy radical²⁹. Another possible explanation is the very fast reactivity of phenoxy radical with o-Semiquinone radical. In addition to the very fast reactivity of phenoxy radical with the O-semiquinone radical, the absence of phenoxy radical may be accounted for the very low phenoxy radical formation below the limit of detection of the EPR cavity. Given that we had vaporized Catechol at a very low rate (2.5×10^{-3} mmol/min) and that to avoid catechol condensation on the wall due to its very low vapor pressure, all the transfer lines from the vaporizer to the cold finger of the Dewar need to be maintained at constant and elevated temperatures ($\sim 80^\circ\text{C}$). Very often, condensation can not be avoided, supporting the idea that

little of catechol pyrolysis products reach the detector. Consequently, phenoxy radical that we believe of very low concentration can not be observed through its EPR spectrum acquisition.

Likely, the hydroxyCPD radical was not observed from the pyrolysis of catechol. As in phenoxy radicals case, the hydroxyCPD may form but has very short life span in our experimental conditions. We concluded that phenoxy radical and hydroxyCPD are not dominant radicals in our experimental conditions. To definitely conclude that hydroxyCPD and phenoxy radical were formed in trace during the pyrolysis of CT, we performed GC-MS products analysis. The atmospheric pressure pyrolysis of Catechol allowed collecting both radicals onto the finger of the Dewar and pyrolysis products in a trap held at 77K and placed on the atmospheric line.

The online CT pyrolysis products collection has been performed simultaneously with radical accumulation. The GC-MS analysis of the products was performed.

Several compounds have been detected ranging from C₆ to C₁₂. Extensive Catechol pyrolysis products have been reported in the literature. The yield of naphthalene at temperature below 800 °C is extremely low compared to other PAHs^{39, 46, 50}. In our GC-MS analysis of the pyrolysis products of catechol, our findings are consistent with the literature; we can only detect trace of naphthalene that confirms the formation of CPD at 750 °C. Additionally, two to three member ring compounds were detected. The detection of 1H-Indenol gives evidence of the formation of labile radicals such as hydrocyclopentadienyl radical, while that of Fluorene confirms not only the formation of CPD radical but also of aliphatic radicals such as ethenyl, and acetylenyl radicals⁴⁶

4.4 Radicals from Tobacco

As it can be expected from the pyrolytic study of catechol, hydroquinone and phenol, the pyrolysis of tobacco with the noble goal of identifying persistent free radicals, is very

complicated for several reasons. For the pyrolysis of pure compounds such as catechol, hydroquinone and phenol, the complications that arise from the convolution of several radicals in the acquired spectra, and the difficulties that necessitated additional experimental and mathematical tools in interpreting the spectra in order to assign radicals were signs that the study of tobacco, a very complex compound made of not only the precursors studied, but of hundreds of other organic compounds⁵¹ including pectin, protein, some metals, lignin, cellulose, cryogenic acids⁵², will not be an easy task. However, we have diligently investigated the temperature dependence gas-phase pyrolysis of tobacco that we believe is a very strong step to future study.

Semiquinone type radicals have been reported in cigarette smoke^{53, 54}. The detection method use can be the direct collection of Total Particulate Matter (TPM) on a filter (usually cellulose filter) or the extraction of the TPM in solution. The free radicals from TPM have been classified in two categories. The first category is made of radicals directly formed during the burning of tobacco and the smoking process and the second category encompasses free radicals that are not initially present in the smoke, but are formed when TPM is exposed to oxygen or biological media⁵⁵. The first category is termed primary radicals whereas the second is termed secondary radicals⁵⁶.

A nonsmoker is basically exposed to secondary radicals that are also termed Environmental Tobacco Smoke (ETS)⁵⁷. Further classification put semiquinone radicals in the second category⁵⁵, therefore as an ETS. TPM radicals have been accepted as semiquinone radicals^{58, 59}. However, recent publications have demonstrated existence or coexistence of carbon-centered radicals and oxygen-centered radicals in TPM. The g-value, one important radical's characteristic that allows the distinction between carbon-centered radicals ($g \sim 2.003$) and oxygen-centered radicals ($g \sim 2.004-2.005$)⁶⁰ become un-operational when the EPR spectra are the convolution of several radicals³¹. Thus identification after detection of radicals in TPM

becomes very important issue. Given the successful identification of radicals from the pyrolysis of precursors employing the LTMI-EPR technique, we have studied radicals from online gas-phase tobacco smoke employing the same technique.

The EPR spectra from the pyrolysis of tobacco at 350 ° C display a featureless singlet line visibly comparable to the featureless singlet line spectra from the gas-phase pyrolysis of catechol and hydroquinone. We believe that the featureless singlet line spectra obtained from the online pyrolysis of tobacco is the superposition of the EPR signal of several radicals and therefore its assignment to a given radical is impossible at the present time given that the EPR g-value and the spectra widths are not enough for this purpose ³¹. However, in the hypothesis that the EPR singlet line from the pyrolysis of tobacco arises as the signal of only one radical, which means the complete termination at the experimental temperature of all other radicals, we have compared its characteristics to the EPR signals obtained from the study of the precursors.

- **Comparison with Phenol's Radicals**

There was no common characteristic to the singlet line spectra observed from tobacco pyrolysis and the spectra from phenol. In the low temperature region (below 600°C) non well resolved five lines spectra with g-value at the center of 2.0058 were observed from phenol pyrolysis: the phenoxy radical. Generally, tobacco pyrolysis EPR spectra show singlet line. At higher temperature, phenol pyrolysis yielded CPD radical which can't be found anywhere in the tobacco pyrolysis EPR spectra.

This observation may be due to the fact that even if CPD radicals are formed, they terminated by radical-radical reaction, given that tobacco burning releases several compounds.

- **Comparison with p-Semiquinone and o-Semiquinone Radicals**

The room temperature catechol and hydroquinone photolysis and pyrolysis at temperature below 600°C yielded featureless singlet line that we assigned, based on the combination of both

experimental and mathematical tools and literature, to o-Semiquinone (o-SQ) and p-Semiquinone (p-SQ) respectively. The featureless singlet line EPR spectra observed from the low temperature (320-380°C) pyrolysis of tobacco resemble apparently o-SQ and p-SQ. Herein,

we are going to compare the EPR characteristics of tobacco pyrolysis single line EPR spectra to those of o-SQ and p-SQ.

Our calculations using the SimFonia software showed that the singlet line EPR spectra from the pyrolysis of tobacco at low temperature have the following characteristics. The g-values vary between 2.00368 - 2.00399. This range of g-values is consistent with surface-associated carbon-centered radicals where the unpaired electron is vicinal to an oxygen containing functional group⁶¹ and partially delocalized, polymeric, phenoxy type radicals^{60, 62}. The peak to peak widths (ΔH_{p-p}) of the EPR spectra from the pyrolysis of tobacco vary between 8.008 and 10.16G. These ΔH_{p-p} values are wider than the one of ($\Delta H_{p-p} = 6.6G$) reported in reference⁶³ and that led to the conclusion that p-SQ types radicals were in Tobacco Particulate Matter (TPM). However, the extraction technique used in the cited study may have a narrowing effect on the width of the spectra. with $\Delta H_{p-p} \sim 12.60-15.60G$ ⁶⁵. To only base our reasoning on those values to assume that the radicals from pyrolysis of tobacco are semiquinone types radicals seems inconsistent at the present time. Thus the nature of radicals in tobacco pyrolysis needs further investigation.

4.5 Effects of Oxygen on the Nature of Radicals

The persistence of free radicals is defined as their resistance to react with oxygen for longer period of time. In this paragraph, we are interested on the effect of trace of oxygen on radicals. The pure p-SQ radical generated in our study has the following characteristics: g-values $\sim 2.0044-2.0049$, and $\Delta H_{p-p} \sim 12G$ ^{64, 65}.

The pure o-SQ generated has g-values ~ 2.0052 - 2.0061

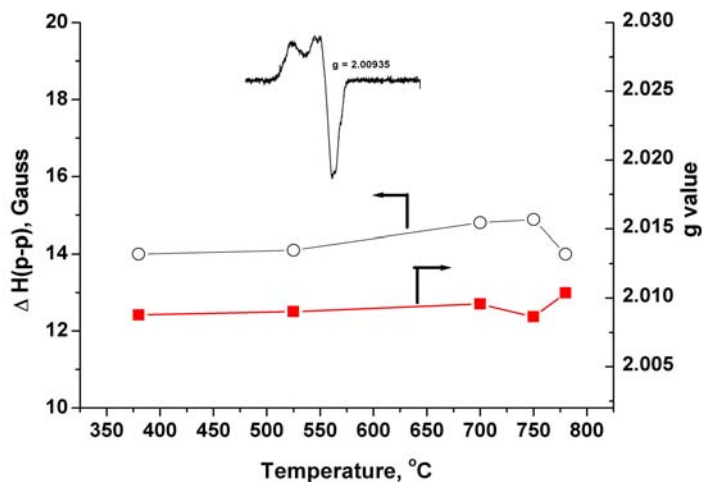


Figure 4.7 Temperature dependence of g-values and ΔH_{p-p} of radicals from the pyrolysis of HQ in CO_2 in presence of traces of O_2 (~ 700 ppm). The top spectrum was detected from HQ pyrolysis at 435°C ($g = 2.00935$). The delivery rate of HQ up to the cold zone in flow of CO_2 was higher ($\sim 10^{-2}$ mmol/min) than in neat pyrolysis ($\sim 10^{-3}$ mmol/min).

In fact EPR spectrum of CH_3O_2 (C-A) in **Figure.3.30** overlaps the spectrum A and a spectrum C is generated, where all resolved lines were merged and we have RO_2 like radical EPR spectrum, C in general.

In **Figure 4.7** a temperature dependence of g-values and ΔH (p-p) of radicals from pyrolysis of HQ in CO_2 in presence of traces of O_2 (~ 700 ppm) is presented. This group of spectra according to their spectral parameters ($g = 2.0078 - 2.0100$ and ΔH (p-p) = $14 - 14.9$ G (**Figure4.7**)) were different from the group of spectra produced from neat pyrolysis of HQ. They were much broader and possessed high g values (a representative spectrum at pyrolysis temperature at 435°C with $g = 2.00935$ is presented on the top of **Figure.4.7**).

The reason for such differences could be the different experimental pyrolysis conditions. It is reasonable that the change of g value by increasing the pyrolysis temperature can be caused by the formation of new type of radicals in wide temperature region (400 - 750°C). The

broadening of EPR spectra from 9.5 – 12.2 G (neat HQ Pyrolysis) to 14 – 14.9 G (pyrolysis in CO₂, in presence of traces of oxygen, **Figure.4.7**) can be attributed not only to the formation of new type of radicals (for instance RO₂) but also to the effects of concentration broadening (high delivery rate of HQ), ion pairing, polar interactions of frozen radicals on cold finger etc ^{67, 68}. For instance, concentration broadening or ion pairing of EPR spectra of radicals can be evaluated by comparison of the color of the deposits on the finger during neat pyrolysis of HQ (colorless) and pyrolysis in CO₂ (blue in case of HQ, and pink in case of CT). Indeed at higher concentrations, benzosemiquinone anion radicals exhibit a strong blue hue in frozen solution ⁶⁹. The reason for this color is thought to be due to radical complexes in the concentrated systems ^{69,70}.

An influence of ionic environment on broadening the EPR spectra of radicals in solid phase, for instance for char radicals from cellulose pyrolysis has been found in presence of ionic compounds like alkali carbonates, bicarbonates, NaCl ⁷¹.

4.6 References

1. L. Khachatryan, Adoukpe, J., Maskos, M., and Dellinger, B., "Formation of Cyclopentadienyl Radicals from the Gas-Phase Pyrolysis of Hydroquinone, Catechol, and Phenol," *Environ. Sci. Technol.*, *40*, 5071-5076 (2006).
2. D.K. Russell, Davidson, I.M.T., Ellis, A.M., Mills, G.P., Pennington, M., Povey, I.M., Raynor, J.B., Saydam, S., Workman, A.D., "Mechanism of pyrolysis of tricarbonyl(cyclopentadienyl)manganese and tricarbonyl(methylcyclopentadienyl)manganese," *Organometallics*, *14* (1995), 3717-23.
3. A.S. Jeevarajan, and Fessenden, R.W., "Unusual chemically induced dynamic electron polarization of electrons by photoionization," *J.Chem.Phys*, *96* (1992), 1520-23.
4. A. Bussandri, and Willigen, H. van, "Photoionization of phenolates and scavenging of hydrated electrons by NO₃⁻: A study of the reaction mechanism by FT-EPR " *J.Phys. Chem.*, *105* (2001), 4669-75.
5. A. Bussandri, and Willigen, H. van, "FT-EPR study of the wavelength dependence of the photochemistry of phenols," *J.Chem.Phys*, *106* (2002), 1524-32.

6. L. Batt, Benson, S.W., "Pyrolysis of Di-tertiary butyl peroxide: Temperature gradients and chain contribution to the rate," *J.Chem.Phys*, *36* (1962), 895-901.
- 7.M.F.R. Mulcahy, Williams, D.J., and Wilmshurst, J.R., "Reactions of free radicals with aromatic compounds in the gaseous phase " *Aust.J.Chem.*, *17* (1964), 1329-41.
- 8.a.P. Yip. C.K., H.O., "Thermal decomposition of di-tert-butyl peroxide in binary mixtures near the critical point," *Can.J.Chem.*, *49* (1971), 2290-96.
- 9.T. Yamaji, Noda, Y., Yamauchi, S., and Yamauchi, J., "Multi-Frequency ESR Study of the Polycrystalline Phenoxy Radical of r-(3,5-Di-tert-butyl-4-hydroxyphenyl)-N-tert-butyl nitron in the Diamagnetic Matrix," *J. Phys. Chem. A* *110* (2006), 1196-200.
10. B.S. Prabhananda, *J.Chem.Phys*, *59* (1983), 2509-12.
11. C.C. Felix, and Prabhananda, B.S. , *J.Phys. Chem.*, *80* (1984), 3078-81.
12. O. Burghaus, Plato, M., Rohrer, M., Mobius, K., MacMillan, F., Lubitz, W., *J.Phys. Chem.*, *97* (1993), 7639-47.
13. G. Feber, Isaacson, R.A., Okamura, M.Y., Lubitz, W., "In Springer Series in Chemical Physics; Michel-Beyerle, M.E., Ed.," *Springer-Verlag, Berlin.*, (1985), 174-89.
14. S. Un, Tang, X-S., Diner, B.A., *Biochemistry*, *35* (1996), 679-84.
15. F. Graf, Loth, K., and Gunthard, H-H., "Chlorine hyperfine splittings and spin density distribution of peroxy radicals. An ESR and Quantum chemical study.," *Helvetica Chimica Acta.*, *60* (1977), 710-21.
16. H. Hiroyuki Nishide, Kaneko, T., Nii, T., Katoh, K., Tsuchida, E., and Lahti, P.M., "Poly(phenylenevinylene)-Attached Phenoxy Radicals: Ferromagnetic Interaction through Planarized and δ -Conjugated Skeletons," *J.Am.Chem.Soc.*, *118* (1996), 9695-704.
17. P.J. Barker, Davies, A.G., and Tse, M-W. , "The photolysis of cyclopentadienyl compounds of tin and mercury. Electron spin resonance spectra and electronic configuration of the cyclopentadienyl, deuteriocyclopentadienyl, and alkylcyclopentadienyl radicals. ," *J. Chem. Soc., Perkin Transaction 2*, (1980), 941-48.
18. G. NIST Chemical Kinetics Database 17, MD, . (1998).
19. A.J. Collussi, Zabel, F., and Benson, S.W., "The very low-pressure pyrolysis of phenyl ethyl ether, phenyl allyl ether, and benzyl methyl ether and the enthalpy of formation of the phenoxy radical.," *Inern. J. Chem. Kin.*, *9* (1977), 161-78.
- 20.R. Liu, Morokuma, K., Mebel, A.M., Lin, M.C., "Ab initio study of the mechanism for the thermal decomposition of the phenoxy radical," *J.Phys. Chem.*, *100* (1996), 9314-22.

21. a.W. Ihm. H., J.M., "Stepwise Dissociation of Thermally Activated Phenol on Pt(III)," *J.Chem.Phys, B*, 104 (2000), 6202-11.

22. J.A. Manion, and Louw, R., "Rates, products, and mechanisms in the gas-phase hydrogenolysis of phenol between 922 and 1175 K," *J.Phys. Chem.*, 93 (1989), 3563-74.

23. C.A. McFerrin, R.W. Hall and B. Dellinger, "Ab Initio study of the formation and degradation reactions of semiquinone and phenoxy radicals," *Theochem, accepted* (2007).

24. C. Horn, Roy, K., Frank, P., and Just, T., "Shock-tube study on the high-temperature pyrolysis of phenol " *27th Symp.(Intern.) on Combustion / The Combustion Institute, Pittsburgh, PA*, (1998), 321-28.

25. R.J. Kee, Rupley, F.M., Miller, J.A., Coltrin, M.E., Grcar, J.F., Meeks, E., Moffat, H.K., Lutz, A.E., Dixon-Lewis, G., Smooke, M.D., Warnatz, J., Evans, G.H., Larson, R.S., Mitchell, R.E., Petzold, L.R., Reynolds, W.C., Caracotsios, M., Stewart, W.E., Glaborg, P., Wang, C., Adigun, O., Houf, W.G., Chou, C.P., and Miller, S.F., "Chemkin Collection, Release 3.7, Reaction Design, Inc.," *San Diego, CA*, (2002).

26. L.A. Khachatryan, Burcat, A., and Dellinger, B., "An Elementary Reaction Kinetic Model for the Gas-Phase Formation of 1,3,6,8- and 1,3,7,9-Tetrachlorinated Dibenzo-p-dioxins from 2,4,6 -Trichlorophenol," *Combustion and Flame*, 132 (2003), 406-21.

27. F. Berho and R. Lesclaux, "The phenoxy radical: UV spectrum and kinetics of gas-phase reactions with itself and with oxygen," *Chemical Physics Letters*, 279 (1997), 289-96.

28. C.F. Melius, M.E. Colvin, N.M. Marinov, W.J. Pitz and S.M. Senkan, "Reaction mechanisms in aromatic hydrocarbon formation involving the C₅H₅ cyclopentadienyl moiety," *26th Symposium (International) on Combustion; The Combustion Institute: Pittsburgh, PA.*, 26 (1996), 685-92.

29. B. Dellinger, S. Lomnicki, L. Khachatryan, Z. Maskos, R. Hall, J. Adoukpe, McFerrin. C. and H. Truong, "Formation and stabilization of persistent free radicals " *ScienceDirect, Proceedings of the Combustion Institute*, 31 (2007), 521-28.

30. L. Khachatryan, Adoukpe, J., Maskos, Z., Dellinger, B., "Formation of cyclopentadienyl radical from the gas-phase pyrolysis of hydroquinone, catechol and phenol," *Environ. Sci. Technol.*, 40 (2006), 5071-76.

31. L. Khachatryan, Adoukpe, J., and Dellinger, B., "Phenoxy and cyclopentadienyl radicals from the gas-phase pyrolysis of phenol," *J.Phys.Chem., A*, 112, pp 481-487 (2008).

32. B. Dellinger, Lomnicki S.; Khachatryan, L.; Maskos, Z.; Hall, R., W.; Adoukpe, J.; McFerrin, C.; Truong, H., "Formation and stabilization of persistent free radicals," *Proceedings of the Combustion Institute* 31 (2007), 521-28.

33. Hieu Truong, Slawo Lomnicki and B. Dellinger, "Mechanisms of molecular product and persistent radical formation from the pyrolysis of hydroquinone," *Chemosphere, in press* (2007).

34. M. Karni, I. Oref and A. Burcat, "Ab-Initio calculations and ideal gas thermodynamic functions of cyclopentadiene and cyclopentadiene derivatives," *J.Phys. Chem. Ref. Data*, 20 (1991), 665-83.
35. X. Zhong and J.W. Bozzelli, "Thermochemical and kinetic analysis of the H, OH, HO₂, O, and O-2 association reactions with cyclopentadienyl radical," *Journal of Physical Chemistry A*, 102 (1998), 3537-55.
36. M.T. Cocivera, M.; Groen, A., *Journal of American Chem. Society*, 94 (1972), 6598.
37. R.F. Pottie and F.P. Lossing, "Free radicals by mass spectrometry. XXIX. Ionization potentials of substituted cyclopentadienyl radicals," *Division of Pure Chemistry, National research Council, Ottawa, Canada*, (1962), 269-71.
38. C.F. Melius, Colvin, M.E., Marinov, N.M., Pitz, W.J., Senkan, S.M., "Reaction mechanisms in aromatic hydrocarbon formation involving the C₅H₅ cyclopentadienyl moiety," *Proc. Combust. Inst.*, 26 (1996), 685-92.
39. H. Truong, Copper II Oxide Mediated Formation and Stabilization of Combustion Generated Persistent Free Radical In *Chemistry Department*, (Baton Rouge: Louisiana State University, 2007), 157.
40. K. Loth, Graf, F., and Gunthard, H-H., "Effects of intramolecular and intermolecular proton transfer processes onto the ESR spectra of o-semiquinone radicals.," *Chemical Physics Letters*, 45 (1977), 191-96.
41. J.G. Calvert, and Pitts, J.N. Jr, "Photochemistry," *John Wiley & Sons, Inc.* (1966), 499.
42. P. Neta, and Fessenden, R.W., "Hydroxyl radical reactions with phenols and anilines as studied by ESR.," *J.Phys. Chem.*, 78 (1974), 523-29.
43. H.M. McConnell, *Journal of Chemical Physics*, 24 (1956), 764.
44. H.M.a.C. McConnell, D.B., *Journal of Chemical Physics*, 28 (1958), 107.
45. J.A. Weil, Bolton, J.R., Wertz, J.E., "Electron Paramagnetic Resonance," *J.Wiley & Sons, Inc., NY*, (1994).
46. E.B. Ledesma, Marsh, N.D., Sandrowitz, A.K., and Wornat, M.J, "An Experimental Study on the Thermal Decomposition of Catechol," *Proc. Combust. Inst.*, 29 (2002), 2299-306.
- 47.C.E. Evans, and Dellinger, B., "Mechanisms of Dioxin Formation from the High-Temperature Pyrolysis of 2-Chlorophenol," *Environ. Sci.&Technol.*, 37 (2003), 1325-30.
48. T. Sakai, and Hattori, M., "Thermal Decomposition of Catechol, Hydroquinone and Resorsinol.," *Chemistry Letters*, (1976), 1153-56.
49. A.V. Friderichsen, Shin, E-J., Evans, R.J., Nimlos, M.R., Dayton, D.C., Ellison, G.B., "The pyrolysis of anisole (C₆H₅OCH₃) using a hyperthermal nozzle," *Fuel*, 80 (2001), 1747-55.

50. N.D. Marsh, Ledesma, E. B., Sandrowitz, A. K., and Wornat, M. J., "Yields of Polycyclic Aromatic Hydrocarbons from the Pyrolysis of Catechol [ortho-Dihydroxybenzene]: Temperature and Residence Time Effects.," *Energy&Fuels*, 18(1) (2004), 209-17.
51. D.D. Davis, Nielsen, M.T(ed), "TOBACCO. Production, Chemistry and Technology," *Chapter 12, Smoke Chemistry, Baker, R.R.* (1999), 398-439.
52. G.H. Bokelman, Ryan, W. S., "Analyses of Bright and Burley tobacco laminae and stems.," *Beitr. Tabakforsch.*, 13 (1985), 29-36.
53. W.A. Pryor, Stone, K., Zang, L-Y., and Bermudez, E., "Fractionation of Aqueous Cigarette Tar Extracts: Fractions that Contain the Tar Radical Cause DNA Damage," *Chem.Res. Toxicol.*, 11 (1998), 441-48.
54. B. Dellinger, W.A. Pryor, R. Cueto, G.L. Squadrito and W.A. Deutsch, "The role of combustion-generated radicals in the toxicity of PM2.5," *Proceedings of the Combustion Institute*, 28 (2000), 2675-81.
55. B.B. Halliwell, and Poulsen, H.E. Editors, "Cigarette Smoke and Oxidative Stress," *Springer-Verlag, Berlin Heidelberg*, (2006).
56. Z.D. Maskos, B., "Formation of the Secondary Radicals from the Aging of Tobacco Smoke," *Energy & Fuel*, 22 (2008), 382-88.
57. R.R.P. Baker, C.J., "The Origins and Properties of Environmental Tobacco Smoke," *Environ Int*, 16:231245 (1990).
58. W.A. Pryor, Hales, B.J., Premovic, P.I., Church, D.F., "The radicals in cigarette tar: Their nature and suggested physiological implications," *Science*, 220 (1983), 425-27.
59. W.A. Pryor, "Oxy-Radicals and Related Species: Their Formation, Lifetimes, and Reactions," *Annual Review of Physiology*, 48 (1986), 657-67.
60. Z. Maskos, Khachatryan, L., Cueto, R., Pryor, W.A., and Dellinger, B, "Radicals from the Pyrolysis of Tobacco," *Energy & Fuels*, 19 (2005), 791-99.
- 61.T.M. Flicker, Green, S. A., "Detection and separation of gas-phase carbon-centered radicals from cigarette-smoke and Diesel exhaust.," *Analytical Chemistry*, 70 (1998), 2008-12.
62. S. Lomnicki, Dellinger, B., "A detailed mechanism of the surface-mediated formation of PCDD/F from the oxidation of 2-chlorophenol on a CuO/silica surface.," *Journal of Physical Chemistry A*, 107 (2003), 4387-95.
63. W.A. Pryor, Prier, D. G., Church, D. F., "Electron spin resonance study of mainstream and sidestream smoke: Nature of the free radicals in gas-phase smoke and in cigarette tar.," *Environmental Health Perspectives*, 47 (1983), 345-55.

64. J. Adoukpe, Khachatryan, L; Dellinger B., "Radicals from the Gas-Phase Pyrolysis of Hydroquinone 1. Temperature dependence of the total radical yield.," *Fuels and Energy Submitted*, (2008).
65. J. Adoukpe, Khachatryan, L; Dellinger B., "Radicals From the Thermal Degradation of Catechol," *in Preparation*, (2008).
66. L. Khachatryan, Niazyan, O., Mantashyan, A.H., Vedeneev, V.I., Teitel'boim, M.A.,, "Experimental determination of the equilibrium constant of the reaction $\text{CH}_3 + \text{O}_2 \rightleftharpoons \text{CH}_3\text{O}_2$ during the gas-phase oxidation of methane.," *Int.J.Chem.Kin.*, *14* (1982), 1231-41.
67. D.J.E. Ingram, "Free radicals as studied by Electron Spin Resonance," *Butterwords Publ. Limited* (1958), 210.
68. B.J. Hales, "Immobilized Radicals. 3. Anisotropic saturation of Semiquinones in Protic Solvents," *The Journal of Chemical Physics*, *65* (1976), 3767-72.
69. B.J. Hales, "Immobilized Radicals. I. Principal Electron Spin Resonance Parameters of the Benzosemiquinone Radical," *Journal of the American Chemical society*, *97* (1975), 5993-97.
70. D. Campbell, and Symons, M.C.R., "Unstable intermediates. Part LXVII. ESR spectrum of cyclohexadienyl radicals from resorcinol: the mechanism of radiation damage," *J.Chem.Soc. (A)*, *9/840* (1969), 2977-78.
71. J.-W. Feng, Zheng, S., and Maciel, G.E., "EPR investigation of the effects of inorganic additives on the charring and char/air interactions of cellulose," *Energy & Fuels*, *18* (2004), 1049-65.

CHAPTER 5: SUMMARY

Combustion-generated Particulate Matter (PM) toxicity is attributed to their association with semiquinone type radicals¹⁻⁴ supposedly formed from redox cycling of catechol (CT), hydroquinone (HQ) and structurally similar compounds found in woods, biomass, fuels and tobacco⁵⁻¹².

However, semiquinone type radicals have only been reported in the pyrolysis of tobacco^{13, 14}. Given that other organic materials such as woods, biomass coals, etc contain CT, HQ and phenols, semiquinone type radicals being solely found in tobacco burning is quite surprising. It is therefore very important to investigate the exact nature of radicals formed from the pyrolysis of CT, HQ, and phenols to compare to those formed in tobacco. In the following paragraphs, summary of the key findings, employing CT, HQ, phenols and tobacco will be presented.

5.1 Cyclopentadienyl Radical

From **Scheme 4.1**, thermal degradation of CT, HQ, and phenols should lead to phenoxy radical that further decomposes to CPD by CO elimination¹⁵. In our gas-phase phenol thermal degradation study, CPD and phenoxy radicals are respectively identified as pyrolysis products and their EPR gas-phase spectra acquired.

The pyrolysis of phenol from 400 to 1000° C shows a linear time dependence of radical signal intensity **Figure 5.1** while the temperature dependence shows a sudden increase from 700°C **Figure 5.2**.

In this study, and according to **Scheme 4.1**, CPD radical was detected as the end point of phenol (low and high temperatures), catechol and hydroquinone (high temperature) thermal degradation.

The identification of CPD radical was rendered easy first by pyrolysing the tricarbonylcyclopentadienylmanganese ($\eta^5\text{-C}_5\text{H}_5\text{Mn}(\text{CO})_3$) at 250°C¹⁶. The pure CPD radical, a

six lines EPR spectrum, exhibits an isotropic 1:5:10:10:5:1, with a g value of 2.00431, characteristic of carbon-centered radicals, and shows a linear microwave power dependence consistent with reports in the literature ¹⁷. This spectrum was compared to those from pyrolysis of CT, HQ and phenol in step by step annealing experiments. The CPD radical from phenol, CT and HQ pyrolysis matches perfectly the pure CPD radical from $\eta^5\text{-C}_5\text{H}_5\text{Mn(CO)}_3$.

The pyrolysis of phenol, CT, and HQ at various temperatures yielded a mixture of radicals from which the most abundant and persistent at temperatures above 800 °C are CPD radicals. At temperatures above 850°C, all annealed spectra from the pyrolysis of HQ resulted in an EPR spectrum with 6 lines, $\Delta\text{H (p-p)} \sim 3.0$ G, a g-value of 2.00430, and a hyperfine splitting constant ~ 6.0 G. Those characteristics link to the CPD radical that we compared with the pure CPD radical from the pyrolysis of the tricarbonylcyclopentadienylmanganese ($\eta^5\text{-C}_5\text{H}_5\text{Mn(CO)}_3$) at

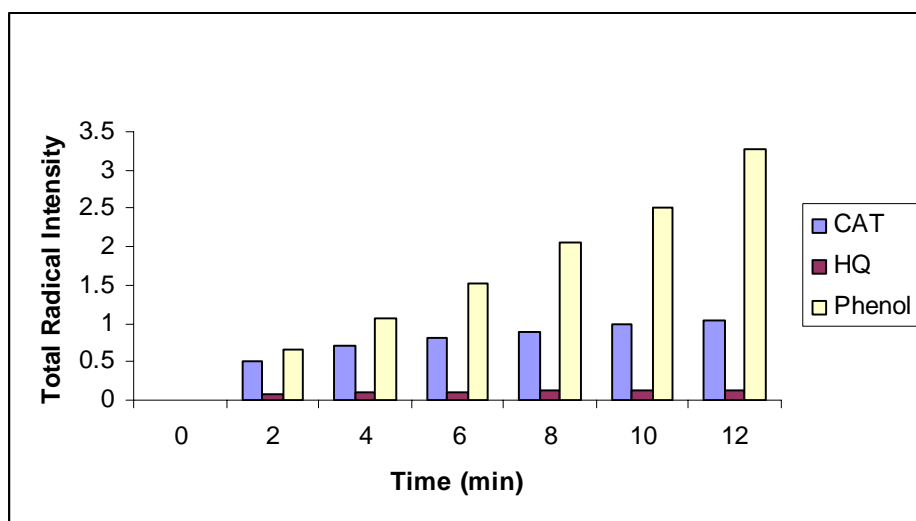


Figure 5.1 A comparative total radical yields from 0 to 12min accumulation time of radicals from the pyrolysis of CT(blue), HQ(red) and Phenol(yellow). HQ shows the lowest yield. While total radical from phenol keeps an increasingly linear trend, saturation is reached at approximately 10 min of total radical accumulation from CT and HQ

250°C ¹⁶. They were perfect matches. Our calculation led to the conclusion that CPD radicals were dominant at temperature above 850°C during the pyrolysis of HQ.

5.2 Phenoxy Radical

The gas-phase phenoxy radical EPR spectrum has not been reported in the literature. Its primary precursor should be phenol which is used in this study to characterize the under-investigation radical. Several experimental techniques were used and/or combined to positively assign the EPR spectrum of phenoxy radical as a non-resolved five lines spectrum. The photo-excitation of phenol at 250-300nm¹⁸⁻²⁰ was performed at room temperature. It yielded a non-resolved five lines spectrum with a $g = 2.0060$, characterizing an oxygen centered radical. This spectrum was compared to the pure phenoxy radical spectrum generated from the thermal degradation of phenol at 250°C in di-tert-butylperoxide (DTBP) under CO₂ flow. The DTBP is known to react with phenol by extracting the hydrogen atom from the hydroxyl group of phenol²¹⁻²³. The five line spectrum obtained from the reaction of the DTBP with phenol has a g value of 2.00582, an oxygen-centered radical. A perfect match was observed when the two spectra were superposed to the one from the thermal degradation of phenol at temperature below 500°C conclusively leading to the identification of gas-phase phenoxy radical EPR spectrum.

However the phenoxy radical EPR spectrum was impossible to detect in the mixture of radicals from the pyrolysis of HQ and CT. Even though the left hand side broadening of acquired EPR spectra of products of the pyrolysis of HQ and CT as in the case of the pyrolysis of phenol, is the evidence of the presence of phenoxy radical, the latter is completely lost during annealing.

In addition to CPD and phenoxy radical from the pyrolysis of phenol, the hydroxyhexadienyl was observed

5.3 Ortho-Semiquinone and Para-Semiquinone Radicals

Unlike the pyrolysis of phenol, the time dependence of radical intensity from the pyrolysis of Hydroquinone and Catechol showed saturation towards the end of the accumulation period as

depicted by **Figure 5.1**. The temperature dependence of HQ pyrolysis showed an increase in signal intensity from 300 to 850°C, followed by a decrease above 850°C. From **Scheme 4.1**, p-Semiquinone (p-SQ), o-Semiquinone (o-SQ), CPD, phenoxy, and Hydroxycyclopentadienyl (HO-CPD) radicals are more likely the most Persistent Free Radicals (PFRs) to form from the pyrolysis of HQ and CT. We have positively identified and acquired p-SQ, and o-SQ radical from the pyrolysis at low temperature of HQ and CT respectively.

A featureless singlet line EPR spectrum was detected from the pyrolysis of HQ at 400°C with $g = 2.0048-2.005$ attributable to oxygen-centered radicals. The photolysis reaction of HQ yielded an EPR spectrum with singlet line and $g = 2.0044$. Both spectra with a ΔH (p-p) = 12 G were superposed and matched each other. Based on those considerations (singlet line, g-value and ΔH (p-p)), we have assigned to this spectrum the para-Semiquinone (p-SQ) radical. Also, it is known that between 500 and 600°C, the major product of the pyrolysis of HQ is the para-Benzoquinone (p-BQ) formed through expulsion of one hydrogen atom from the p-SQ radical²⁴. Our calculations showed that in the mixture of phenoxy, CPD and p-SQ radicals, p-SQ is the dominant radical at temperatures below 750°C.

The pyrolysis of CT between 400 and 600°C yielded a featureless singlet and strong line EPR spectrum with $g = 2.0058-2.0061$ and a ΔH p-p = 13.5-15.0 G attributable to oxygen-centered radicals. We have performed CT photolysis. The photolysis reaction of CT yielded a weak EPR spectrum with singlet line, $g = 2.0052$, and a ΔH (p-p) = 12.60-15.6G very close to the values reported in the literature for hydroxypyrimidines radicals in aqueous solution²⁵. Both EPR spectra from CT pyrolysis and photolysis were superposed and matched each other quite well except for the height of the spectrum from the pyrolysis which was greater than that of photolysis. This slight difference is attenuated with pyrolysis at lower temperature, but then the spectra have a splitting at the center. Unlike HQ, the literature data to confidently assign spectra

observed at low temperature pyrolysis of CT is missing. We have than to rely on experimental variation and mathematical tools to solve the identification issue. We have successfully identified o-SQ radical from the pyrolysis of CT at low temperature very much comparable to the photolysis radical.

5.4 Hydroxycyclopentadienyl Radical

At the present time, our experiments and mathematical manipulations did not allow us to acquire OHCPD radical EPR spectrum. However, the GC-MS analysis of the pyrolysis products of CT revealed the formation of fluorene ($m/z = 166$), and 1H-Indenol ($m/z = 132$) and its isomer 1H-Inden-1-one_2,3_ dihydro, acenaphthylene ($m/z = 152$), Benzofuran-7-methyl, Benzofuran-2-methyl ($m/z = 132$). The detection of 1H-Indenol gives evidence of the formation of labile radicals such as hydroxycyclopentadienyl radical, while that of fluorene confirms not only the formation of CPD radical but also of aliphatic radicals such as ethenyl, and acetylenyl radicals²⁶.

A computer-generated Hydroxycyclopentadienyl radical EPR spectrum, a five line spectrum

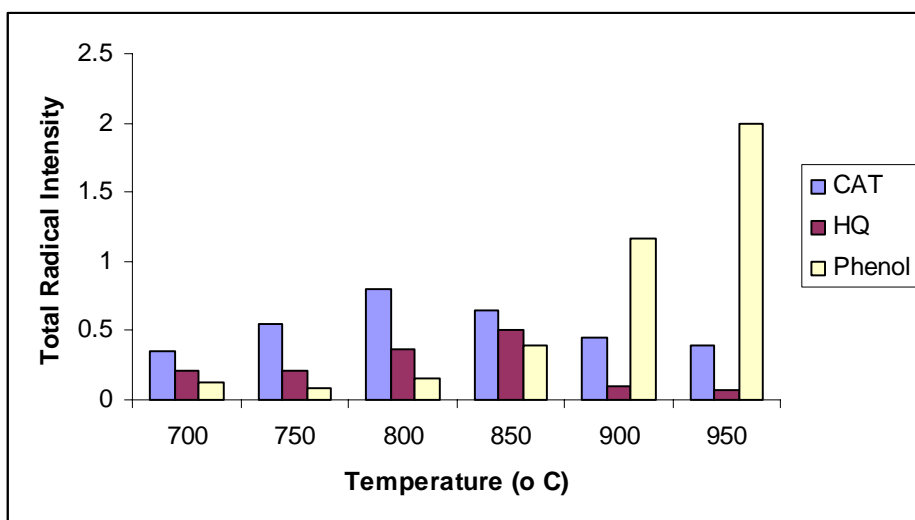


Figure 5.2 Temperature Dependence of Total Radical Yield. CT values to the scale, HQ values have been multiplied by 2 and Phenol's value divided by 10. CT and HQ have the same trends with maximum at 800°C and 850 °C while Phenol's values have a sudden increase by 800 °C.

with intensity distribution 1:4:6:4:1 was compared with the EPR spectra from the pyrolysis of HQ in all temperature regions. There was no match. However, the GC-MS analysis of the atmospheric pressure pyrolysis products of HQ revealed the formation of, in addition to naphthalene, indene and Hydroxyindene, supposedly results of the CO elimination from either Hydroxynaphthalene or Dihydroxynaphthalene themselves results of the condensation of one molecule of CPD and one of OHCPD, or the condensation of two molecules of OHCPD. The formation of indene and Hydroxyindene during the pyrolysis of HQ is the evidence of OHCPD gas-phase formation. We concluded that OHCPD is formed but were not persistent enough to acquire its EPR spectrum with the various techniques we used in the present study.

5.5 Methylperoxide Radical

It has been demonstrated that the pyrolysis of CT and HQ promotes formation of methyl (CH_3), ethyl (CH_3CH_2)^{27, 26} and acetylene²⁶ that contributed to the formation of PAHs. In our effort to identify persistent free radicals formed from the pyrolysis of CT, HQ and phenol, we have had a close look at the effect of traces of oxygen on the shape of radicals. In the HQ case, we found that increasing oxygen concentration from 15ppm to 700ppm yielded broader EPR spectra which widths increase with oxygen concentration. Mathematical manipulations using Simphonia software helped to extract a resulting EPR spectrum with a total width of 75-80 G, hyperfine splitting at the bottom of spectra was $\sim 5.42\text{G}$ with a g-value of 2.010. The spectrum known in the literature as methyl peroxide radical spectrum^{28, 29} exhibits exactly same characteristics as the one we detected in our study. We have then positively identified the methyl peroxide radical as a persistent radical in addition to p-SQ, and CPD radicals.

5.6 Radicals from Tobacco

Semiquinone type radical has been reported in tobacco^{14, 30, 31}. CT and HQ are known to be major constituents of mainstream tobacco smoke. Our thermal degradation of pure compound of

CT and HQ showed formation of o-SQ and p-SQ respectively in addition to CPD, phenoxy and OHCPD radicals. It is therefore expected that the gas-phase pyrolysis of tobacco should yield radicals comparable to those formed by the pyrolysis of the precursors. The pyrolysis of tobacco did not give any radical which EPR spectra are close to those of CPD, phenoxy and OHCPD. Instead, featureless singlet line EPR spectra comparable to those of o-SQ and p-SQ were acquired during the pyrolysis of all blends of tobacco. A comparative study of their characteristics was inconclusive. Therefore, we can not, at the present time confirm that the gas-phase radicals formed during the pyrolysis of tobacco are either o-SQ or p-SQ. They are just singlet line that gives no further information on their nature. Further investigation on persistent gas-phase radicals yielded by the pyrolysis of tobacco is therefore needed to do a comparative study of the already determined persistent free radicals from the precursors in the present work with the probable persistent radicals from tobacco.

Table 5.1 gives a summary of the environmentally persistent free radicals observed from the pyrolysis of catechol, hydroquinone, and phenol, along with their respective temperature region of dominance.

5.7 Radical from Tobacco Compared to Those from Precursors

The gas-phase low pressure pyrolysis of pure compounds such as catechol, hydroquinone and phenol, major components of mainstream tobacco smoke, yielded variety of radicals among which we have identified cyclopentadienyl, phenoxy, o-Semiquinone, p-Semiquinone, and hydroxycyclopentadienyl. Given that catechol, hydroquinone and phenol are found in mainstream tobacco smoke, it is expected that the low pressure pyrolysis of tobacco would yield radicals comparable to those from the precursors. The present thorough study did not give the expected results. Several possible explanations to this fact are proposed in the following paragraphs

Table 5.1. Summary of Key Findings

| Precursors | 300-700 | 700-800 | 800-850 | 850-1000 |
|--------------|---------------------------|---|--|----------|
| Phenol | Phenoxy (trace of CPD) | Mixture (phenoxy, CPD) Phenoxy > CPD | Mixture (phenoxy, CPD) CPD > Phenoxy | CPD |
| Hydroquinone | p-Semiquinone | Mixture (p-SQ, phenoxy, OHCPD, CPD) p-SQ dominates | Mixture (p-SQ, phenoxy, OHCPD, CPD) CPD dominates | CPD |
| Catechol | o-Semiquinone | Mixture (o-SQ, phenoxy, CPD, OHCPD) o-SQ dominates | Mixture (o-SQ, phenoxy, CPD, OHCPD) CPD dominates | CPD |
| Tobacco | Singlet line | | | |

The first possible explanation is experimental. During the pyrolysis of pure compounds, the complications that arise from the convolution of several radicals and that necessitated additional experimental and mathematical tools in interpreting the spectra in order to assign radicals were

signs that the study of tobacco, a very complex compound made of not only the precursors studied, but of hundreds of other organic compounds³² including pectin, protein, lignin, cellulose, cryogenic acids³³, and some metals will not be an easy task. It is possible that the free

radicals that are formed during the pyrolysis of tobacco either terminate by radical-radical recombination or convolute in the singlet EPR signal that was observed.

Semiquinone type radicals have been reported in cigarette smoke^{34, 35}. The photolysis at room temperature of catechol and hydroquinone as well as their pyrolysis at low temperature yielded singlet line EPR spectra that we identified to o-semiquinone and p-semiquinone respectively. The pyrolysis of tobacco also yielded a singlet line EPR spectrum. Logically, the possible comparison is between the latter and the o-semiquinone and p-semiquinone radicals.

The g-values, one of EPR spectra characteristics used to associate carbon-centered or oxygen-centered radicals were found to vary between 2.00368 and 2.00399 for the singlet line spectra from the pyrolysis of tobacco. This range of g-values characterizes surface-associated carbon-centered radical³⁶ and partially delocalized, polymeric, phenoxy type radicals^{37, 38} reported in the literature. o-semiquinone and p-semiquinone radicals that we have identified have higher g-values (2.0044-2.0061). Therefore based on the g-values we can not clearly say what radicals from the pyrolysis of tobacco give the singlet line EPR spectrum observed. Another EPR spectra characteristic is the peak to peak width of the spectrum.

The width of the singlet EPR spectrum from the pyrolysis of tobacco varies between 8.008 to 10.156 G, higher than the ~ 6.6G reported in the literature³⁹ and that led to the conclusion that p-SQ types radicals were in Tobacco Particulate Matter (TPM). However, the pure p-SQ radical generated in our gas phase pyrolysis/photolysis study has the following characteristics: g-values ~ 2.0044-2.0049, and $\Delta H_{p-p} \sim 12G$ ^{15, 40}. The pure o-SQ generated has g-values ~ 2.0052-2.0061 with $\Delta H_{p-p} \sim 12.60-15.60G$ ⁴⁰. Those two sets of values (g-values and peak-to-peak widths) do not match their counterpart from tobacco gas-phase pyrolysis. At this point of our study, there is no conclusive assignment of the singlet line EPR spectrum from the pyrolysis of tobacco.

The second possible explanation of the non assignment of radical from tobacco compared to those from the precursors may be the pyrolysis environment of tobacco. As said previously, tobacco is made of hundred of organic compounds and metal. The rapid destruction of the formed radicals either by radical-radical reaction, or radical interaction with surfaces (metal, tobacco ash) may explain their non appearance in the EPR spectra. Metal surface bound radical was reported in the literature ^{41, 42}. Given that tobacco contain metals, it is possible that even if the radicals are formed, they do not exit the tobacco bed before their destruction. Consequently, they can not reach the cold finger of the Dewar to be detected by EPR.

It may be possible to get a better understanding of radicals formed from tobacco pyrolysis employing the Electron Nuclear Double Resonance (ENDOR) technique. This technique described as EPR detected NMR (Nuclear Magnetic Resonance) allows simultaneous detection of paramagnetic species and nuclei in the vicinity of the unpaired electron, thus giving the precise structure of the molecule under investigation ^{43, 44}

Another experimental tool that will give very good insights in understanding the decomposition pathway of the precursors is the Time of Flight (TOF) associated with Mass Spectroscopy. When combined with the Resonance Enhanced Multiphoton Ionization, TOF-MS is an ideal tool to accurately identify decomposition fragments of the precursors ⁴⁵⁻⁴⁷. Without any doubt, the fragmentation of the precursor will allow not only a qualitative but also a quantitative study of its decomposition pathway.

5.8 Concluding Remarks

The reported studies were designed to determine if potentially environmentally persistent free radicals could be formed from the pyrolysis of suspected precursors, phenol, HQ, and CT. Environmental persistence requires a combination of stability (resistance to decomposition) and low reactivity (slow rate of reaction with other radicals and molecules, particularly molecular

oxygen). Our pyrolysis experiments did address their high temperature stability but did not address reactivity with oxygen which would be the major route of destruction of these radicals in the atmosphere and, under some conditions, in combustion systems.

The thorough study of phenol, HQ and CT thermal degradation revealed that all three precursors have similar thermal degradation behavior. Below 600°C, the pyrolytic decomposition of each precursor is characterized by a dominant simple dissociation of the hydroxyl hydrogen, leading to phenoxy, o-SQ and p-SQ for phenol, CT, and HQ, respectively. The calculated O-H bond dissociation energies of phenol, CT and HQ are consistent with the temperatures of initiation of decompositions (300-400°C and 500°C, respectively). Intermediate temperature pyrolysis (600-800°C) of the precursors yielded complex mixtures of radicals identifiable only by annealing and microwave power dependence experiments. Phenoxy radical was identified in this mixture for each precursor. Above 800°C, the dominant radical from each precursor was CPD radical.

Our experiments demonstrated that during annealing of the matrix, CPD still persisted, while other radicals were annihilated, presumably by radical-radical recombination. It is not clear from the pyrolysis experiments alone if CPD is less reactive than the other radicals or survives because of its initially high concentration. The dominance of CPD radical over phenoxy and semiquinone radicals was quite surprising in the light of the stability of phenoxy and semiquinone radicals proposed in the literature^{48, 49}. However, our reaction kinetic model for the pyrolysis of phenol⁵⁰ is consistent with the high CPD/phenoxy ratio that leads to the dominance of CPD over phenoxy radical in the intermediate pyrolysis temperature region.

Based on our results, phenoxy, o-SQ, p-SQ, and CPD are all formed from these precursors under some pyrolysis conditions. O-SQ, p-SQ, and phenoxy are not stable above 600 C and

decompose to form CPD. CPD is stable enough to survive in measureable concentrations above 800 C.

The question is now whether it is reactive with molecular oxygen. O-SQ, p-SQ, and phenoxy are expected to be less reactive because they can exist in oxygen-centered structures that resist reaction with oxygen. In contrast, CPD is a purely carbon-centered radical that may react with oxygen. Reaction kinetic studies of the rate of reaction of these radicals with oxygen should be conducted to determine their reactivity. Reaction kinetic studies of the rate of destruction of phenoxy, o-SQ, p-SQ, and CPD as a function of initial radical concentration should be performed to determine their stability. The combination of these studies will define their persistence under combustion conditions..

5.9 References

1. B.. Dellinger, Pryor, W. A.; Cueto, R.; Squadrito, G. L.; Hedge, V.; Deutsch, W. A. 2001, 14, 1371-1377., "Role of free radicals in the toxicity of airborne fine particulate matter.," *Chem. Res. Toxicol.*, 14 (2001), 1371-77.
2. Z.a.Z. Meng, Q., "Oxidative damage of dust storm fine particles instillation on lungs, hearts and livers of rats " *Environmental Toxicology and Pharmacology* 22 (2006), 277-82.
3. K.B. Donaldson, D. M.; Mitchell, C.; Dineva, M.; Beswick, P.; Gilmour, P.; MacNee, W., "Free Radical Activity of PM10: Iron-mediated Generation of Hydroxyl Radicals," *Environ Health Perspect*, 105 (1997), 1285-89.
4. G.L. Squadrito, B. Dellinger, R. Cueto, W.A. Deutsch and W.A. Pryor, "Quinoid Redox Cycling as a Mechanism for Sustained Free Radical Generation by Inhaled Airborne Particulate matter," *Free Radical Biology & Medicine*, 31 (2001), 1132-38.
5. C.G.S. Nolte, J. J.; Cass, G. R.; Simoneit, B. R. T., "Highly polar organic compounds present in wood smoke and in the ambient atmosphere. ," *Environmental Science & Technology* 35 (2001), 1912-19.
6. G.E.M. Troughton, J. F.; Chow, S. Z., " Lignin utilization. II. Resin properties of 4-alkyl-substituted catechol compounds. ," *Forest Products Journal* 22 (1972), 108-10.
7. R.E. Font, M.; Garcia, A. N., , "Toxic by-products from the combustion of Kraft lignin. *Chemosphere* 2003, 52, (6), 1047-1058," *Chemosphere*, 52 (2003), 1047-58.

8. B.R.T. Simoneit, Biomass burning - "A review of organic tracers for smoke from incomplete combustion. ," *Applied Geochemistry*, 17 (2002), 129-62.
9. M.D.F. Hays, P. M.; Geron, C. D.; Kleeman, M. J.; Gullett, B. K, "Open burning of agricultural biomass: Physical and chemical properties of particle-phase emissions. ." *Atmospheric Environment* 39 (2005), 6747-64.
10. R.H. Visser, A. A. M.; Hovestad, A.; Stevens, T. W., "Identification of organic compounds in waste water of wood gasifiers with capillary gas chromatography," *Proc. Int. Symp. Capillary Chromatogr*, 6 (1985), 281-87.
11. P.M.C. Fine, G. R.; Simoneit, B. R. T., "Chemical characterization of fine particle emissions from the fireplace combustion of wood types grown in the Midwestern and Western United States," *Environmental Engineering Science* 21 (2004), 387-409.
12. P.M.C. Fine, G. R.; Simoneit, B. R. T., "Chemical characterization of fine particle emissions from fireplace combustion of woods grown in the northeastern United States," *Environmental Science & Technology* 35 (2001), 2665-75.
13. W.A. Pryor, Prier, D.G., and Church, D.F., "ESR Study of mainstream and sidestream cigarette smoke:Nature of free radicals in gas-phase smoke and in cigarette tar.," *Environmental Health Perspectives*, 47 (1983), 345-55.
14. W.A. Pryor, Hales, B.J., Premovic, P.I., Church, D.F., "The radicals in cigarette tar: Their nature and suggested physiological implications," *Science*, 220 (1983), 425-27.
15. J. Adoukpe, L. Khachatryan; Dellinger B., "Radicals from the Gas-Phase Pyrolysis of Hydroquinone 1. Temperature dependence of the total radical yield.," *Fuels and Energy Submitted*, (2008).
16. D.K. Russell, Davidson, I.M.T., Ellis, A.M., Mills, G.P., Pennington, M., Povey, I.M., Raynor, J.B., Saydam, S., Workman, A.D., "Mechanism of pyrolysis of tricarbonyl(cyclopentadienyl)manganese and tricarbonyl(methylcyclopentadienyl)manganese," *Organometallics*, 14 (1995), 3717-23.
17. P.J. Barker, Davies, A.G., and Tse, M-W. , "The photolysis of cyclopentadienyl compounds of tin and mercury. Electron spin resonance spectra and electronic configuration of the cyclopentadienyl, deuteriocyclopentadienyl, and alkylcyclopentadienyl radicals. ," *J. Chem. Soc., Perkin Transaction* 2, (1980), 941-48.
18. A.S. Jeevarajan, and Fessenden, R.W., "Unusual chemically induced dynamic electron polarization of electrons by photoionization," *J.Chem.Phys*, 96 (1992), 1520-23.
19. A. Bussandri, and Willigen, H. van, "Photoionization of phenolates and scavenging of hydrated electrons by NO₃⁻ : A study of the reaction mechanism by FT-EPR " *J.Phys. Chem.*, 105 (2001), 4669-75.

20. A. Bussandri, and Willigen, H. van, "FT-EPR study of the wavelength dependence of the photochemistry of phenols," *J.Chem.Phys*, *106* (2002), 1524-32.
21. L. Batt, Benson, S.W., "Pyrolysis of Di-tertiary butyl peroxide: Temperature gradients and chain contribution to the rate," *J.Chem.Phys*, *36* (1962), 895-901.
22. M.F.R. Mulcahy, Williams, D.J., and Wilmshurst, J.R., "Reactions of free radicals with aromatic compounds in the gaseous phase " *Aust.J.Chem.*, *17* (1964), 1329-41.
23. Yip. C.K. and H.O. Pritchard, "Thermal decomposition of di-tert-butyl peroxide in binary mixtures near the critical point," *Canadian Journal of Chemistry*, *49* (1971), 2290-96.
24. Hieu Truong, Slawo Lomnicki and B. Dellinger, "Mechanisms of molecular product and persistent radical formation from the pyrolysis of hydroquinone," *Chemosphere*, *in press* (2007).
25. H.M.T. Novais, J. P.; Steenken, S., "Structure of radicals derived from hydroxypyrimidines in aqueous solution," *J.Chem. Soc. Perkin Trans.*, *2* (2002), 1412-17.
26. E.B. Ledesma, Marsh, N.D., Sandrowitz, A.K., and Wornat, M.J, "An Experimental Study on the Thermal Decomposition of Catechol," *Proc. Combust. Inst.*, *29* (2002), 2299-306.
27. T. Sakai, and Hattori, M., "Thermal Decomposition of Catechol, Hydroquinone and Resorsinol.," *Chemistry Letters*, (1976), 1153-56.
28. L. Khachatryan, Niazyan, O., Mantashyan, A.H., Vedeneev, V.I., Teitel'boim, M.A.,, "Experimental determination of the equilibrium constant of the reaction $\text{CH}_3 + \text{O}_2 \rightleftharpoons \text{CH}_3\text{O}_2$ during the gas-phase oxidation of methane.," *Int.J.Chem.Kin.*, *14* (1982), 1231-41.
29. M. Carlier, Pauwels, J.P., and Sochet, L-R., "Application of ESR techniques to the study of gas-phase oxidation and combustion phenomena," *Oxidation Communication*, *6* (1984), 141-56.
30. L.Y. Zang, Stone, K., and Pryor, W.A., "Detection of Free Radicals in Aqueous Extracts of Cigarette Tar by ESR," *Free Radical Biol. Med.*, *19* (1995), 161-67.
31. W.A. Pryor, "Cigarette smoke radicals and the role of free radicals in chemical carcinogenicity.," *Environmental Health Perspectives*, *105* (1997), 875-82.
32. D.D. Davis, Nielsen, M.T(edt), "TOBACCO. Production, Chemistry and Technology," *Chapter 12, Smoke Chemistry*, Baker, R.R. (1999), 398-439.
33. G.H. Bokelman, Ryan, W. S., "Analyses of Bright and Burley tobacco laminae and stems.," *Beitr. Tabakforsch.*, *13* (1985), 29-36.
34. W.A. Pryor, Stone, K., Zang, L-Y., and Bermudez, E., "Fractionation of Aqueous Cigarette Tar Extracts: Fractions that Contain the Tar Radical Cause DNA Damage," *Chem.Res. Toxicol.*, *11* (1998), 441-48.

35. B. Dellinger, W.A. Pryor, R. Cueto, G.L. Squadrito and W.A. Deutsch, "The role of combustion-generated radicals in the toxicity of PM_{2.5}," *Proceedings of the Combustion Institute*, 28 (2000), 2675-81.
36. T.M. Flicker, Green, S. A., "Detection and separation of gas-phase carbon-centered radicals from cigarette-smoke and Diesel exhaust.," *Analytical Chemistry*, 70 (1998), 2008-12.
37. Z. Maskos, Khachatryan, L., Cueto, R., Pryor, W.A., and Dellinger, B, "Radicals from the Pyrolysis of Tobacco," *Energy & Fuels*, 19 (2005), 791-99.
38. S. Lomnicki, Dellinger, B., "A detailed mechanism of the surface-mediated formation of PCDD/F from the oxidation of 2-chlorophenol on a CuO/silica surface.," *Journal of Physical Chemistry A*, 107 (2003), 4387-95.
39. W.A. Pryor, Prier, D. G., Church, D. F., "Electron spin resonance study of mainstream and sidestream smoke: Nature of the free radicals in gas-phase smoke and in cigarette tar.," *Environmental Health Perspectives*, 47 (1983), 345-55.
40. J. Adoukpe, L. Khachatryan; Dellinger B., "Radicals From the Thermal Degradation of Catechol," *in Preparation*, (2008).
41. B. Dellinger, S. Lomnicki, L. Khachatryan, Z. Maskos, R. Hall, J. Adoukpe, McFerrin. C. and H. Truong, "Formation and stabilization of persistent free radicals " *ScienceDirect, Proceedings of the Combustion Institute*, 31 (2007), 521-28.
42. H. Truong, Copper II Oxide Mediated Formation and Stabilization of Combustion Generated Persistent Free Radical In *Chemistry Department*, (Baton Rouge: Louisiana State University, 2007), 157.
43. R.L.B. R. B. Clarkson, K. Rothenberger, and H. Crookham, . "ENDOR of Perylene Radicals Adsorbed on Alumina and Silica-Alumina Powders. I. The Ring Protons," *J. Catalysis*, 106 (1987), 500.
44. T.M.Z. F. Jiang, J. B. Cornelius, R. B. Clarkson, R. B. Gennis, and R. L. Belford, "Nitrogen and Proton ENDOR of Cytochrome d, Hemin, and Metmyoglobin in Frozen Solutions," *J. Am. Chem. Soc.*, 115 (1993), 10293-99
45. M.N.R.A.S.R.L.R.A.M.A.J.O.-E.C.M.W.C.R.S.C.A.d. Lange2, "Resonance enhanced multiphoton ionization (REMPI) and REMPI-photoelectron spectroscopy of ammonia," *Eur. Phys. J. D 4*, 189-197, D 4 (1998), 189-97.
46. C.M. Gittins, Castaldi,M.J., Senkan,S.M., Rohlfig,E.A," "Real-Time Quantitative Analysis of Combustion Generated Polycyclic Aromatic Hydrocarbons by Resonance Enhanced Multiphoton Ionization Time of Flight Mass Spectrometry," *Anal. Chem*, 69 (1997), 286.

47. A. Marshall, Ledingham, K.W.D., Singhai, R.P., , "Trace Detection of Benzene Vapor in a Simple Ion Chamber Employing Laser Induced Resonance Enhanced Multiphoton Ionization in the 246-265 nm Wavelength Region," *Analyst*, 120 (1995), 2069-73.
48. J.A. Manion, and Louw, R., "Rates, products, and mechanisms in the gas-phase hydrogenolysis of phenol between 922 and 1175 K," *J.Phys. Chem.*, 93 (1989), 3563-74.
49. C.A. McFerrin, R.W. Hall and B. Dellinger, "Ab Initio study of the formation and degradation reactions of semiquinone and phenoxy radicals," *Theochem*, *accepted* (2007).
50. C. Horn, Roy, K., Frank, P., and Just, T., "Shock-tube study on the high-temperature pyrolysis of phenol " *27th Symp.(Intern.) on Combustion / The Combustion Institute, Pittsburgh, PA*, (1998), 321-28.

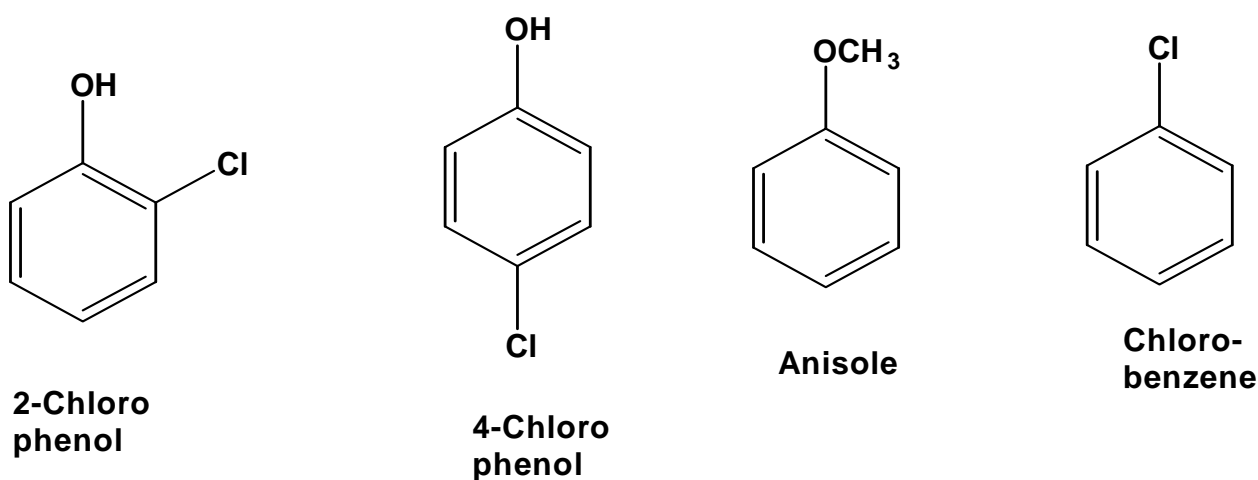
APPENDIX 1: ATMOSPHERIC PRESSURE PYROLYSIS OF 2-CHLOROPHENOL, 4-CHLOROPHENOL, ANISOLE, AND CHLOROBENZENE

1 Introduction

After a thorough look at the pyrolysis gas-phase products of catechol, hydroquinone and phenol, we performed the atmospheric pressure pyrolysis of compounds that have similar structure as the latter. The objective here was to see the decomposition pathway of compounds that mimic each of previously studied molecules. We anticipated that the change in the substituents on the benzene ring may reveal the real primary decomposition pathway of the compounds studied.

We employed 2-chlorophenol, 4-chlorophenol, chlorobenzene and anisole to respectively mimic catechol, hydroquinone, and phenol. Benzene was employed as reference compound. We pyrolyzed each of the compounds in the same experimental conditions as described in the present work. The pyrolysis temperature was 750C.

2. Molecular Formula of 2-Chlorophenol, 4-Chlorophenol, Anisole, and Chlorobenzene



The EPR spectra from the chlorinated phenol revealed one additional resolved line and one unresolved line in the spectra. This was not observed in the primary studies. The GC-MS pyrolysis products analysis confirmed that the primary decomposition pathway of the phenols

was through CO elimination as can be seen in the formation of chlorinated naphthalene. However, non-substituted dioxin formation from chlorophenol suggested chlorine atom

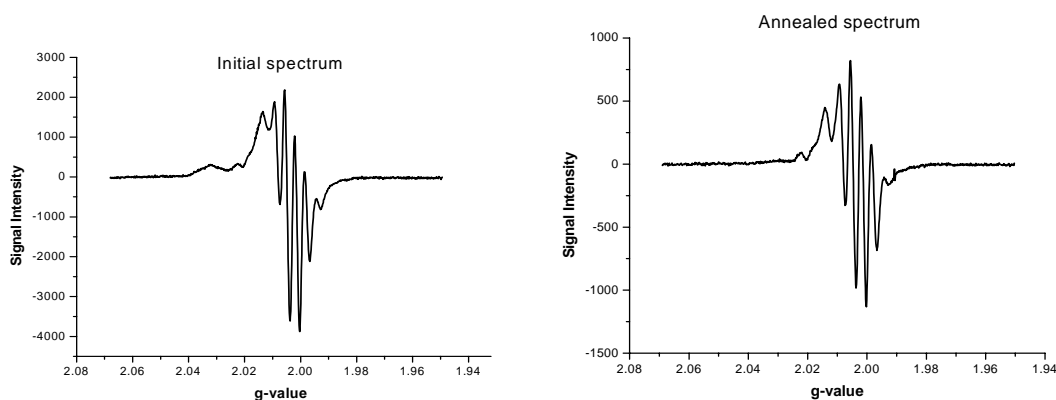


Figure A1- EPR spectra of radicals emerging from the pyrolysis of 2-Chlorophenol. The initial spectrum shows a shoulder with an additional line. After annihilation, the shoulder is removed but the additional line remained.

elimination prior to CO elimination.

2-2 EPR Spectra of the Pyrolysis of 4-Chlorophenol

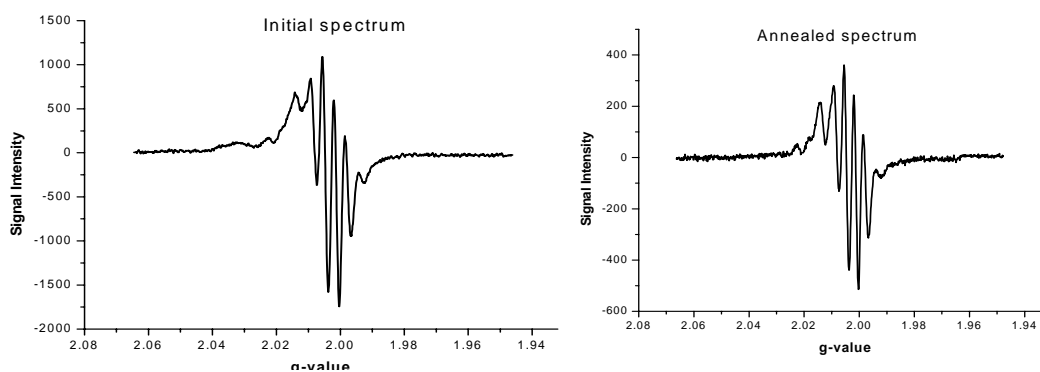


Fig A 2-EPR spectra of radicals emerging from the pyrolysis of 4-Chlorophenol. The initial spectrum shows a shoulder with an additional line. After annihilation, the shoulder is removed but the additional line remained

2-3 EPR Spectrum of the Pyrolysis of Anisole

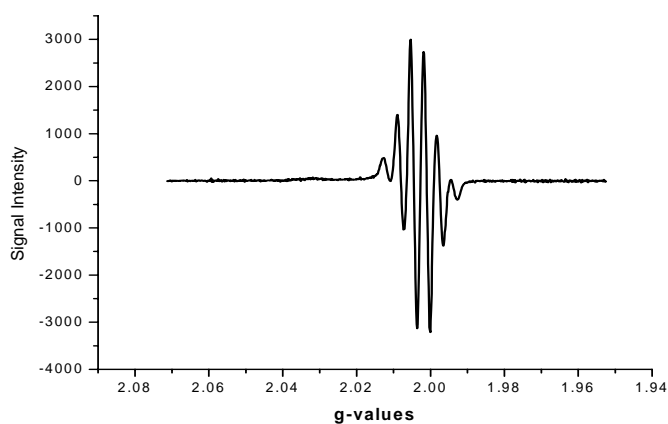


Fig A 3 Initial spectrum from the pyrolysis of Anisole. A clean CPD like was observed at the beginning of the accumulation. There was no need of annealing the clean spectrum

2.4 EPR Spectra of the Pyrolysis of Chlorobenzene

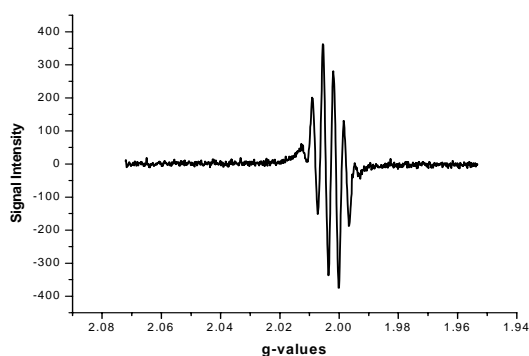


Fig A 4A Annealed spectrum

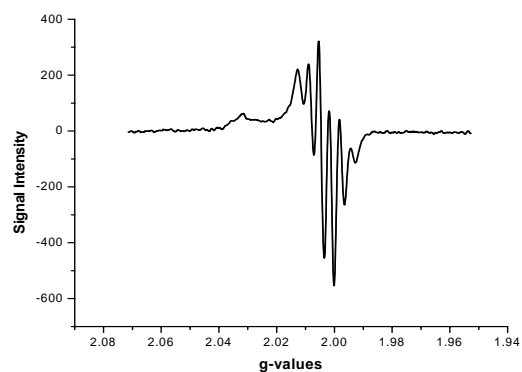


Fig A 4B Unannealed spectrum

The clean CPD radical observed after annihilation suggests a decomposition pathway that eliminates chlorine and carbon atoms or the presence of impurity in the sample may yield the CPD

3 G-C MS Spectra of the Pyrolysis Products of the Precursors

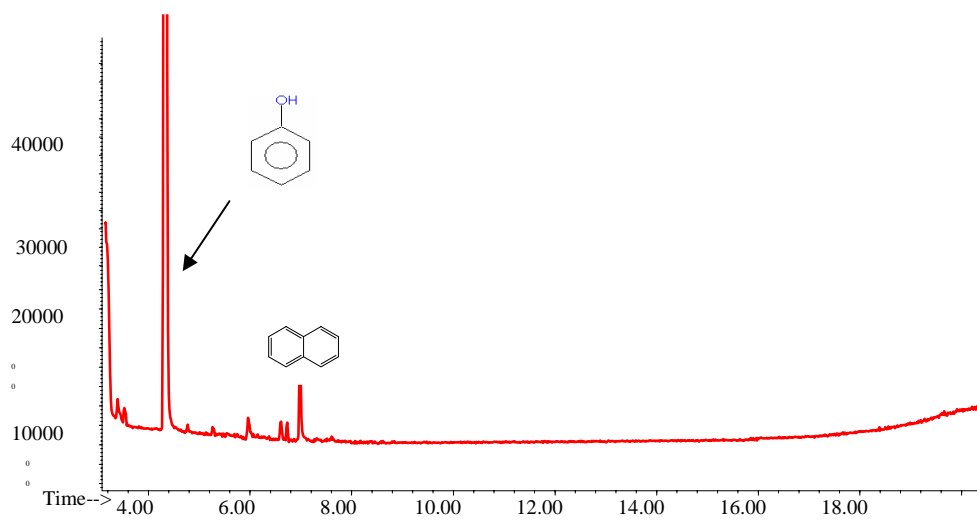


Fig A5 GC-MS of Phenol

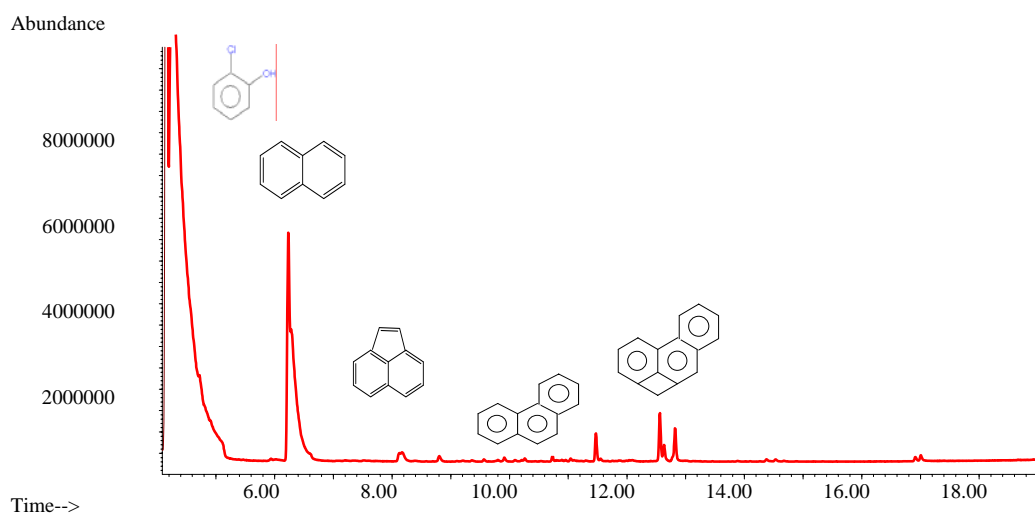


Fig A6 GC-MS of 2-Chlorophenol

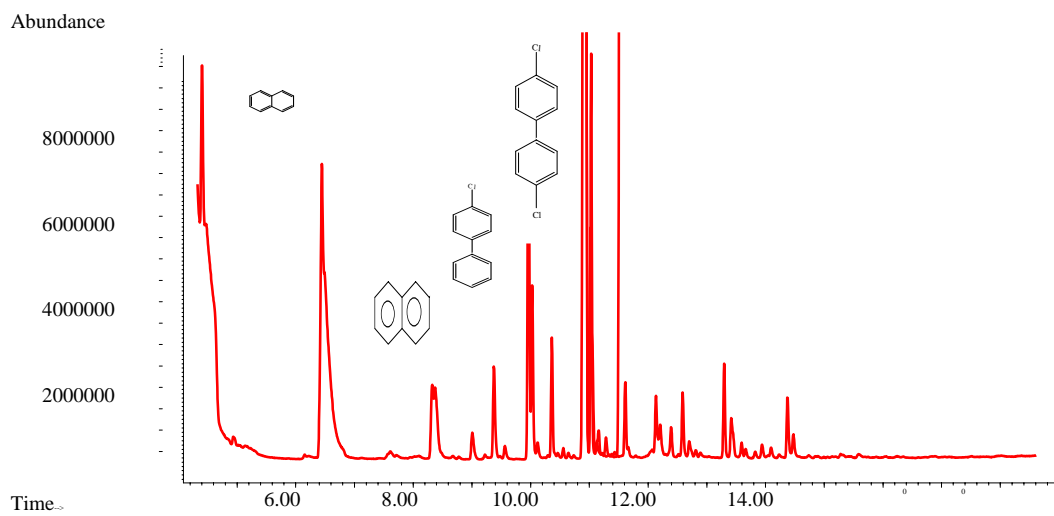


Fig A7GC-MS of Chlorobenzene

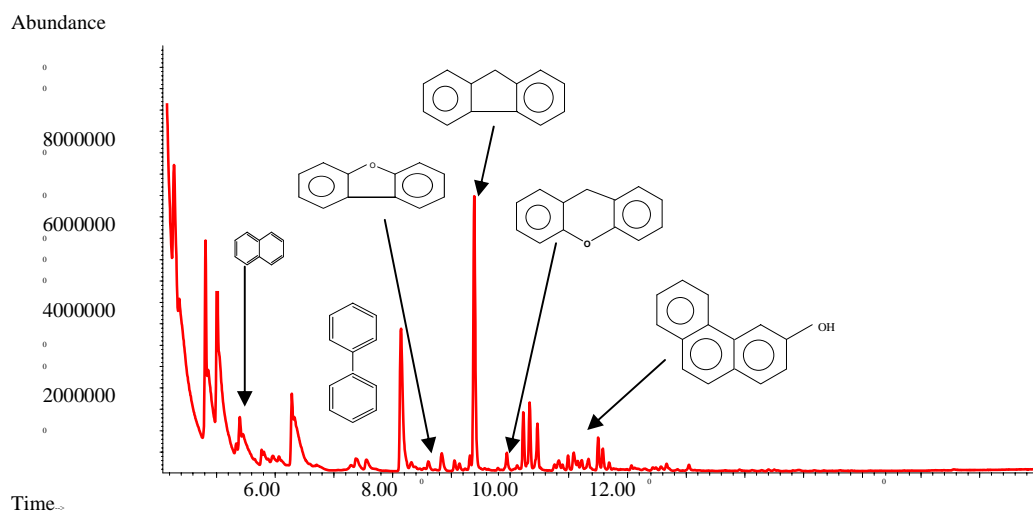


Fig A 8 GC-MS of Anisole

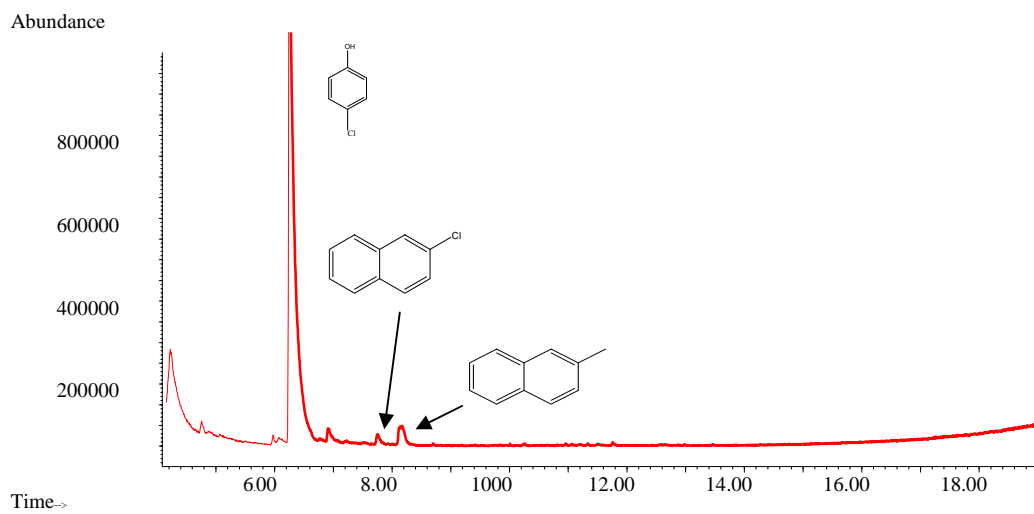


Fig A 9 GC-MS of 4-Chlorophenol

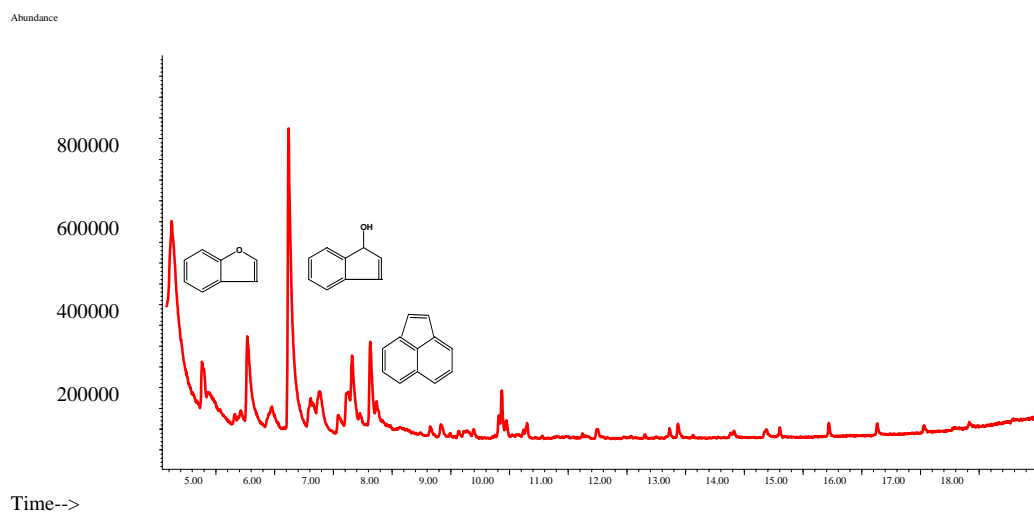


Fig A 10 GC-MS of Catechol

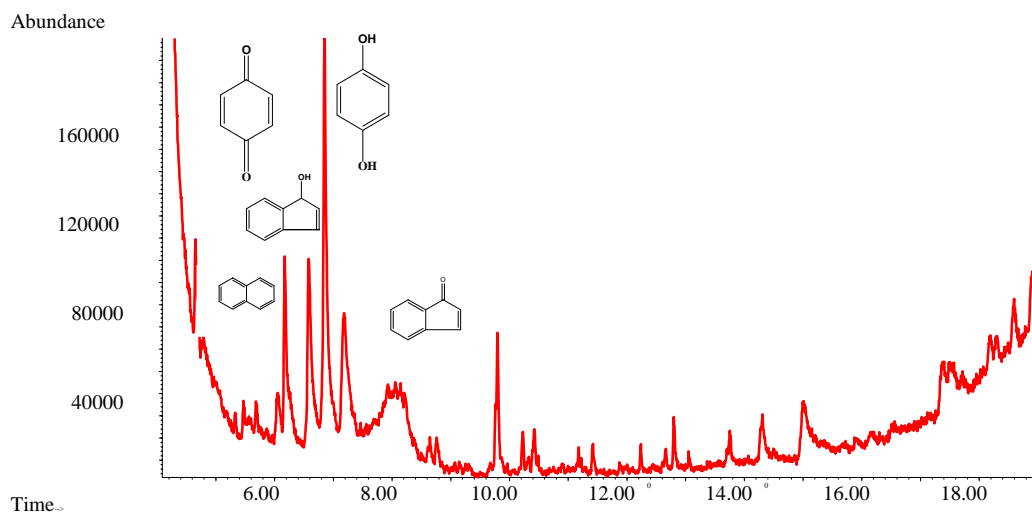


Fig A 11 GC-MS of Hydroquinone

APPENDIX 2: COPYRIGHT AND PERMISSIONS

JULIEN ADOUNKPE

Louisiana State University Department of Chemistry
Choppin Hall, Room 232, Box A23 Baton Rouge, LA 70803

Legal/Permissions

One Lake Street
Upper Saddle River, NJ 0745J; Eax:201-236--3290
Phone- 201-236-328, MiChelle.Johnson;a'?.PearsonEd.c

Fax #: 225-578-0276 Dear Mr. AdouUk'pe:

You have our permission to include content from our text, *QUANTUM CHEMISTRY, Stil Ed. by LEVINE, I'RA N.*, in your dissertation at LOUISIANA STATE UNIVERSITY.

Content to be included is: p. 338 Fig, 11..6

Please credit our material as follows:

LEVINE, IRA N., QUANTUM CHEMISTRY, Sti Edition, @ 2000,p.33\$. Reprinted by permission of Pearson Education, Inc., Upper Saddle River, NJ

Sincerely,

Michelle A. Parnicinne

02/26/2008 14:29 FAX 2027768112
0J001/002



American Chemical Society

Publications Division
Copyright Office

VIA FAX: 225-578-0276

DATE: February 26, 2008

1155 Sixteenth Street, NW
Washington, DC 20036

Phone: (1) 202-872-4368 or -4367

Fax: (1) 202-776-8112 [E-mail: copyright@acs.org](mailto:copyright@acs.org)

To: Julien Adoukpe, Department of Chemistry, Louisiana State University
Choppin Hall Room 232, Box A23, Baton, Rouge. LA 70803

FROM: C_Arleen Courtney, Copyright Associate • *asLLAd e'sP*

Thank you for your request for permission to include your paper(s) or portions of text from your paper(s) in your thesis. Permission is now automatically granted; please pay special attention to the implications paragraph below. The Copyright

If your paper has not yet been published by ACS, we have no objection to your including the text or portions of the text in your thesis/dissertation in **print and microfilm formats**; please note, however, that electronic distribution or Web posting of the unpublished paper as part of your thesis in electronic formats might jeopardize publication of your paper by ACS. Please print the following credit line on the first page of your article: "Reproduced (or 'Reproduced in part) with permission from [JOURNAL NAME], in press (or'submitted for publication'). Unpublished work copyright [CURRENT YEAR] American Chemical Society." Include appropriate information.

If your paper has already been published by ACS and you want to include the text or portions of the text in your thesis/dissertation in **print or microfilm formats**, please print the ACS copyright credit line on the first page of your article: "Reproduced (or'Reproduced in part) with permission from [FALL REFERENCE CITATION.] Copyright (YEAR) American Chemical Society." Include appropriate information.

Submission-to a **Dissertation Distributor**; If you plan to submit your thesis to UMI or to another dissertation distributor, you should not include the unpublished ACS paper in your thesis if the thesis will be disseminated electronically, until ACS has published your paper. After publication of the paper by ACS, you may release the entire thesis (**not the individual ACS article by itself**) for electronic dissemination through *the* distributor, ACS's copyright credit line should be printed *on* the first page of the ACS paper.

Use **on an Intranet**: The inclusion of your ACS unpublished or published manuscript is pennitted in your thesis in print and microfilm formats. if ACS has published your paper you may include the *manuscript in your thesis* on an intranet that is not publicly available. Your *ACS article cannot* be posted electronically on a publicly available medium (i_e. one that is not password protected), such as but not limited to, electronic archives, Intrruet, library server, etc. The only material from your paper that can be posted on a public electronic medium is the article abstract, fig=s, and tables, and you may link to the article's DOI or post the *article's* author-directed URL link provided by ACS. This paragraph does not pertain to the dissertation distributor paragraph above.

6/07/06

0

VITA

Julien Adoukpe was born on January 26, 1965, in Abomey-Calavi, Benin Republic (West Africa). He successively earned a Master of Science degree in physics with minor in chemistry in December 1990, a teaching certificate in September 1991 from the National University of Benin, and a postgraduate degree in rural engineering with specialization in energies from the Inter States College of Rural Engineering in July 1992, in Ougadougou, Burkina Faso. After a decade of teaching in Beninese public schools and of research action development in environmental field with the US-Peace Corps of Benin, He earned the prestigious Fulbright scholarship to undergo environmental studies at Louisiana State University (LSU) in Baton Rouge, Louisiana. In August 2002, He joined Dr Barry Dellinger's group at LSU department of chemistry where He found a very pleasant working environment. After his master's degree in environmental chemistry in August 2004, his master's in environmental studies in December 2007, Mr. Adoukpe will receive his Doctor of Philosophy degree in May 2008. He is very grateful to God for everything He has achieved in his life, and particularly in the United States of America.